Université Paris Diderot (Paris 7) Sorbonne Paris Cité
ED 560 - STEP'UP - "Sciences de la Terre et de l'Environnement
et Physique de l'Univers de Paris"

Thèse de Doctorat
Physique théorique

The nonperturbative renormalization group for quantum field theory in de Sitter space

présentée par

Maxime GUILLEUX

pour l'obtention du titre de

Docteur de l'Université Paris Diderot (Paris 7) Sorbonne Paris Cité

Thèse dirigée par Dr Julien Serreau
Laboratoire AstroParticule et Cosmologie

soutenue publiquement le 28 septembre 2016 devant le jury composé de :

Pr	Jihad	Mourad	Président du jury
Dr	Julien	Serreau	Directeur de thèse
Pr	Ali	Kaya	Rapporteur
Pr	Emil	Akhmedov	Rapporteur
Pr	Bertrand	Delamotte	Examinateur
Dr	Dario	Benedetti	Examinateur

A René. A Gabrielle.

Acknowledgments

I am grateful to the many people who have contributed in any way to this project. I would like to thank Julien first, for taking me as his Ph.D. student. I have learned a lot by working with him, all the while enjoying myself very much.
I thank the jury members, Bertrand Delamotte, Dario Benedetti, and Jihad Mourad. I am especially grateful to the referees, Emil Akhmedov and Ali Kaya.
It was a pleasure to work among the theory group at APC. It has proved to be a rich scientific environment thanks to all its members.
Thanks also to all those at APC laboratory who where around me : the fellows in office 424A, both old and new, as well as all the students in the lab. It's been a great experience and a pleasure to work alongside you.
Teaching was a great experience and a fun part of my PhD. For this I am thankful to Sara Ducci and the rest of the pedagogical team.
Thanks to all the friends and family who were close by in these demanding times. And thank you, Marie, for being a part of my life.

Contents

Introduction **ix**

Conventions **xiii**

1 General setup **1**
1.1 Cosmology: from expansion to inflation . . . 2
1.1.1 An expanding Universe . . . 2
1.1.2 The inflationary epoch . . . 2
1.1.3 Primordial fluctuations . . . 4
1.2 Quantum field theory in de Sitter space . . . 5
1.2.1 de Sitter space . . . 5
1.2.2 The in-in formalism . . . 6
1.2.3 Physical momentum representation . . . 8
1.2.4 Loop expansion . . . 9
1.2.5 Resummation techniques . . . 11
1.3 Non Perturbative Renormalization Group . . . 14
1.3.1 Regulated effective action . . . 14
1.3.2 Boundary condition for the effective action . . . 16
1.3.3 Flow of the effective action . . . 17
1.3.4 Choosing the regulator . . . 18
Conclusion . . . 20

2 Flow of the effective potential **21**
2.1 The Local Potential Approximation . . . 22
2.1.1 Two-point correlators . . . 22
2.1.2 Flow of the potential . . . 24
2.2 From subhorizon to superhorizon scales . . . 26
2.2.1 Minkowski regime . . . 26
2.2.2 Infrared regime and dimensional reduction . . . 29
2.3 Equivalent approaches . . . 30
2.3.1 zero-dimensional field theory . . . 30
2.3.2 Relation to the stochastic approach . . . 31
2.3.3 Relation to Euclidean de Sitter space . . . 32
2.4 The large-N limit . . . 33

2.4.1 Generalizing to $O(N)$ theories . . . 34
2.4.2 Flow of a ϕ^4 theory . . . 35
2.4.3 Symmetry restoration . . . 36
2.4.4 Mass (re)generation . . . 40
2.4.5 Correlation length . . . 43
2.5 Finite N . . . 44
2.5.1 Goldstone contributions . . . 44
2.5.2 Convexification . . . 45
Conclusion . . . 48

3 NPRG in Minkowski space 49
3.1 Derivative expansion . . . 50
3.1.1 LPA' . . . 50
3.1.2 Flow of the potential . . . 51
3.2 Anomalous dimension . . . 52
3.2.1 Flow of the inverse propagator . . . 52
3.2.2 Flow of Z_k through frequency derivative . . . 54
3.2.3 Flow of Z_k through momentum derivative . . . 55
3.2.4 Critical exponents at the Wilson-Fischer fixed point . . . 56
3.2.5 Concerning regulators . . . 58
3.3 Conclusion . . . 60

4 Beyond the LPA 61
4.1 Derivative expansion in de Sitter space . . . 62
4.1.1 Derivative couplings in curved space-time . . . 62
4.1.2 Prescription for the anomalous dimension . . . 63
4.1.3 Correlators in the LPA' . . . 65
4.2 Anomalous dimension of a single field . . . 67
4.2.1 General expression . . . 67
4.2.2 Heavy UV regime . . . 70
4.2.3 Light IR regime . . . 71
4.3 Anomalous dimension in $N > 1$ . . . 71
4.3.1 Generalizing to $O(N)$ theories . . . 71
4.3.2 Light IR regime . . . 74
4.4 Influence on the flow of the potential . . . 74
4.4.1 Dimensional reduction and modified RG scale . . . 74
4.4.2 Field expansion . . . 76
Conclusion . . . 78
4.4.3 Heavy UV regime . . . 80
4.5 first order derivative expansion and anomalous dimension in the symmetric phase . . . 81

Conclusion 83

Appendices **87**
A Hankel functions cheat sheet . . . 88
A.1 General relations . . . 88
A.2 Infrared regime . . . 88
A.3 Ultraviolet regime . . . 89
B Explicit calculation of $B(\nu, k, x)$ . . . 90
C Dimensionally reduced RG flow . . . 92
D Dimensionally reduced integral for large N . . . 93
E Truncation effects for $N = 1$ . . . 95
F Correlator functions . . . 97
G Ultraviolet flow of the inverse correlator . . . 99
G.1 Tadpole contribution . . . 99
G.2 Sunset contributions . . . 100
H Infrared flow of the inverse correlator . . . 102
H.1 Tadpole contribution . . . 102
H.2 Sunset contributions . . . 102
H.3 $0(N)$ case . . . 104

Bibliography **117**

Introduction

The study of quantum field theory in curved space-time is currently an active topic [1–16]. For physical phenomena where gravitational and quantum dynamics interplay, this treatment is a first step towards quantum gravity with many interesting results. Prominent examples are the spontaneous Hawking/Unruh radiation from black holes [17–19], the possibility of gravitationally induced phase transitions in the early Universe [20–22], and the amplification of cosmological perturbations during the inflation era [23].

This last phenomenon puts a great deal of attention on de Sitter space [24–27]. Because its symmetry is maximal, it is a preferred playground to understand the nontrivial quantum effects that occur in a period of accelerated expansion [28, 29]. For light scalar fields relevant to inflation, the nontrivial kinematics in de Sitter space provides a mechanism to generate the primordial power spectrum. At tree order, their quantum fluctuations are enhanced on large scales, seeding the classical fluctuations in the CMB and the formation of Large Scale Structures at later times [30, 31].

The gravitational enhancement of these superhorizon fluctuations is also problematic when computing loop corrections. Infrared and secular divergences appear in the quantum corrections to scalar field dynamics in de Sitter space [32, 33], signaling genuine nonperturbative effects which require resummations [13, 34]. Dealing with these divergences is a crucial issue in the context of quantum field theory on de Sitter space. For instance, these have led some authors [35–37] to conjecture that dS space might be unstable against quantum fluctuations. It has been argued in [33, 38] that secular divergences are very generic in cosmological space-times. In fact, they are a well-known artifact of perturbative approaches in non-stationary (nonequilibrium) systems even in flat space, where advanced resummation methods have been developed to treat them consistently [39–41]. It is of utmost importance to develop similar tools in the cosmological case in order to get control on loop corrections at late times or, in the de Sitter case, for superhorizon modes, relevant for inflationary cosmology.

Specific techniques beyond standard perturbation theory have already been developed to capture the dynamics of the relevant modes. This ranges from the effective stochastic approach put forward in Ref. [42, 43] to various quantum field theoretical methods suitably adapted to de Sitter space; see Refs. [44–57] for a (non exhaustive) list of examples. In particular, such methods allow one to study how an interacting scalar theory cures its infrared and secular problems, e.g., with the dynamical generation of a nonzero mass.

Nonperturbative renormalization group (NPRG) methods are particularly adapted

for dealing with nontrivial infrared physics in many instances, from critical phenomena in statistical physics to the long distance dynamics of non-Abelian gauge fields [58–61]. Such techniques have recently been formulated in de Sitter space-time[1] in Refs. [65, 66], where they have been used to study the renormalization group (RG) flow of O(N) scalar field theories at superhorizon scales. In the present thesis, we undertake a systematic study of NPRG techniques in de Sitter space. We extend previous studies in the simplest approximation (LPA) and obtain original results concerning the onset of gravitational effects as one integrates out modes from sub to superhorizon scales. Finally, we develop the formalism beyond the LPA and lay the basis for more general approximations. In particular, we discuss the derivative expansion, widely used in statistical physics.

This manuscript is organized as follows. The first chapter is devoted to a general overview of the inflationary era and the current interest for light scalar fields in de Sitter space. We introduce the setup in which quantum field theory can be formulated as a functional integral, and give a brief summary of the results of perturbative theory, namely the ability to produce the desired near-invariant power spectrum at tree level as well as the problematic infrared and secular divergences that appear in loop corrections to massless field dynamics. We discuss a selection of resummation methods that have been developed to address these issues: the stochastic approach, which has been most widely used, as well as Schwinger-Dyson equations and large-N techniques. We conclude this chapter with an introduction to the nonperturbative renormalization group, from the concept of infrared regulation to the resulting flow equation for the effective action.

In the second chapter, we provide a complete analysis of the flow of the effective potential in the local potential approximation (LPA), generalizing the findings of [65, 66]. In particular, we study in detail the onset of gravitational effects as one integrates out momentum modes from subhorizon scales, where the physics is essentially that of Minkowski space, to superhorizon and deep superhorizon scales, where the space-time curvature plays a predominant role and leads to dramatic effects. In this regime, the strongly amplified field fluctuations lead to an effective dimensional reduction of the flow, which becomes identical to that of a zero-dimensional theory. This phenomenon has significant consequences which we investigate in detail. First and foremost is that the effective potential of the resulting theory in the infrared can be described in terms of a usual integral, as opposed to a functional one, which can be computed exactly (sometimes analytically). This analysis allows for nontrivial bridges with other approaches, in particular, the widely used stochastic approach of [42] Starobinsky:1994bd and the Euclidean de Sitter approach [64]. On the one hand, we show explicitly that the weight of the integral defining the effective potential in the IR is identical to the late-time stationary probability distribution function of the stochastic approach. On the other hand, we also show that the dimensionally reduced flow in Lorentzian de Sitter is identical to the RG flow in Euclidean de Sitter which is eventually driven by a single degree of freedom, the zero mode of the compact space. Finally, we discuss the phenomenon of radiative symmetry restoration, previously advocated in [67–70] and first decribed in this context in [66]. We find that no spontaneously broken symmetry is possible in the

[1] See also [62–64] for other recent applications in curved spaces.

effective potential, in any dimension and regardless of the bare potential.

In the third chapter we develop the equivalent setup in Minkowski space. This serves to prove that the de Sitter RG flow admits a proper flat space limit as we take $H \to 0$. We find indeed that this limit coincides with the Minkowskian calculation, which we compare to usual flat space results from statistical physics. Because our regulator acts on spatial momenta only, leaving frequencies unregulated, our flow equation is different from the usual Euclidean one. A study of the critical properties around the Wilson-Fischer fixed point shows a good agreement between the two methods, indicating that our regulation scheme works appropriately in this limit. Finally, we introduce the derivative expansion in the context of flat space and implement the LPA' scheme as an improvement of the LPA. This lays the groundwork for similar improvements in de Sitter space and provides once again a point of comparison with the limit $H \to 0$.

In the last chapter, we pave the way for NPRG techniques in de Sitter space beyond the LPA. The derivative expansion is especially relevant to the physics of long wavelength fluctuations which we are interested in, and a great deal of work is devoted to formal questions concerning its very formulation in general curved space-times. Besides the large range of possible couplings to gravity that are generated, the non-commutation of the isometry generators poses peculiar problems which are absent in flat space. We solve this issue in de Sitter space by considering spatially homogeneous but time dependent field configurations. This allows us to define a prescription for the flow of each term in the derivative expansion. To put the formalism at work, we consider the simplest extension of the LPA, which includes a renormalization of the standard kinetic term (field renormalization factor). A large part of this work is devoted to the computation of its flow, the so-called running anomalous dimension. We are able to show that the derivative expansion thus defined admits a proper flat space limit when we take $H \to 0$. In the opposite regime, for light infrared modes, a remarkable result is that the effective potential remains the same as in the LPA, so that the field renormalization does not bring any corrections to the stochastic approach.

Conventions

- We work in $D = d + 1$ space-time dimensions with signature $(-, +, ..., +,)$.
- The Einstein summation convention is to be understood whenever Lorentz indices are repeated.
- K denotes a comoving momentum, and k the renormalization scale.
- x denotes a space-time point $(\mathbf{x}, \eta)$, where $\mathbf{x}$ is a spatial point and η (conformal) time.
- The Fourier transform is defined as :

$$\tilde{F}(\mathbf{K}) = \int d^d x e^{-i\mathbf{K}\mathbf{x}} F(\mathbf{x}) \qquad F(\mathbf{x}) = \int \frac{d^d K}{(2\pi)^d} e^{i\mathbf{K}\mathbf{x}} \tilde{F}(\mathbf{K}) \tag{1}$$

- We work in natural units $\hbar = c = 1$. Unless specified otherwise, we also set the de Sitter curvature $H = 1$.
- We denote the step function as $\theta(x) = \begin{cases} 1 \text{ if } x > 0 \\ 0 \text{ otherwise} \end{cases}$

On the electronic version of this thesis

The table of contents contains links to each section. We have also added a link back to the table of contents in the page number of each page to navigate back and forth between sections.

Chapter 1

General setup

In the beginning there was nothing, which exploded.

– Terry Pratchet, *Lords and Ladies*

Contents

1.1 Cosmology: from expansion to inflation 2

1.1.1 An expanding Universe 2

1.1.2 The inflationary epoch 2

1.1.3 Primordial fluctuations 4

1.2 Quantum field theory in de Sitter space 5

1.2.1 de Sitter space 5

1.2.2 The in-in formalism 6

1.2.3 Physical momentum representation 8

1.2.4 Loop expansion 9

1.2.5 Resummation techniques 11

1.3 Non Perturbative Renormalization Group 14

1.3.1 Regulated effective action 14

1.3.2 Boundary condition for the effective action 16

1.3.3 Flow of the effective action 17

1.3.4 Choosing the regulator 18

Conclusion 20

1.1 Cosmology: from expansion to inflation

1.1.1 An expanding Universe

One of the fundamental consequences of general relativity is the possibility of a dynamical space-time [71]: given a specific content of matter and energy, the Universe can be expanding or contracting. Assuming spatial homogeneity and isotropy, one can follow this expansion through a single function of time, the scale factor $a(t)$. It encodes the time evolution of spatial distances: $\dot{a}(t) > 0$ for expansion, i.e. growing physical distances. The time evolution of the scale factor is set by the matter-energy density through the Friedmann equations. In the Big Bang scenario this density is successively dominated by radiation, matter, and then dark energy corresponding respectively to $a(t) \propto t^{\frac{1}{2}}, t^{\frac{2}{3}}$ and e^{Ht} [72].

The consistency of these theoretical predictions has been checked by measurement of the galaxy redshift [73, 74], proving that objects are receding from each other at large scales. Other observations, such as the Cosmic Microwave Background [75] or Big Bang Nucleosynthesis [76] confirm the hot dense state of the Universe some 13.6 billion years ago.

1.1.2 The inflationary epoch

Several reasons motivate the alteration of this simplest model by adding another era [77]. Let us briefly discuss two such problems:

- Horizon problem: The CMB observations show an extremely homogeneous early Universe where distant regions where at thermal equilibrium. Yet in the simplest Big Bang model, the time between the primordial singularity and the CMB emission is not sufficient for these regions to be causally connected, let alone at the same temperature.

- Flatness problem: The two first eras – radiation, and matter dominated – correspond to decelerated expansion. From the Friedmann equations this implies that the total density should depart from the critical density over time. Observations however find the density to be very close to its critical value at present day.

Both these problems are not fundamental flaws of the model but consist in extreme fine tuning: we could always assume that the Universe started at thermal equilibrium on very large scales and with a density extremely close to criticality. This is quite uncomfortable however and it would be preferable to have a dynamical explanation.

The simplest (and most elegant) way to overcome these fine tuning problems is to introduce an early phase of *accelerated* expansion, as sketched in figure 1.1. The horizon problem is solved because there is now more time[1] since the primordial singularity for all regions of the observed Universe to achieve thermal equilibrium. The flatness problem is also solved because the accelerated expansion brings the total density closer to its critical value, explaining the observed value today in an natural way.

[1] Precisely, there is more conformal time. Inflationary models do not necessarily add cosmological time. Figure 1.1 features cosmological time and is therefore nothing more than a sketch of inflation.

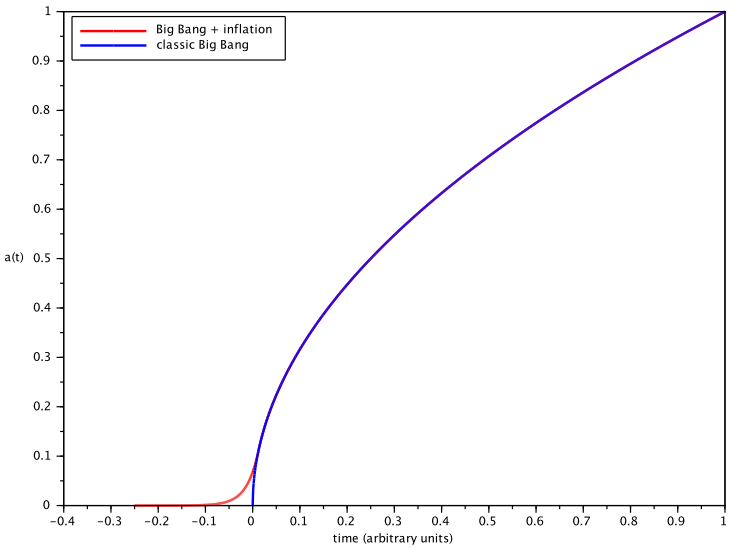


Figure 1.1: Rough picture of the scale factor in the early Universe with and without inflation. The inflation era consists in a primordial accelerated expansion which explains the causal connection of the Universe on large scales.

The accelerated expansion must be sourced by some content of matter-energy. Radiation and ordinary matter produce only decelerated expansion. Dark energy, in the form of a cosmological constant, would dominate for all posterior times which doesn't allow for the rest of cosmology to take place. Models of inflation are therefore built with some new kind of matter. The simplest one, called the slow-roll model, requires a single scalar field called the inflaton [78, 79]. Considering its action,

$$S[\phi] = \int d^4x\sqrt{-g}\left(\frac{1}{2}g^{\mu\nu}\partial_\mu\phi\partial_\nu\phi - V(\phi)\right), \tag{1.1}$$

then the inflaton behaves as a perfect fluid when assuming isotropy and homogeneity. Its density and pressure are:

$$\rho = \frac{1}{2}\dot{\phi}^2 + V(\phi), \tag{1.2}$$

$$p = \frac{1}{2}\dot{\phi}^2 - V(\phi). \tag{1.3}$$

This field starts out of equilibrium, i.e. with a uniform value that does not minimise its self-interaction potential. If this potential energy is large compared to the kinetic energy, this results in a negative pressure, typically $\rho = -p$, sourcing an exponential expansion. The above condition implies that the field density rolls slowly down the potential, which puts some constraints on the shape of the potential (see Fig 1.2). The inflation epoch ends when the kinetic and potential energies become comparable. Coupled to ordinary matter, it then produces the classical content of matter-energy of the early Universe during the phase of reheating.

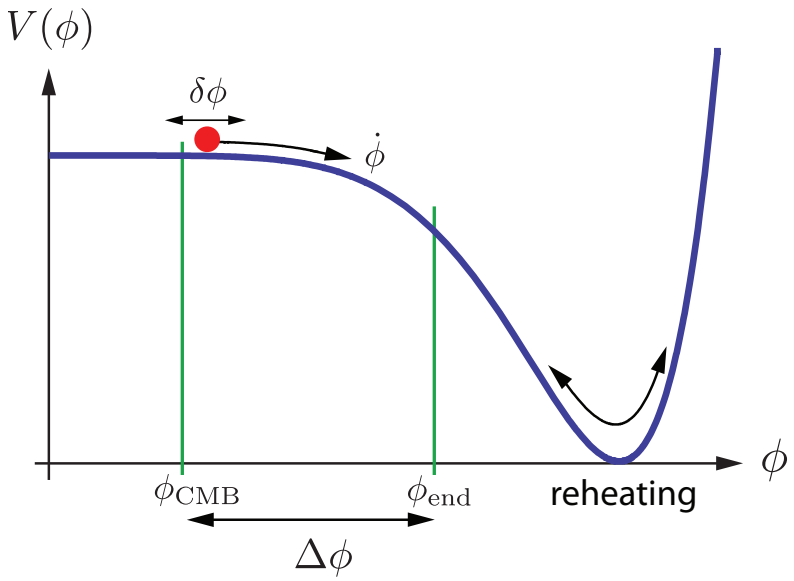


Figure 1.2: Self-interacting potential of the inflaton field. Inflation starts as the field is out of its equilibrium value. The shape of the potential is designed to generate a slow roll during which the pressure is negative, generating accelerated expansion. Inflation ends as the slope increases towards the minimum, and the inflaton decays into ordinary fields to generate the hot universe of the Big Bang scenario.

1.1.3 Primordial fluctuations

The slow-roll model has an excellent theoretical as well as observational success. The scales involved are typically an expansion of some 60 e-folds in 10^{-32} seconds in order to match observations. The next step is to study cosmological perturbations, i.e. primordial fluctuations in energy/density and their evolution by gravitational instability to form the Large Scale Structures at present day.

At this point, a number of reasons point that these fluctuations should be of quantum origin and not classical. On one hand, classical fluctuations pose a fine tuning problem in order to both match observations and remain small with respect to the background value during inflation [30]. On the other hand, tree level computation of quantum fluctuations give remarkable predictions for the primordial power spectrum, from its flatness on large scales to the coherence of all modes leading to the Baryonic Acoustic Oscillations. Our current paradigm for inflation is therefore that a perfectly homogeneous quantum field sources statistical fluctuations in the early cosmology.

Because the precision of observations is increasing, and for want of a consistent quantum theory, it is necessary to understand and compute loops on an expanding background. There some problems arise: the scalar and tensor modes built from the fluctuations of the field and the metric behave as massless fields at tree order. This

is responsible for non-trivial divergences in loops [32, 33] which signal nonperturbative physics and call for resummation techniques [34, 68, 80, 81]. This is the issue we will be adressing in this thesis. To simplify the complicated task of coupling a quantum field to gravitational degrees of freedom, we consider a test field on a fixed expanding background. In the next section, we define this background, illustrate the tree level and loop computations, and give a brief review of some nonperturbative methods that have been used so far.

1.2 Quantum field theory in de Sitter space

1.2.1 de Sitter space

de Sitter space is particularly adapted to study questions of QFT in an expanding Universe, because of its simplicity and relevance to inflation. It is simple because it is the unique maximally symmetric space-time with positive curvature. The D-dimensional de Sitter space, dS_D, can be visualised as the hyperboloid

$$-X_0^2 + \Sigma_{i=1}^{D} X_i^2 = \frac{1}{H^2} \tag{1.4}$$

embedded in a $D+1$-dimensional Minkowski space

$$ds^2_{D+1} = -dX_0^2 + \Sigma_{i=1}^{D} dX_i^2. \tag{1.5}$$

In this work, we will restrict ourselves to a causal patch of this manifold, the Poincaré patch, which is half of the full de Sitter hyperboloid (see figure 1.3). See [72] for a complete description. The metric on this patch can be written as

$$ds^2 = -dt^2 + a(t)^2 d\mathbf{x}^2 \qquad \text{with} \quad a(t) = e^{Ht}, \qquad t \in]-\infty; +\infty[, \tag{1.6}$$

$$= a(\eta)^2(-d\eta^2 + d\mathbf{x}^2) \qquad \text{with} \quad a(\eta) = \frac{-1}{H\eta}, \qquad \eta \in]-\infty; 0[, \tag{1.7}$$

where $\mathbf{x} = (x_1, \dots x_d)$ and $D = d+1$. The conformal time η is defined by $d\eta = dt/a(t)$. The exponential growth of the scaling factor is a typical feature of slow-roll inflationary models[2].

Although we will not use them, we mention another set of useful coordinates for the Poincaré patch, the Lemaître-Painlevé-Gulstrand coordinates[3]:

$$\mathbf{X} = a(t)\mathbf{x}. \tag{1.8}$$

The metric in these coordinates writes

$$ds^2 = -(1 - H^2\mathbf{X}^2)dt^2 - 2H\mathbf{X}.d\mathbf{X}dt + d\mathbf{X}^2, \tag{1.9}$$

where it is made obvious that this space is stationary (although inhomogeneous). This is a key feature in understanding the spectral accumulation for large wavelength modes which we will discuss later. In what follows, unless specified otherwise we will set $H = 1$, that is, work in units of H.

[2] More precisely, the growth is almost exponential with H varying slowly in time until the breakdown of this regime and the end of inflation.

[3] Here, $\mathbf{X}$ is not to be mistaken for the $D+1$ Minkowski coordinates $X_0..X_D$.

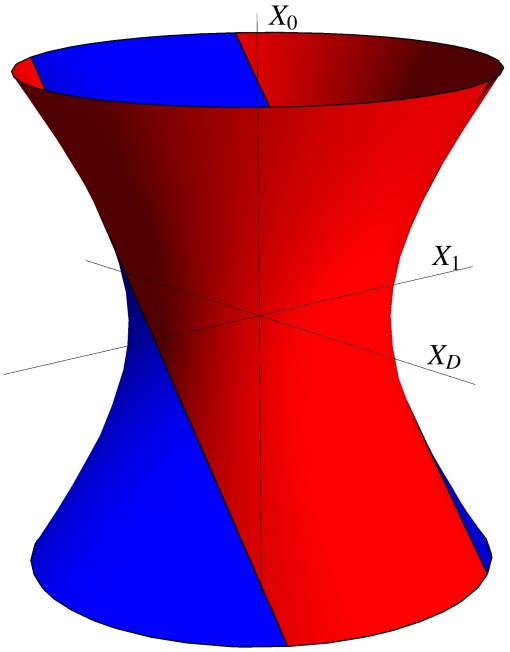


Figure 1.3: Representation of de Sitter space as a hyperboloid embedded in $D+1$ Minkowski space. The Poincaré patch in red corresponds to the region $X_0 + X_D > 0$.

1.2.2 The in-in formalism

The success of functional approaches for quantum field theory in flat space-time has led to the development of powerful tools. Starting from the action, the generating functional is defined as

$$Z[J] = e^{iW[J]} = \int \mathscr{D}\varphi \ \exp\left(iS[\varphi] + i\int_x J\varphi\right). \tag{1.10}$$

The action of a scalar field typically writes

$$S[\varphi] = -\int_x \left(V(\varphi) + \frac{1}{2}(\partial\varphi)^2\right), \tag{1.11}$$

where $V(\varphi)$ is the self-interaction potential. From this functional, one can extract the average value of any observable $\mathcal{O}$ in the presence of a source:

$$\langle\mathcal{O}\rangle_J = e^{-iW[J]} \int \mathscr{D}\varphi \ \mathcal{O}[\varphi] \ \exp\left(iS[\varphi] + i\int_x J\varphi\right). \tag{1.12}$$

The difficulty is of course to compute a functional integral, for which we will introduce the functional renormalization group. Before doing so, however, we must adapt this formalism to the context of an expanding background. The first step for this is to convariantize quantities in the following way:

- Space-time derivative ∂_μ must be replaced by covariant derivatives ∇_μ.



Figure 1.4: Closed time path of the Schwinger-Keldish (in-in) formalism. By defining the field on this time path $\mathcal{C}$, one can construct the generating functional for expectation values similarly to the generating functional for matrix elements in the in-out formalism.

- Space-time integrals must have the covariant measure $\int_x \equiv \int d^D x\sqrt{-g}$, where g is the determinant of the metric $g_{\mu\nu}$.
- Functional derivatives must be made covariant, e.g. $\dfrac{\delta_c \bullet}{\delta J(x)} \equiv \dfrac{\delta \bullet}{\sqrt{-g}\delta J(x)}$.
- Space-time delta functions must be made covariant[4] : $\delta(x,x') = \dfrac{\delta^{(D)}(x-x')}{\sqrt{-g}}$.

The second step is to provide a framework in which we can diagonalize the Laplace-Beltrami operator. This is not as trivial as in flat space due to the noncommutation of space and time translation operators. As a consequence, it is difficult to formulate de Sitter symmetries in momentum space. A convenient choice is to diagonalize space translations by going to comoving spatial Fourier space and to treat the time evolution as a non equilibrium problem.

The issue of quantum fields is therefore more conveniently formulated as an initial-value problem [54] rather than the usual in-out formalism. Instead of computing the overlap between an initial and a final state, we are interested in evolving an initial state in time and computing expectation values of products of fields. The Schwinger-Keldish formalism [82, 83] allows us to compute a generating functional for such quantities by defining the fields on a closed time path going from the infinite past to the infinite future and back (see Fig 1.4). Equations (1.10 - 1.12) remain valid where the time integrals are now performed on this contour.

Let us introduce the two-point function which will intervene in most computations:

$$G(x,y) \equiv \langle\varphi(x)\varphi(y)\rangle_J - \langle\varphi(x)\rangle_J \langle\varphi(y)\rangle_J = -iW^{(2)}(x,y), \tag{1.13}$$

where

$$W^{(2)}(x,y) = \frac{\delta_c^2 W[J]}{\delta J(x)\delta J(y)}. \tag{1.14}$$

One can define G equivalently as a time-ordered product in the operator formalism:

$$G(x,y) = \langle\Omega_J|T_{\mathcal{C}}\hat{\varphi}(x)\hat{\varphi}(y)|\Omega_J\rangle - \langle\Omega_J|\hat{\varphi}(x)|\Omega_J\rangle \langle\Omega_J|\hat{\varphi}(y)|\Omega_J\rangle\,, \tag{1.15}$$

where $|\Omega_J\rangle$ is the appropriate state corresponding to the source J. This function and the time ordering are defined on the contour $\mathcal{C}$, and we may write

$$G(x,x') = F(x,x') - \frac{i}{2}\mathrm{sign}_{\mathcal{C}}(\eta-\eta')\rho(x,x'), \tag{1.16}$$

[4]Because we are in the in-in formalism, the Dirac function takes values on the closed time path.

where F and ρ are the statistical and spectral two-point functions respectively. In the operator formalism, they write

$$F(x,x') = \frac{1}{2}\left\langle \Omega_J | \{\hat{\varphi}(x); \hat{\varphi}(x')\} | \Omega_J \right\rangle, \qquad \rho(x,x') = i\left\langle \Omega_J | [\hat{\varphi}(x); \hat{\varphi}(x')] | \Omega_J \right\rangle. \tag{1.17}$$

They are respectively symmetric and antisymmetric:

$$F(x,x') = F(x',x), \qquad \rho(x,x') = -\rho(x',x). \tag{1.18}$$

1.2.3 Physical momentum representation

We will restrict ourselves to quantum states which respect the symmetries of de Sitter space, allowing us to simplify the expression of the two-point correlators. Although they depend on two space-time points, they can be expressed as a function of the de Sitter invariant

$$z(x,x') = \frac{(\mathbf{x}-\mathbf{x}')^2 - (\eta-\eta')^2}{\eta\eta'}, \tag{1.19}$$

so that $G(x,x') = G(z)$. As we have discussed previously, we take a different approach here however since we wish to move to Fourier space for spatial variables. Exploiting spatial translation invariance in comoving coordinates, we write

$$G(x,x') = G(\mathbf{x}-\mathbf{x}', \eta, \eta'). \tag{1.20}$$

Moving to spatial Fourier modes,

$$\tilde{G}(K,\eta,\eta') = \int d^d x e^{-i\mathbf{K}\cdot\mathbf{x}} G(x,\eta,\eta'), \tag{1.21}$$

where $\tilde{G}$ depends only on $K = |\mathbf{K}|$ by isotropy. In general cosmological space-times, the correlator depends separately on the comoving momentum K and the conformal times η, η'. The symmetries of the de Sitter space-time—in fact the affine subgroup [84, 85]—constrain these dependences to be tied together by the gravitational redshift. The correlation function is a nontrivial function of the physical momenta $p = -K\eta$ and $p' = -K\eta'$ only:

$$\tilde{G}(K,\eta,\eta') = \frac{(\eta\eta')^{\frac{d-1}{2}}}{K}\hat{G}(p,p'). \tag{1.22}$$

Similarly, for the inverse correlator[5],

$$\tilde{\Gamma}^{(2)}(K,\eta,\eta') = (\eta\eta')^{\frac{d+3}{2}} K^3 \hat{\Gamma}^{(2)}(p,p'). \tag{1.23}$$

The time-evolution equation can be traded for a (physical) momentum evolution equation; see Refs. [54, 84, 85] for details. Since times are defined on the contour $\mathcal{C}$, in the p-representation the correlators and inverse correlators are functions of physical momenta which also take value on a contour $\hat{\mathcal{C}}$ (see figure 1.5).

[5] We define this quantity properly in the following section.



Figure 1.5: Closed path $\hat{\mathcal{C}}$ of the momentum variable $p = -K\eta$. It goes from infinite past $p = +\infty$ (UV) to infinite future $p = 0$ (IR) and back.

1.2.4 Loop expansion

The late time dynamics of light scalar fields in de Sitter, corresponding to infrared (IR) physical momenta, exhibit some nonperturbative features. To discuss these, we start by detailing the (rather successful) tree-level computation and the issues that arise when computing loops. Working with the conformally rescaled field $u = a^{\frac{d-1}{2}}\phi$, the quantization procedure leads to

$$\hat{u}(x) = \int_{\mathbf{K}} \left(u_K(\eta)\hat{a}_{\mathbf{K}} e^{i\mathbf{K}\cdot\mathbf{x}} + u_K^*(\eta)\hat{a}_{\mathbf{K}}^\dagger e^{-i\mathbf{K}\cdot\mathbf{x}} \right), \tag{1.24}$$

with the canonical commutation relation

$$[\hat{a}_{\mathbf{K}}, \hat{a}_{\mathbf{K}'}^\dagger] = (2\pi)^d \delta^{(d)}(\mathbf{K} - \mathbf{K}') \tag{1.25}$$

ensured by the normalization condition:

$$u_K^* u_K' - u_K'^* u_K = -i. \tag{1.26}$$

For a free massless scalar $\Box\phi = 0$, and therefore the mode functions in $D = 3 + 1$ de Sitter space are solution of

$$\left(-\partial_\eta^2 + \frac{2}{\eta^2} - K^2 \right) u_K(\eta) = 0. \tag{1.27}$$

The general solution writes

$$u_K(\eta) = \alpha_K \frac{e^{-iK\eta}}{\sqrt{2K}} \left(1 - \frac{i}{K\eta} \right) + \beta_K \frac{e^{iK\eta}}{\sqrt{2K}} \left(1 + \frac{i}{K\eta} \right), \tag{1.28}$$

where α_K and β_K must be set by initial conditions. The de Sitter isometries imply that these coefficients are independent of K [86]. This is obvious in the p-representation,

$$\hat{u}(p) \equiv \sqrt{K} u_K(\eta), \tag{1.29}$$

where $\hat{u}$ must be a function of $p = -K\eta$ only. The normalization condition (1.26) translates to

$$|\alpha|^2 - |\beta|^2 = 1, \tag{1.30}$$

which is not sufficient to constrain these parameters fully. Transformations of the parameters (α, β) respecting (1.30) are called Bogolyubov transformations; they select a vacuum state among the so-called α-vacua [87]. Indeed, unlike in Minkowski space where the vacuum is defined uniquely by selecting positive frequencies, this condition cannot

be fulfilled at all times in de Sitter space. Selecting an initial vacuum state in the infinite past results in particle creation with respect to this vacuum at later times.

The physical choice is to impose positive frequency for all modes in the infinite past, that is when $p = -K\eta \gg 1$. This means that modes of short wavelength are not sensitive to the space-time curvature. This, in particular, satisfies the so-called Hadamard conditions [88], that is, the short distance behavior of correlators is independent of the curvature and identical to that in Minkowski space. This can be seen as a statement of the equivalence principle for quantum fields. In this regime, the mode function must have the same expression as in flat space:

$$u_K(\eta) \underset{p\gg 1}{\to} \frac{e^{-iK\eta}}{\sqrt{2K}}. \tag{1.31}$$

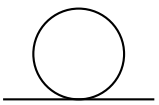
This fixes $\alpha = 1$ and $\beta = 0$. This choice corresponds to the Bunch-Davies vacuum [89], for which the mode function writes

$$u_K(\eta) = \frac{e^{-iK\eta}}{\sqrt{2K}}\left(1 - \frac{i}{K\eta}\right). \tag{1.32}$$

The power spectrum is then computed as

$$\left\langle \hat{\phi}_{\mathbf{K}}(\eta)\hat{\phi}_{\mathbf{K}'}(\eta)\right\rangle = (2\pi)^3\delta^{(3)}(\mathbf{K}+\mathbf{K}')\frac{H^2}{2K^3}(1+K^2\eta^2), \tag{1.33}$$

which can be directly related to scalar fluctuations in the CMB. Extending this analysis to quasi-de Sitter space allows us to link features of the spectrum to the shape of the slow-roll potential. Although observations are very well matched to the tree level analysis, there are open questions in this field that require resummation techniques. Indeed, it is clear from (1.32) that the mode function receives a strong enhancement at low momentum $p \ll 1$, so that loop corrections are infrared divergent. For example, the tadpole in a $\lambda\phi^4$ theory writes:



$$\propto \lambda \int_{\mathbf{K},\mathbf{K}'} \left\langle \hat{\phi}_{\mathbf{K}}(\eta)\hat{\phi}_{\mathbf{K}'}(\eta)\right\rangle \sim \int \frac{d^3K}{K^3}, \tag{1.34}$$

which is logarithmically divergent in the IR. It is interesting to note that the same issue arises in $D = 2$ in flat space-time, where nontrivial physics occur [59]. Here, infrared problems occur in any dimension because the power spectrum (1.33) behaves as K^{-d} in $D = d + 1$ space-time dimensions.

To regulate these divergences in de Sitter space, an infrared cutoff $-K\eta > \mu$ must be introduced. It must act on physical momenta in order to conserve the symmetries of de Sitter space. This generates time-dependent corrections to non-local contributions $\sim \ln\big(a(\eta)\big)$ which also diverge at late times.

Infrared and secular divergences signal the nonperturbative aspect of light fields in de Sitter space. A number of resummation techniques have already been applied to treat them. We give a brief (and incomplete) review of these techniques with some main results.

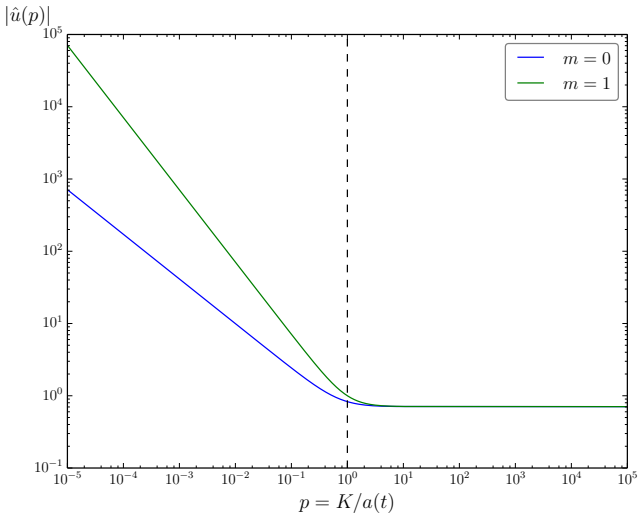


Figure 1.6: One point function of a free field in $D = 3 + 1$ dimensions. In the UV ($p > 1$) the behavior is the same as in flat space ($\hat{u} = \text{const}$ in the p-representation). The IR regime ($p < 1$) exhibits a strong spectral accumulation. The massless case corresponds to $\hat{u} \sim p^{-3/2}$, leading to the infrared divergences discussed in the main text. A non-vanishing mass dampens this spectral accumulation as $p^{-\nu}$ where $\nu = \sqrt{9/4 - m^2}$.

1.2.5 Resummation techniques

Similar nonperturbative issues arise in various instances of QFT, from bosonic fields at high temperature (e.g. quark gluon plasma [90]) to condensed matter systems at a second order phase transition [59] or genuine non equilibrium quantum fields [39–41]. Various nonperturbative or resumption techniques have been developed to tackle IR issues in flat space. In recent years, some efforts have been dedicated to adapting some of these methods to de Sitter space physics. Here, we review some of them. We start with the stochastic approach, which has been developed specifically to de Sitter. We then illustrate large-N and Schwinger-Dyson techniques.

Stochastic approach

The stochastic approach proposed by Starobinsky and Yokoyama in Ref. [43] is based on exploiting the specific aspects of the de Sitter kinematics to write down an effective theory for light fields on superhorizon scales. The idea is to separate the field operator as

$$\hat{\phi}(x) = \varphi(x) + \int_{\mathbf{K}} \theta\big(K - \epsilon a(t)\big)\big[\hat{a}_{\mathbf{K}}\phi_{\mathbf{K}}(t)e^{-i\mathbf{K}\cdot\mathbf{x}} + \hat{a}^{\dagger}_{\mathbf{K}}\phi^{*}_{\mathbf{K}}(t)e^{i\mathbf{K}\cdot\mathbf{x}}\big], \tag{1.35}$$

where ϵ is a small constant. φ contains the long-wavelength contributions, which can be treated as a stochastic variable sourced by the short wavelength modes. The Langevin equation it obeys is derived from the equation of motion $\Box\hat{\phi} + V'(\hat{\phi}) = 0$ after several

simplifications. First, the large-wavelength modes are considered spatially homogenous, so that they depend only on time. Second, this time evolution is slow enough to neglect second order time derivatives[6]. Finally, the UV modes are treated as noninteracting massless fields in the Bunch-Davies vacuum. The evolution of φ is then given by [43,50]

$$\dot{\varphi}(t) + \frac{1}{3}V'(\varphi(t)) = \xi(t), \tag{1.36}$$

where $\xi(t)$ is a stochastic sourcing of IR modes by UV modes. Its correlation properties are given by the massless free mode function, so that it is gaussian with

$$\langle \xi(t)\xi(t')\rangle = \frac{1}{4\pi^2}\delta(t-t'). \tag{1.37}$$

Using standard manipulations, Eq. (1.36) can be turned into the following Focker-Planck equation for the probability distribution $\mathcal{P}(\varphi, t)$ of the stochastic process

$$\partial_t \mathcal{P} = \frac{1}{d}\frac{\partial}{\partial\varphi}\left\{\frac{\partial V_{\rm soft}}{\partial\varphi}\mathcal{P} + \frac{1}{\Omega_4}\frac{\partial\mathcal{P}}{\partial\varphi}\right\}, \tag{1.38}$$

where $\Omega_4 = 8\pi^2/3$ is the volume of the 4−sphere. The latter admits a stationary attractor solution at late times (i.e., in the deep infrared), given by

$$\mathcal{P}(\varphi) \propto \exp\big\{-\Omega_4 V(\varphi)\big\}. \tag{1.39}$$

Equal-time correlation functions on superhorizon scales can then be computed as moments of this distribution. For instance, one has

$$\langle\varphi^2(t)\rangle \underset{t\to\infty}{\to} \frac{\int d\varphi\,\varphi^2\,\mathcal{P}(\varphi)}{\int d\varphi\,\mathcal{P}(\varphi)}. \tag{1.40}$$

A particularly interesting case is when the field is massless and interacting, $V(\varphi) = \lambda\varphi^4$. At late times,

$$\langle\varphi^2\rangle = \frac{\Gamma(3/4)}{4\Gamma(5/4)}\frac{1}{\sqrt{\Omega_4\lambda}}, \tag{1.41}$$

so that a squared mass $\propto\sqrt{\lambda}$ is generated. In particular, this non-analytic result illustrates the nonperturbative nature of infrared modes in de Sitter space.

Large-N resummation

$O(N)$ scalar theories generalize the single field case by considering N fields $\varphi_1\ldots\varphi_N$ with rotational invariance. Of particular interest is the large N limit $N\to\infty$ where a number of approximations become exact. It is possible, for example, to resum all the contributions to the mass in a $\lambda\phi^4$ theory [70]. We start with the bare action

$$S[\varphi] = -\int_x\left\{\phi_a(\Box + m^2)\phi_a + \frac{\lambda}{4!N}(\phi_a\phi_a)^2\right\}, \tag{1.42}$$

[6]This can be generalized to take into account the field derivative $\dot{\varphi}$ as a second independent degree of freedom; see Ref. [91].

where summation over repeated indices is to be understood. The self-consistent mass M is then given by the implicit relation

$$M^2(\phi^2) = m^2 + \frac{\lambda}{6}\phi^2 + \frac{\lambda}{6}F, \tag{1.43}$$

where $\phi_a = \langle\varphi_a\rangle/\sqrt{N}$, and F is the free statistical correlation function at equal points with self-consistent mass M. This effectively resums all tadpole loops which are referred to as super daisy diagrams. In the large-N limit, there are no other contributions to the mass. After appropriate UV renormalization and for weak coupling, this equation becomes:

$$M^2(\phi^2) = a(\phi^2) + \frac{bH^4}{M^2(\phi^2)} \tag{1.44}$$

where a is an affine function and b is a positive constant. We thus get the ϕ-dependent mass,

$$M^2(\phi^2) = a(\phi^2) + \sqrt{a^2(\phi^2) + b} \tag{1.45}$$

which is always positive. Since we have kept the dependency on the average field, this result gives the effective potential through the relation $\partial V_{\text{eff}}/\partial\phi_a = M^2(\phi^2)\phi_a$. The fact that this curvature is always positive indicates the the effective potential is strictly convex, forbidding any spontaneously broken symmetry. Furthermore, a and b are both proportional to λ, so that we recover the same result as in the stochastic approach $M^2 \sim \sqrt{\lambda}$ for a vanishing bare mass.

The stochastic approach and large N techniques illustrate how to resum the infrared divergences in local contributions. We now introduce the Schwinger-Dyson equations as a means to resum non-local contributions with secular divergences.

Schwinger-Dyson equations

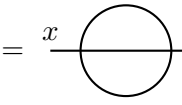
The Schwinger-Dyson equations are a set of relations between the Green's functions of a quantum field theory [92,93]. We summarize here their application to IR dynamics in de Sitter space [55,94]. The inverse propagator can be written as:

$$G^{-1} = G_0^{-1} - \Sigma, \tag{1.46}$$

where $iG_0^{-1}(x,x') = (\Box - M^2)\delta(x,x')$ is the free propagator with resummed mass, and Σ is the non-local self-energy. Convoluting with the full propagator on the right, we get

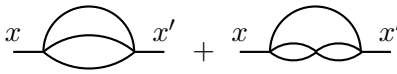
$$(\Box - M^2)G(x,x') - \int_y \Sigma(x,y)G(y,x') = \delta(x,x'). \tag{1.47}$$

This essentially resums the infinite series of self energy insertions. In [55], the authors compute the self-energy at leading order in a $\lambda\phi^4$ theory. It is given by the sunset diagram:

$\Sigma(x,x') =$  $= -\frac{\lambda^2}{6}G_0^3(x,x')$ (1.48)

This is injected in (1.47) and solved exactly in the infrared limit $p, p' \ll 1$. Another possibility is the $1/N$ expansion, where it is possible to resum the infinite series of bubble diagrams [94]:

$$\Sigma(x,x') = \quad + \quad + \dots \tag{1.49}$$



In both cases, the secular divergences of previous perturbative calculations are resummed in a non trivial momentum dependence: the statistical correlator in the p-representation writes

$$\hat{F}(p,p') = c_+ \hat{F}_+(p,p') + c_- \hat{F}_-(p,p'), \tag{1.50}$$

where $\hat{F}_\pm$ are free propagators associated to different masses, and $c_+ + c_- = 1$. Since the free propagator is a power law dependent on the mass (see Fig 1.6), only the contribution $\hat{F}_+$ with the lightest mass contributes deep in the infrared. The difference $c_+ - c_-$ can be seen as a measurement of the non-local corrections to the propagator. For instance, in the limit of weak coupling $c_- \sim \lambda$.

1.3 Non Perturbative Renormalization Group

We now introduce the method that we will be using in this thesis. The Nonperturbative renormalization group (NPRG), also called Functional or Exact RG, is designed to address infrared issues e.g. for statistical systems close to criticality [95]. Because such issues also arise with light scalar fields in de Sitter space, it is of great interest to investigate what information can be obtained by this method. Recent works applying this method have come up with some interesting first results [65, 66]. We make a short presentation here, see [59] for a review and [96–98] for NPRG methods applied to nonequilibrium systems.

1.3.1 Regulated effective action

The NPRG procedure consists in regulating the problematic infrared modes by giving them a large effective mass. This is done by defining the modified action $S_k = S + \Delta S_k$, with

$$\Delta S_k[\varphi] = \frac{1}{2} \int_{x,y} \varphi(x) R_k(x,y) \varphi(y). \tag{1.51}$$

Here, R_k is an IR regulator function that depends on the renormalisation scale k, as well as the momentum p of the modes: this added quadratic term in the action behaves as a large mass term for modes $p < k$, and essentially vanishes for modes above k.

We will give a specific meaning to $R_k(p)$ below. Before, we present the properties that the regulator function must have (see figure 1.7):

- $R_k(p) \underset{p \gg k}{\to} 0$: the infrared regulator leaves the UV modes unaffected.

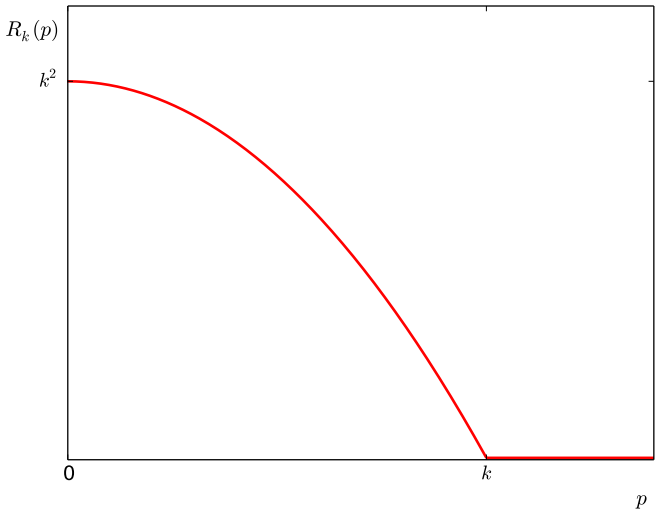


Figure 1.7: Litim [99] regulator $R_k(p) = (k^2 - p^2)\theta(k^2 - p^2)$ as a function of the momentum p. Its purpose is to behave as a large mass $m \sim k$ for modes $p < k$, effectively freezing quantum fluctuations at these scales. The modes $p > k$ are unregulated: these fluctuations are integrated over in the effective action.

- $R_k(p) \underset{p \ll k}{\sim} k^2$: the infrared regulator behaves as a large mass that freezes IR fluctuations.
- $R_k(p) \underset{k \to \infty}{\to} \infty$: all fluctuation modes are frozen by a large mass when the scale is sufficiently large. We will consider this to be effective for k of the order of the UV scale Λ at which the bare action is defined[7].
- $R_k(p) \underset{k \to 0}{\to} 0$: the regulator identically vanishes when the RG scale reaches 0, allowing us to retrieve the full quantum theory.

The goal is to work on the regulated theory, and to lower the RG scale k from Λ to zero in order to progressively integrate out low momentum modes and build the full quantum action of the theory. The generating functional is therefore redefined using the modified action and now also depends on the scale k:

$$Z_k[J] = e^{iW_k[J]} = \int \mathscr{D}\varphi \ \exp\left(iS_k[\varphi] + i\int_x J\varphi\right). \tag{1.52}$$

We could study the variation of this functional with the scale k, but it is preferable to work on the effective action which contains as much information but proves better suited

[7] In statistical physics Λ would typically be related to the microscopic scale of the lattice. In this context however, this scale doesn't necessarily have any meaning other than the initial point of our flow.

for approximation schemes [100]. We define the mean field as

$$\phi(x) \equiv \langle \varphi(x) \rangle_J = \frac{\delta_c W_k}{\delta J(x)}. \tag{1.53}$$

One constructs the regulated effective action by taking the (modified) Legendre transform

$$\Gamma_k[\phi] = W_k[J] - \int_x J\phi - \Delta S_k[\phi], \tag{1.54}$$

where, as usual, the source J_k must be seen as a functional[8] of the mean field ϕ:

$$J_k[\phi](x) = -\frac{\delta_c(\Gamma_k + \Delta S_k)}{\delta\phi(x)}. \tag{1.55}$$

1.3.2 Boundary condition for the effective action

Γ_k is shifted by ΔS_k from the usual effective action for the following purpose: in the UV limit $k \sim \Lambda$, all fluctuation modes are frozen and Γ_Λ is just the classical action S. Let us demonstrate this by taking (1.54) in Eq. (1.52)

$$\exp\left(i\Gamma_k[\phi] + i\Delta S_k[\phi] + i\int_x J_k[\phi]\phi\right) = \int \mathscr{D}\varphi \ \exp\left(iS[\varphi] + i\Delta S_k[\varphi] + i\int_x J_k[\phi]\varphi\right). \tag{1.56}$$

It is tempting to take $\varphi = \phi$ and cancel the functional integral on the right hand side. This is the mean field approximation, in which the fluctuations of the field are neglected. Let us rearrange the previous relation as

$$e^{i\Gamma_k[\phi]} = \int \mathscr{D}\varphi \ e^{iS[\varphi] + i\int_x \Gamma_k^{(1)}(\phi-\varphi)} \exp\left(i\int_{x,y}(\phi-\varphi)(x)R_k(x,y)(\phi-\varphi)(y)\right), \tag{1.57}$$

where (1.55) has been used. Since the regulator behaves like a large mass at $k \sim \Lambda$, all fluctuations are effectively frozen. The second exponential on the right hand side then behaves as a functional Dirac delta

$$\exp\left(i\int_{x,y}(\phi-\varphi)(x)R_k(x,y)(\phi-\varphi)(y)\right) \underset{k\sim\Lambda}{\sim} \delta[\phi-\varphi], \tag{1.58}$$

hence the desired result : $\Gamma_{k\to\Lambda}[\phi] \to S[\phi]$. The mean field approximation is exact in this limit.

On the other hand, when $k \to 0$, the regulator function identically vanishes and $S_k \to S$. Γ_0 is then exactly the Legendre transform of the generating functional W, which is indeed the full quantum action.

[8] Note that as a consequence J_k depends on k.

1.3.3 Flow of the effective action

As we lower k, we take the large modes into account and in the $k \to 0$ limit one retrieves the full quantum action. The transition for k from Λ to 0 is done by computing the variation of Γ_k with k and integrating. The remarkable observation of Wilson [101] is that the variation from $k \to k - \delta k$ can be given in a simple exact form which allows to derive nonperturbative approximation schemes; see also [102]. To find the functional flow equation we derive Eq. (1.54) with respect to k at constant field φ:

$$\partial_\kappa \Gamma_k[\phi]|_\phi = \partial_\kappa W_k[J_k]|_J + \int_x \partial_\kappa J_k|_\phi W_k^{(1)}[J_k] - \int_x \partial_\kappa J_k|_\phi \phi - \partial_\kappa \Delta S_k|_\phi[\phi]. \tag{1.59}$$

The second and third terms cancel out. The first term writes

$$\begin{aligned} \partial_\kappa W_k[J_k]|_J &= e^{-iW_k[J_k]} \int \mathscr{D}\varphi \; \partial_\kappa \Delta S_k|_\varphi[\varphi] \; \exp\left(iS_k[\varphi] + i\int_x J_k\varphi \right) \\ &= \frac{1}{2}\int_{x,y} \partial_\kappa R_k(x,y) \left\langle \varphi(x)\varphi(y) \right\rangle \end{aligned} \tag{1.60}$$

by swapping the functional integral with the two space-time integrals. Notice that the fourth term is simply

$$\partial_\kappa \Delta S_k|_\phi[\phi] = \frac{1}{2}\int_{x,y} \partial_\kappa R_k(x,y)\phi(x)\phi(y) \tag{1.61}$$

$$= \frac{1}{2}\int_{x,y} \partial_\kappa R_k(x,y) \left\langle \varphi(x) \right\rangle \left\langle \varphi(y) \right\rangle . \tag{1.62}$$

By gathering (1.60) and (1.62) we build the regulated connected two-point function. This gives the functional flow equation known as the Wetterich equation [100]:

$$\partial_\kappa \Gamma_k|_\phi[\phi] = \frac{1}{2}\int_{x,y} \partial_\kappa R_k(x,y) G_k(x,y). \tag{1.63}$$

It is more convenient to introduce the flow time $t = \ln k$, and note derivatives with respect to t by $\dot{A} \equiv k\partial_\kappa A$, all other arguments being implicitly held constant. Furthermore, the right hand side can be seen as a trace, leading to the more compact notation:

$$\dot{\Gamma}_k[\phi] = \frac{1}{2}\,\mathrm{Tr}\left[\dot{R}_k G_k\right]. \tag{1.64}$$

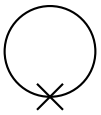
$\dot{\Gamma}_k = \frac{i}{2}$ 

Figure 1.8: Diagrammatic representation of the Wetterich equation (1.63). The full line represents the exact propagator, the cross is $\dot{R}_k$ and the loop stands for the trace integral. This representation leads to flow equations for the complete set of 1PI correlation functions by taking successive field derivatives.

Let us write this equation in a third way by writing the relation between G_k and Γ_k. Deriving (1.53) with respect to $\phi(y)$ we obtain

$$\delta^{(D)}(x-y) = \int_z \frac{\delta J_k(z)}{\delta\phi(y)} W_k^{(2)}(x,z), \tag{1.65}$$

which is to say

$$\int_z \left[\Gamma_k^{(2)}(x,z) + R_k(x,z)\right] G_k(z,y) = i\delta_c^{(D)}(x,y) \tag{1.66}$$

because of (1.13) and (1.55). This standard result of Legendre transformation simply means that $-i[\Gamma_k^{(2)} + R_k]$ is the inverse of the regulated two point correlator in the meaning precised above. Thanks to this and by using the functional property $\delta(\mathrm{Tr}\ln M) = \mathrm{Tr}(M^{-1}\delta M)$ we can write

$$G_k(x,y) = i\frac{\delta}{\delta R_k(x,y)}\,\mathrm{Tr}[\ln(\Gamma_k^{(2)} + R_k)]. \tag{1.67}$$

Replacing in (1.63) we get

$$\dot\Gamma_k[\phi] = \frac{i}{2}\tilde\partial_k\,\mathrm{Tr}[\ln(\Gamma_k^{(2)} + R_k)], \tag{1.68}$$

where

$$\tilde\partial_k \bullet = \int_{x,y} \dot R_k(x,y)\frac{\delta_c \bullet}{\delta R_k(x,y)} \tag{1.69}$$

is a total derivative consisting in deriving with respect to k at fixed $\Gamma_k^{(2)}$, i.e. only in the explicit regulator dependencies. This last expression is reminiscent of first order quantum corrections to the effective action in perturbation theory. We will use this form of the Wetterich equation to compute the flow of the inverse correlator later on.

It is also interesting to read the complexity of this flow: it is a nonlinear functional, integral and partial differential equation! The good news is that it is an exact equation, with a diagrammatic representation as a one-loop structure (see Fig 3.1). There are no known exact solutions however, and we will resort to truncations schemes.

1.3.4 Choosing the regulator

Strictly speaking, the choice of the regulator does not affect the effective action at the end of the flow, but only the path by which we interpolate from $\Gamma_{k=\Lambda} = S$ to $\Gamma_{k=0}$ (see fig. 1.9). That is, the effective action depends on the regulator for intermediate values of k only. In practice, however, we will perform approximations to solve the flow that will result in a dependence of the effective action $\Gamma_{k=0}$ in the choice of our regulator.

Following [65, 66], we choose an infrared regulator of the form

$$\begin{aligned} R_k(x,x') &= -\frac{\delta(\eta-\eta')}{a^D(\eta)}\int \frac{d^dK}{(2\pi)^d} e^{i\mathbf{K}\cdot(\mathbf{x}-\mathbf{x}')} R_k(-K\eta) \\ &= -\delta(t-t')\int \frac{d^dp}{(2\pi)^d} e^{i\mathbf{p}\cdot(\mathbf{X}-\mathbf{X}')} R_k(p). \end{aligned} \tag{1.70}$$

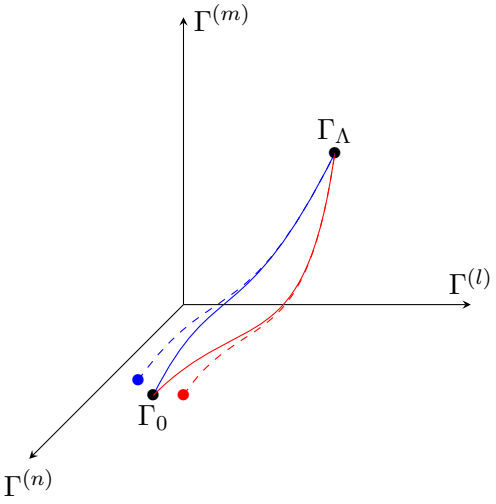


Figure 1.9: RG flow in the theory space of action functionals. Different regulators (red or blue) take the same initial condition to the same effective action through different paths (full lines). Approximations schemes spoil this result and lead to a regulator dependent effective action (dashed lines).

When plugged in Eq. (1.51), one checks that this indeed leads to a momentum-dependent mass term. An important remark is that this only regulates spatial momenta and thus breaks the local Lorentz symmetry of de Sitter space-time. The difficulty of choosing a fully invariant regulator is related to the fact that the distinction between high and low momentum modes is ambiguous in a space with Lorentzian signature. We emphasize though that it is important to regulate physical momenta $p = -K\eta$ in order to keep as many of the de Sitter symmetries as possible [66]. In particular, this guarantees that the affine subgroup of the de Sitter group is left unbroken [84,85] which leads to a consistent[9] truncation of both sides of the flow equation.

We still have to choose the function $R_k(p)$, for which we have much freedom as long as it satisfies the conditions described earlier. It would be optimal to choose a regulator which leads to a least biased effective action in a given approximation scheme. This would require an extensive analysis. Here, our aim is to develop the basis of NPRG methods in de Sitter space and we make the choice of simplicity instead with the Litim-like regulator [99]

$$R_k(p) = (k^2 - p^2)\theta(k^2 - p^2), \tag{1.71}$$

which allow us to perform many computations analytically.

[9] For instance, a regulator on comoving momenta spoils the stationarity of de Sitter space; see Ref. [65].

Conclusion

The early and late universe are characterized by an accelerated expansion. Because to our best knowledge, nature is intrinsically quantum, we are led to study quantum fields in such backgrounds. This is particularly rewarding concerning the inflation era, where light scalar fields can not only source the expansion for a finite time, but also seed the primordial fluctuations that are observed. Unfortunately, the same enhancement of the large scale fluctuations is responsible for infrared and secular divergences in quantum corrections. This signals a breakdown of the perturbative expansion, and requires specific attention.

The topic of quantum fields in de Sitter space can be set up as an out-of-equilibrium problem using the in-in formalism. This enables a formulation in terms of a functional integral, to which we can apply the nonperturbative renormalization group. The first difficulty is to choose a representation for our regulation scheme. Indeed, the time and space-like Killing vectors do not commute in de Sitter space, so that we cannot diagonalize both simultaneously. We have chosen the p-representation, regulating physical momenta and leaving the time-direction unregulated. This breaks part of the de Sitter isometries, with some consequences to be discussed later on.

The resulting flow equation for the effective action admits a universal representation, the Wetterich equation. It is a functional, partial derivative and integral equation. This complexity reflects that of the functional integral encoding the theory, and to extract some information out of it, we must resort to an approximation scheme. In the following chapter, we implement the local potential approximation, which efficiently captures the large scale properties of the theory. This first approximation reproduces a number of results obtained by other methods, and provides some new insights on the physics at hand.

Chapter 2

Flow of the effective potential

Alice: How long is forever? White Rabbit: Sometimes, just one second.
– Lewis Carroll, *Alice in Wonderland*

Contents

2.1 The Local Potential Approximation 22
2.1.1 Two-point correlators 22
2.1.2 Flow of the potential 24
2.2 From subhorizon to superhorizon scales 26
2.2.1 Minkowski regime 26
2.2.2 Infrared regime and dimensional reduction 29
2.3 Equivalent approaches 30
2.3.1 zero-dimensional field theory 30
2.3.2 Relation to the stochastic approach 31
2.3.3 Relation to Euclidean de Sitter space 32
2.4 The large-N limit 33
2.4.1 Generalizing to $O(N)$ theories 34
2.4.2 Flow of a ϕ^4 theory 35
2.4.3 Symmetry restoration 36
2.4.4 Mass (re)generation 40
2.4.5 Correlation length 43
2.5 Finite N 44
2.5.1 Goldstone contributions 44
2.5.2 Convexification 45
Conclusion 48

2.1 The Local Potential Approximation

The functional approach described in the previous chapter is efficient in that the entire information on the physics of the system is encoded in the effective action $\Gamma_{k=0}$. The drawback of this is the cost to retrieve this amount of information : we have already discussed the complexity of the functional flow equation. In the following we shall restrict ourselves to extracting only part of this information, thereby simplifying the flow equation considerably. Specifically, only the infrared sector is interesting[1], the large scale fluctuations being the only ones sensitive to the curvature effects of interest. The modes of wavelength smaller than the curvature radius $1/H$ essentially see a flat space-time and will behave as in Minkowski.

This focus on large wavelength modes means that we are interested in computing the effective action around constant field configurations. As a consequence, the complex structure of this functional may be simplified by dropping space-time derivatives of the field. Furthermore, non-localities can be developed in gradients of the field which can also be dropped at lowest order. The simplest ansatz we can write is therefore

$$\Gamma_k^{LPA}[\phi] = -\int_x \left(V_k(\phi) + \frac{1}{2}\phi\Box\phi \right). \tag{2.1}$$

This is the Local Potential Approximation (LPA). Note that we have kept a kinetic term to maintain the boundary condition $\Gamma_k[\phi] \underset{k\to\infty}{\to} S[\phi]$. At this order in the derivative expansion, we should in principle allow this term to depend on the field and RG scale. We will discuss these improvements in Chapters 3 and 4.

The problem is now to find the flow for V_k, with boundary condition

$$V_k(\phi) \underset{k\to\Lambda}{\to} V(\phi) \tag{2.2}$$

To do this, we must compute both sides of equation (1.63) using the ansatz (2.1) at constant field configuration. The left hand side is simply $-\Omega\dot{V}_k(\phi)$, where $\Omega = \int_x$ is a space-time volume factor. Using the p-representation (1.22), (1.70), the right hand side can be written

$$\frac{1}{2}\,\mathrm{Tr}\left[\dot{R}_k G_k\right] = \frac{1}{2}\Omega \int \frac{d^dp}{(2\pi)^d}\dot{R}_k(p)\frac{\hat{F}_k(p,p)}{p}, \tag{2.3}$$

and the volume factors Ω simplify on both sides as they should. The right-hand side requires the computation of the correlation function, which is defined as the inverse of $\Gamma_k^{(2)} + R_k$ in the LPA ansatz.

2.1.1 Two-point correlators

By taking two covariant derivatives in (2.1) and evaluating at constant field, we get

$$\Gamma_k^{(2)}(\phi, x, x') = -(V_k''(\phi) + \Box_x)\delta(x, x'), \tag{2.4}$$

[1]This is also the case in statistical physics close to criticality, where the focus is on macroscopic physics, e.g. macroscopic magnetization. We shall use it as a guide in devising efficient approximation schemes for our present purposes.

where $\Box_x = \big(-\eta^2\partial_\eta^2 + (D-2)\eta\partial_\eta + \eta^2\nabla_{\mathbf{x}}^2\big)$. After taking a spatial Fourier transform, and with our choice of regulator function, it is straightforward to show that:

$$\big(-V''(\phi) + \Box_{K,\eta} - R(-K\eta)\big)\tilde{G}(K,\eta,\eta') = i\frac{\delta_{\mathcal{C}}(\eta-\eta')}{a^D(\eta)}, \tag{2.5}$$

where $\Box_{K,\eta} = \big(-\eta^2\partial_\eta^2 + (D-2)\eta\partial_\eta - K^2\eta^2\big)$ and the dependency in ϕ is implicit for correlation functions. Moving to the p-representation, we have

$$\left(\partial_p^2 + 1 - \frac{\nu_k^2 - R_k(p) - \frac{1}{4}}{p^2}\right)\hat{G}_k(p,p') = i\delta_{\hat{\mathcal{C}}}(p-p'), \tag{2.6}$$

where

$$\nu_k = \sqrt{\frac{d^2}{4} - V_k''}. \tag{2.7}$$

The delta function on the right hand side is directly related to the time ordering in G_k, while the spectral and statistical correlators (1.16) solve the corresponding homogeneous equation. It is convenient to express the correlators in terms of the mode function:

$$\hat{G}_k(p,p') = T_{\hat{\mathcal{C}}}[\hat{u}_k(p)\hat{u}_k^*(p')], \tag{2.8}$$
$$\hat{F}_k(p,p') = \mathrm{Re}[\hat{u}_k(p)\hat{u}_k^*(p')], \tag{2.9}$$
$$\hat{\rho}_k(p,p') = -2\,\mathrm{Im}[\hat{u}_k(p)\hat{u}_k^*(p')], \tag{2.10}$$

where $\hat{u}_k$ is solution of the homogeneous equation associated to (2.6). For the Litim regulator $R_k(p) = (k^2-p^2)\theta(k^2-p^2)$, this reduces to [65, 66]:

$$p < k, \qquad \Big[\partial_p^2 - \frac{\bar{\nu}_k^2 - \frac{1}{4}}{p^2}\Big]\hat{u}_k(p) = 0, \tag{2.11}$$

$$p > k, \qquad \Big[\partial_p^2 + 1 - \frac{\nu_k^2 - \frac{1}{4}}{p^2}\Big]\hat{u}_k(p) = 0, \tag{2.12}$$

with

$$\bar{\nu}_k^2 = \nu_k^2 - k^2. \tag{2.13}$$

The boundary conditions are imposed by the renormalizability condition, which selects the Bunch-Davies vacuum as the state in the infinite past [89]. For an interacting theory, this state can be quite complicated. To avoid this issue, we define the interacting theory by switching on interactions adiabatically from the infinite past. In this case, we can consider the free Bunch-Davies vacuum as the state in the infinite past $p \to \infty$. It is characterized by the boundary conditions

$$\hat{F}_k(p,p')|_{=p'\to\infty} = \frac{1}{2}, \tag{2.14}$$
$$\partial_p\hat{F}_k(p,p')|_{=p'\to\infty} = 0, \tag{2.15}$$
$$\partial_p\partial_{p'}\hat{F}_k(p,p')|_{=p'\to\infty} = \frac{1}{2}, \tag{2.16}$$

and the solution in terms of the mode function then reads

$$\hat{u}_k(p) = \sqrt{\frac{\pi p}{4}} e^{i\varphi_k} \left[c_k^+ \left(\frac{p}{k}\right)^{\bar{\nu}_k} + c_k^- \left(\frac{k}{p}\right)^{\bar{\nu}_k} \right] \quad \text{for } p \leq k,$$
$$\hat{u}_k(p) = \sqrt{\frac{\pi p}{4}} e^{i\varphi_k} H_{\nu_k}(p) \qquad \text{for } p \geq k, \tag{2.17}$$

where $\varphi_k = \frac{\pi}{2}(\nu_k + 1/2)$, $H_\nu(p)$ is the Hankel function of the first kind, and where the coefficients

$$c_k^\pm = \frac{1}{2}\left[H_{\nu_k}(k) \pm \frac{k}{\bar{\nu}_k} H'_{\nu_k}(k) \right] \tag{2.18}$$

ensure the continuity of $\hat{u}_k(p)$ and of its first derivative at $p = k$. Because we have chosen the Litim regulator, which has a discontinuous first derivative, we see that there is a sharp transition from the unregulated modes ($p > k$) to the regulated ones. This is shown in figure 2.1.

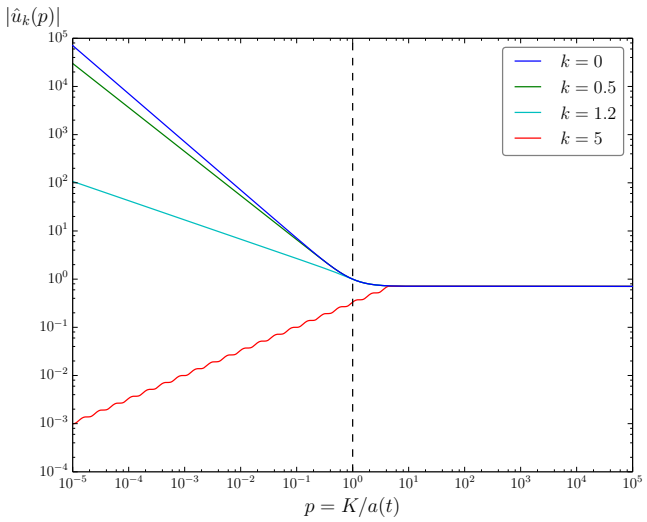


Figure 2.1: Regulated one point function of a massless field[2] in $D = 3 + 1$ dimensions. In the UV ($p > k, H$) the behavior is the same as in flat space (p^0 in the p-representation). In the IR ($p < H$) the unregulated function (in blue) exhibits a strong spectral accumulation. In the presence of a regulator, however, there is a change of power law effective as soon as $p = k$. For large values of the RG scale (in red), $\bar{\nu}_k \in i\mathbb{R}$ and $\hat{u}_k$ is the sum of two imaginary power laws. The dampening saturates and oscillations appear.

2.1.2 Flow of the potential

The potential flow in terms of the one point function is

$$\dot{V}_k = \frac{1}{2} \int \frac{d^d p}{(2\pi)^d} \dot{R}_k(p) \frac{|\hat{u}_k(p)|^2}{p}. \tag{2.19}$$

[2] we have set $V_k'' = 0$ for all these curves. This should not be read as a flow of the one-point function, as we expect mass to be generated as $k \to 0$.

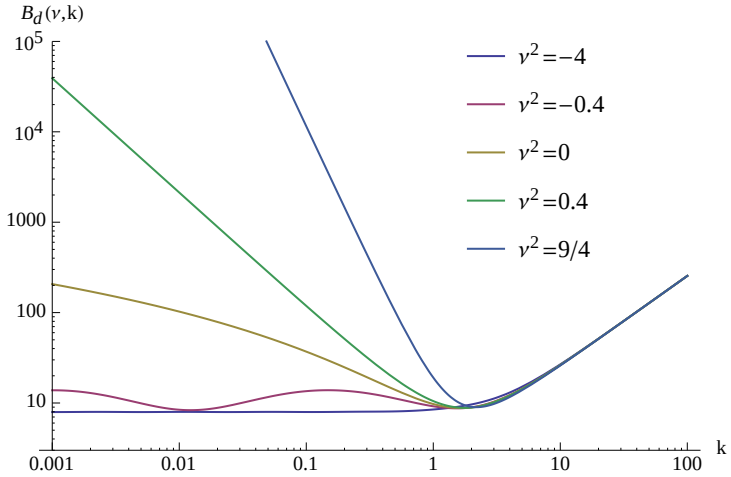


Figure 2.2: The function $B_d(\nu, k)$ [see Eq. (2.21)] in $D = 3 + 1$ dimensions versus k for various (real and imaginary) values of ν. In the UV regime $k \gtrsim 1$ the function $B_d(\nu, k) \sim k$, which reproduces the Minkowski beta function for the potential. Imaginary values of ν correspond to regions of field space where the curvature of the potential $V_k'' > d^2/4$. In that case, the function $B_d(\nu, k)$ shows a bounded oscillatory behavior for $k \lesssim 1$ and it is essentially constant for large field curvatures, $V_k'' \gg d^2/4$. For $\nu = 0$, this turns into a logarithmic behavior, which reflects the gravitational enhancement of superhorizon fluctuations. Finally, real positive values of ν correspond to regions of field space where the curvature of the potential $V_k'' < d^2/4$ and are most sensitive to space-time curvature effects. The logarithmic enhancement is turned into a power law $k^{-2\nu}$.

The momentum integral in Eq. (2.19) can be computed explicitly with the Litim regulator using the expressions (2.17). Indeed, $\dot{R}_k$ ensures that the momenta in the integral are strictly below the RG scale, where the integrand is simply a combination of power laws. In agreement with previous results [65], we obtain the functional beta function for the potential (see appendix B):

$$\dot{V}_k \equiv \beta(V_k'', k) = \frac{C_d\ k^{d+2}}{k^2 + V_k''} B_d(\nu_k, k), \tag{2.20}$$

where $C_d = \pi\Omega_d/[16d(2\pi)^d]$, with $\Omega_d = 2\pi^{d/2}/\Gamma(d/2)$, and where we have defined the function (see Fig. 2.2)

$$B_d(\nu, k) = \frac{\left(d^2 - 2\nu^2 + 2k^2\right)\left|H_\nu(k)\right|^2 + 2k^2\left|H_\nu'(k)\right|^2 - 2dk\,\mathrm{Re}\left[H_\nu^*(k)H_\nu'(k)\right]}{e^{\pi\mathrm{Im}(\nu)}}. \tag{2.21}$$

We stress that we keep the full field dependency on both sides of (2.20), although not written explicitly for simplicity. This is therefore a functional flow.

Let us discuss the structure of the β-function (2.20). We have purposefully expressed it as a product involving $B_d(\nu, k)$, because setting B_d to a constant allows us to retrieve

the d-dimensional flat space flow[3]. This is a remarkable fact which deserves some attention.

First of all, the de Sitter β-function has the same denominator $k^2 + V_k''$ as the Euclidean flow, although the reason is quite different. In flat space, it is simply the value of the inverse propagator at momentum $p < k$. In de Sitter space, it is the result of integrating a growing and a decaying mode and is therefore a feature of the space-time expansion. This denominator plays a crucial role in the convexification of the potential which we will discuss later.

Second, the dimension of the flow appears to be d instead of $D = d + 1$. This also signals the influence of the external scale H and can be traced back to our choice of regulator (1.70). Indeed, by embracing the p-representation we effectively work with d variables, having absorbed all time dependencies in physical momenta. This is flagrant in Eq. (2.19) where the trace integral is d-dimensional.

With these remarks in mind, we can perceive the factorization of the d-Euclidean flow as a "standard provision" of NPRG. The function $B_d(\nu, k)$ then encodes the non-trivial gravitational modifications to this flow. In the following, we will therefore study the asymptotic regimes of this function and the consequences on the flow.

2.2 From subhorizon to superhorizon scales: The onset of gravitational effects

There are two flowing scales in the game, k and V_k'', along with the constant Hubble scale H. This allows for a number of asymptotic regimes depending on their relative values. We distinguish essentially a Minkowskian regime, where no curvature effects are observed, and a light infrared regime where these effects are maximal.

2.2.1 Minkowski regime

The first case of interest is when all fluctuating modes are effectively heavy in units of the space-time curvature. The latter then ceases to play a role in the flow equation and one expects to find the Minkowski limit. There are several ways to realize this.

Large RG scale

First, the RG scale can be greater than all other scales. Using the asymptotic behavior of the Hankel functions in Eq. (2.21), one finds

$$H_\nu(k) \sim \sqrt{\frac{2}{\pi k}} \exp\{ik - i\frac{\pi}{2}(\nu + 1/2)\} \qquad \text{and} \qquad B_d(\nu, k) \approx \frac{8k}{\pi}. \tag{2.22}$$

The beta function (2.20) takes the following form:

$$\beta(V_k'', k) \approx \frac{8C_d k^D}{\pi}, \tag{2.23}$$

[3]Numerical prefactors are irrelevant to the discussion here, and can be absorbed by a rescaling of the potential and the field which is equivalent to a change of initial conditions.

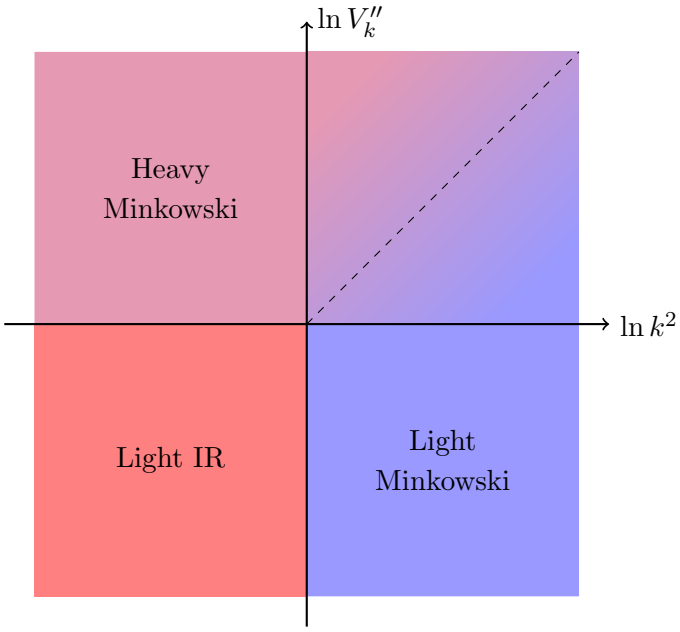


Figure 2.3: Different regimes of the β-function, depending on the relative values of V_k'' and k^2 in units of H. Whenever one of those two scales is large, we observe a flat-space behavior. It can correspond to either a light scenario $k^2 \gg V_k''$ or a heavy scenario $k^2 \ll V_k''$. On the other hand, if both scales are small with respect to H then we fall in the light IR regime where gravitational effects are maximal.

which is identical to that obtained by deriving the flow equation directly in Minkowski space in the limit $k^2 \gg V_k''$ (see chapter 3).

Large potential curvature

The second possibility is for the potential curvature V_k'' to be greater than all other scales[4]. In this case, the index $\nu_k^2 \approx -V_k''$. We then have, for $m \gg k$,

$$H_{im}(k) \sim \sqrt{\frac{2}{\pi m}} \left(\frac{k}{2m}\right)^{im} \exp\{im - i\frac{\pi}{2}(im + 1/2)\} \quad \text{and} \quad B_d(im, k) \approx \frac{8m}{\pi}, \tag{2.24}$$

so that the flow function reduces to

$$\beta(V_k'', k) \approx \frac{8C_d k^{D+1}}{\pi\sqrt{V_k''}}, \tag{2.25}$$

which is the Minkowski beta function in the limit $V_k'' \gg k^2$.

[4]In this discussion we consider only convex regions of the potential $V_k'' > 0$ for simplicity.

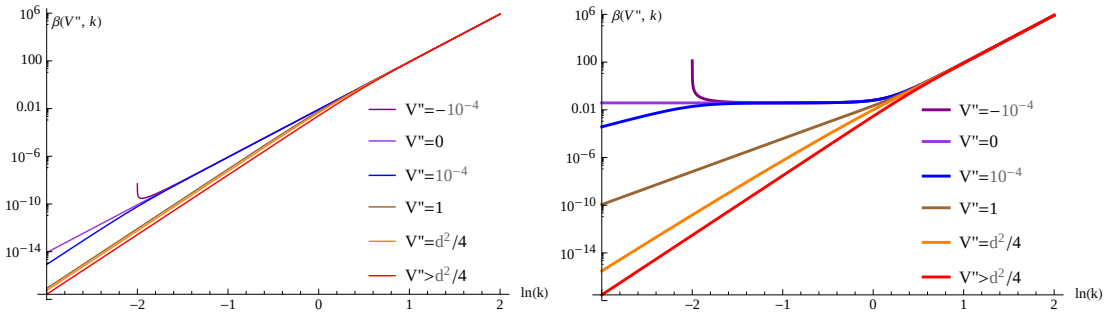


Figure 2.4: The beta function $\beta(V_k'', k)$ of the effective potential as a function of $\ln k$ for different values of the potential curvature V_k'' in Minkowski (left) and de Sitter (right) space-times in $D = 3 + 1$. The de Sitter beta function coincides with the Minkowski one for all values of V_k'' in the regime of subhorizon scales $k \gg 1$ and for all values of k when $V_k'' \gg 1$. Curvature effects become sizable on superhorizon scales for $V_k'' \sim d^2/4$ [see Eq. (2.7)] and the de Sitter beta function is qualitatively different from the Minkowski one for small curvatures of the potential $V_k'' \ll d^2/4$. In particular, its slope is dramatically reduced and even turns to zero for $V_k'' \ll k^2 \ll 1$ as a result of the gravitationally induced amplification of infrared fluctuations. This corresponds to the phenomenon of effective dimensional reduction described in the main text. Also shown is the case of negative potential curvature, for which the beta function diverges as $k^2 \to V_k''$. In such regions of field space, the potential undergoes a strong RG flow which lowers the absolute value of the negative curvature.

General case

The general case can be obtained, when either k or V_k'' are large, using the mixed asymptotic behavior for $m, k \gg 1$:

$$H_{im}(k) \sim \sqrt{\frac{2}{\pi}} \frac{1}{(k^2+m^2)^{\frac{1}{4}}} \exp\left(i\sqrt{k^2+m^2} - im \sinh^{-1}\left(\frac{m}{k}\right) + \frac{m\pi}{2} - i\frac{\pi}{4}\right), \tag{2.26}$$

leading to

$$B_d(\nu, k) \underset{k, V_k'' \gg 1}{\approx} \frac{8\sqrt{k^2+V_k''}}{\pi}. \tag{2.27}$$

The beta function (2.20) thus reads, in the UV regime,

$$\beta\left(V_k'', k\right) \approx \frac{8C_d}{\pi} \frac{k^{d+2}}{\sqrt{k^2+V_k''}}, \tag{2.28}$$

which is identical to the Minkowski beta function. The right-hand side of (2.28) is plotted as a function of the RG scale k for various values of V_k'' in the left panel of Fig. 2.4.

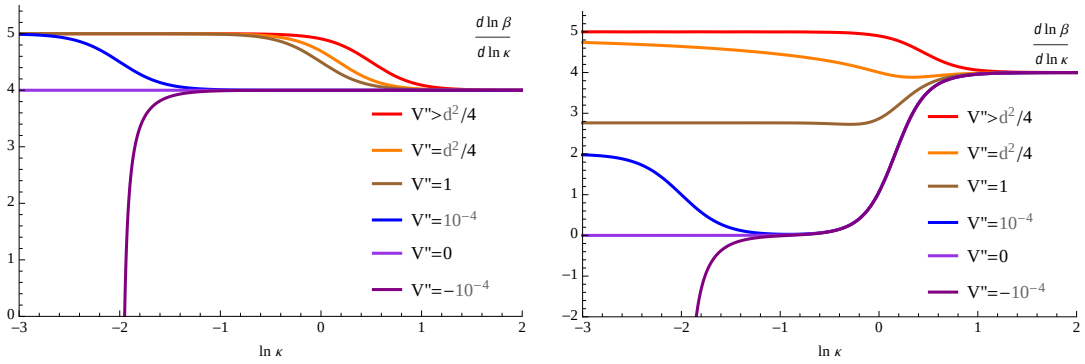


Figure 2.5: The same as Fig. 2.4 but for $k\partial_k \ln \beta(V_k'', k)$. This shows the various power law behaviors in the different regimes of interest for the Minkowski (left) and the de Sitter (right) beta functions. In the former case, one has $\beta \sim k^D$ for $k^2 \gg V_k''$ and $\beta \sim k^{D+1}$ for $k^2 \ll V_k''$. In the latter case, there is an extra dimensionful parameter and the structure is more complex. The Minkowski scaling is reproduced either for $k^2 \gg 1$ or for $V_k'' \gg 1$ but there are strong modifications in the infrared regime $k \ll 1$ for $V_k'' \lesssim d^2/4$. The gravitationally induced logarithmic and power law enhancements (2.29) and (2.31) are clearly visible. The modified power law behavior in the infrared as compared to the flat space-time case results in an effective dimensional reduction up to the zero-dimensional scaling for $V_k'' \ll 1$.

2.2.2 Infrared regime and dimensional reduction

The Minkowski beta function (2.28) receives sizable corrections at superhorizon scales $k \lesssim 1$ when the curvature of the potential $V_k'' \lesssim d^2/4$. This corresponds to ν_k^2 increasing from (large) negative to positive values. For instance, for $V_k'' = d^2/4$ ($\nu_k = 0$), one has

$$B_d(0,k) = \frac{4d^2}{\pi^2} \ln^2\left(\frac{k}{2}\right) - \frac{8d}{\pi^2} \ln\left(\frac{k}{2}\right) + O(k^0). \tag{2.29}$$

This shows a (double) logarithmic enhancement as compared to the Minkowski case in the corresponding regime. This effect gets more dramatic as V_k'' is further decreased (ν_k is further increased to positive values). For $\nu \in R^+$ and $k \lesssim 1$, the Hankel functions behave as

$$H_\nu(k) \sim \frac{\Gamma(\nu)}{i\pi}(2/k)^\nu, \tag{2.30}$$

and we obtain

$$B_d(\nu,k) \underset{k,V_k''\ll 1}{\approx} d(d+2\nu)\frac{\Gamma^2(\nu)}{\pi^2}\left(\frac{2}{k}\right)^{2\nu}\left[1+\mathcal{O}(k^2)\right]. \tag{2.31}$$

The logarithmic enhancement of Eq. (2.29) is turned into a power law $k^{-2\nu}$, which reflects the strong gravitational amplification of infrared fluctuations. In the case of

small potential curvature $|V_k''| \ll 1$, one has $\nu_k \approx d/2$, and the beta function reads

$$\beta\left(V_k'', k\right) \approx \frac{1}{\Omega_{D+1}} \frac{k^2}{k^2 + V_k''}, \tag{2.32}$$

where we used $\Omega_{D+1} = 4\pi^{d/2+1}/[d\Gamma(d/2)]$. The various regimes of the beta function in de Sitter space are illustrated in Fig. 2.4 together with their Minkowski counterparts.

Equation (2.32) reproduces the result of Ref. [66] obtained directly in the infrared limit. As pointed out there, the beta function (2.32) describes an effective Euclidean RG flow in zero space-time dimension.[5] For instance, in the regime $V_k'' \ll k^2 \ll 1$, the flow function $\beta(V_k'', k) \sim k^0$, to be compared to the canonical scaling in D dimensions $\sim k^D$. Below we shall make this statement more precise by showing that the beta function (2.32) describes a RG flow on the D-dimensional sphere S_D, that is, the Euclidean de Sitter space. As a measure of the effective dimensional reduction we show the logarithmic slope of the beta function in the various regimes of interest in Fig. 2.5.

	IR: $k \ll 1$ and $V_k'' \ll 1$	general case	UV: $k \gg 1$ or $V_k'' \gg 1$
$\beta_V =$	$\frac{1}{\Omega_{D+1}} \frac{k^2}{k^2 + V_k''}$	$\frac{C_d k^{d+2}}{k^2 + V_k''} B_d(\nu_k, k)$	$\frac{8C_d}{\pi} \frac{k^{d+2}}{\sqrt{k^2 + V_k''}}$
Interpretation	0-dimensional Euclidean Flow	modified d-dimensional flow	Minkowskian flow (unregulated frequencies)

Table 2.1: β-function in the different regimes.

2.3 Equivalent approaches

The light infrared regime highlights the effects of space-time curvature on the flow. Several other approaches reproduce the same features, and are worth describing.

2.3.1 zero-dimensional field theory

This effective dimensional reduction signals the fact that the solution of the flow equation governed by the beta function (2.32) can be written as an effective zero-dimensional field theory[6]. Indeed, we introduce the following ordinary integral

$$e^{-\Omega_{D+1}\mathcal{W}_k(J)} = \int d\varphi \, e^{-\Omega_{D+1}\left[V_{\rm eff}(\varphi) + J\varphi + \frac{k^2}{2}\varphi^2\right]}, \tag{2.33}$$

where $V_{\rm eff}(\varphi)$ is a function to be specified below. Repeating the steps leading to the Wetterich equation, it is easy to check that the modified Legendre transform

$$V_k(\phi) = \mathcal{W}_k(J) - J\phi - \frac{k^2}{2}\phi^2, \quad \text{with} \quad \frac{\partial \mathcal{W}_k(J)}{\partial J} = \phi, \tag{2.34}$$

[5] A similar dimensional reduction phenomenon has been observed for fermionic degrees of freedom in spaces with constant negative curvature [62, 103].

[6] We thank T. Morris for bringing this to our attention.

satisfies the flow equation (2.32). One can adjust the function $V_{\rm eff}(\varphi)$ so as to produce the appropriate initial conditions[7] for the infrared flow at a scale $k_0 \sim 1$. All solutions of the flow equation in the deep de Sitter regime can thus be written as Eq. (2.33). In particular, it is remarkable that, in this regime, the original D-dimensional Lorentzian theory, with complex weight $\exp(iS)$ eventually flows to a zero-dimensional Euclidean-like integral, with real weight $\exp(-\Omega_{D+1}V_{\rm eff})$.

2.3.2 Relation to the stochastic approach

The phenomenon of dimensional reduction described above is deeply related with the stochastic approach proposed by Starobinsky and Yokoyama in Ref. [43]. We have described in chapter 1 how the superhorizon modes are described by a single degree of freedom with an effective Langevin equation [43, 50]

$$\partial_t \varphi_a(t) + \frac{1}{d}\frac{\partial V_{\rm soft}(\varphi)}{\partial \varphi_a(t)} = \xi_a(t), \tag{2.35}$$

where $V_{\rm soft}(\varphi)$ is the potential seen by the long wavelength modes (see below). The short wavelength modes are responsible for the stochastic sourcing which is delta correlated:

$$\langle \xi_a(t)\xi_b(t')\rangle = \frac{\Gamma(d/2)}{2\pi^{\frac{d}{2}+1}}\delta_{ab}\delta(t-t'). \tag{2.36}$$

Using standard manipulations, Eq. (2.35) can be turned into the following Focker-Planck equation[8] for the probability distribution $\mathcal{P}(\varphi, t)$ of the stochastic process

$$\partial_t \mathcal{P} = \frac{1}{d}\frac{\partial}{\partial\varphi_a}\left\{\frac{\partial V_{\rm soft}}{\partial\varphi_a}\mathcal{P} + \frac{1}{\Omega_{D+1}}\frac{\partial\mathcal{P}}{\partial\varphi_a}\right\}. \tag{2.37}$$

The latter admits an $O(N)$-symmetric stationary attractor solution at late times (i.e., in the deep infrared), given by

$$\mathcal{P}(\varphi) \propto \exp\big\{-\Omega_{D+1}V_{\rm soft}(\varphi)\big\}. \tag{2.38}$$

Equal-time correlation functions on superhorizon scales can then be computed as moments of this distribution. This coincides with the outcome (2.33) of the above RG analysis in the limit $k \to 0$, provided one identifies $V_{\rm soft}(\varphi) = V_{\rm eff}(\varphi) \approx V_{k_0}(\varphi)$. For instance, one has

$$\langle\varphi_a\varphi_b\rangle = \frac{\int d^N\varphi\,\varphi_a\varphi_b\,\mathcal{P}(\varphi)}{\int d^N\varphi\,\mathcal{P}(\varphi)} = \frac{1}{\Omega_{D+1}}\frac{\partial^2\mathcal{W}_{k=0}(J)}{\partial J_a\partial J_b}\bigg|_{J=0}. \tag{2.39}$$

The relevant potential to be used in the stochastic approach is thus not the microscopic one (at the UV scale Λ) but the one evolved down to the horizon scale k_0, which makes perfect physical sense.

The present NPRG approach thus sheds a new light on the basic principles underlying the stochastic approach. Moreover, it clarifies the relation between the stochastic approach and the Euclidean de Sitter approach, as we now discuss.

[7] In the case $N = 1$, one can show that $V_{\rm eff}(\varphi) \approx V_{k_0}(\varphi)$ if $V''_{\rm eff}(\varphi) \ll k_0^2$. For arbitrary N, the inequality should be satisfied by the largest eigenvalue of the curvature matrix $\partial^2 V_{\rm eff}(\varphi)/\partial\varphi_a\partial\varphi_b$.

[8] A correspondance between the Focker-Planck equation and the renormalization group has also been discussed in [104]. There, the authors consider the time evolution as an RG flow, so that the late-time equilibrium corresponds to a fixed point solution.

2.3.3 Relation to Euclidean de Sitter space

Another interesting consequence of the dimensional reduction concerns the relation between Lorentzian and Euclidean de Sitter spaces, the latter being nothing but the D-dimensional sphere S_D. It has been pointed out in [50] that, for what concerns the calculation of static quantities (e.g., equal-time correlators) on superhorizon scales, the nonperturbative physics of the zero mode on the sphere reproduces the results of the stochastic approach. However, the origin of this result has remained unclear.

The present NPRG approach allows us to clarify this point. As we have discussed above, the stochastic approach emerges as the result of the effective dimensional reduction of the RG flow due to the strong enhancement of infrared fluctuations in the Lorentzian case. A similar dimensional reduction takes place in the Euclidean case for more obvious reasons since the sphere is compact.[9] The spectrum of the theory is thus discrete and all heavy modes decouple for scales below the first excited level, leaving the zero mode as the only fluctuating degree of freedom.

The effective dimensional reduction for a scalar field theory ($N = 1$) on the sphere has been studied in detail by means of NPRG techniques in Ref. [64]. There the author finds, employing the LPA and a Litim regulator, that the beta function for the effective potential on length scales larger than the sphere radius exactly reproduces the one obtained in [66] for the Lorentzian theory on superhorizon scales, Eq. (2.32). Below, we provide a short alternative description of the origin of the dimensional reduction on the sphere.

The regularized generating functional for connected correlation functions is given by

$$e^{-\overline{W}_k[J]} = \int \mathcal{D}\varphi \exp\left(-\bar{S}[\varphi] - \Delta\bar{S}_k[\varphi] - \int_x J_a\varphi_a\right), \tag{2.40}$$

where we denote Euclidean quantities by an overall bar (we do not need to be more specific here) and $\int_x$ is the invariant integration on the unit sphere S_D. One decomposes the fields on the discrete basis of eigenfunctions of the corresponding Laplacian operator

$$\varphi(x) = \sum_{\vec{L}} \varphi_{\vec{L}} Y_{\vec{L}}(x), \tag{2.41}$$

where $\vec{L} = (L, L_{D-1}, \ldots, L_1)$ is a vector of integer numbers with $L \geq L_{D-1} \geq \ldots \geq |L_1|$ and where the spherical harmonics satisfy

$$\Box_{S_D} Y_{\vec{L}}(x) = -\lambda_L Y_{\vec{L}}(x), \tag{2.42}$$

with $\lambda_L = L(L + D - 1)$, and are normalized as

$$\int_x Y^*_{\vec{L}}(x) Y_{\vec{L}'}(x) = \delta_{\vec{L},\vec{L}'}. \tag{2.43}$$

[9] Dimensional reduction is spaces with compact dimension has been discussed in [105]. The number of effective dimension is simply given by the number of noncompact dimensions.

The zero mode is the constant $Y_0 = 1/\sqrt{\Omega_{D+1}}$, with Ω_{D+1} the volume of the unit sphere S_D. The infrared regulator in Eq. (2.40) can be written as

$$\Delta\bar{S}_k[\varphi] = \frac{1}{2}\sum_{\vec{L}} \bar{R}_k(L)\,|\varphi_{\vec{L}}|^2, \tag{2.44}$$

where the function $\bar{R}_k(L)$ provides a large effective mass for modes such that $\lambda_L \lesssim k^2$. Because the spectrum is discrete, it is essentially constant for scales below the first nonzero mode $k^2 \lesssim D$. For a potential curvature lower than the first level, $V'' \lesssim D$, and for scales $k^2 \lesssim D$, the nonzero modes effectively behave as heavy modes and decouple in the flow equation. The physics of the zero mode is nonperturbative and must be treated separately [49, 50]. For instance, employing the following regulator[10]

$$\bar{R}_k(L) = \Big(k^2 - \lambda_L\Big)\,\theta\Big(k^2 - \lambda_L\Big), \tag{2.45}$$

one has $\bar{R}_k(L) = k^2\delta_{L,0}$ for $k^2 < D$. Writing the field as

$$\varphi(x) = \bar{\varphi} + \hat{\varphi}(x), \tag{2.46}$$

with $\bar{\varphi} = \varphi_0 Y_0 = \int_x \varphi(x)/\Omega_{D+1}$, we define the generating function for the fluctuations of the zero mode as $\overline{W}_k[J = \text{const.}] = \Omega_{D+1}\overline{\mathcal{W}}_k(J)$, which reads

$$e^{-\Omega_{D+1}\overline{\mathcal{W}}_k(J)} = \int d\bar{\varphi}\, e^{-\Omega_{D+1}\left[\bar{V}_{\text{eff}}(\bar{\varphi}) + \frac{k^2}{2}\bar{\varphi}^2 + J\bar{\varphi}\right]}. \tag{2.47}$$

Here we wrote $\mathcal{D}\varphi = d\bar{\varphi}\mathcal{D}\hat{\varphi}$ and we defined the effective potential for the zero mode as

$$e^{-\Omega_{D+1}\bar{V}_{\text{eff}}(\bar{\varphi})} = \int \mathcal{D}\hat{\varphi}\, e^{-\bar{S}[\varphi]}. \tag{2.48}$$

Equation (2.47) coincides with the Lorentzian result Eq. (2.33)—and thus with the stochastic approach as discussed above—provided one identifies the respective effective potentials V_{eff} and $\bar{V}_{\text{eff}}$.

2.4 The large-N limit

We now discuss the actual RG flow from subhorizon to superhorizon scales. We first consider the limit of a large number of field components, $N \to \infty$, for which the flow equation for the potential is exactly given by the LPA [106] and can be solved analytically in the interesting infrared regime. Furthermore, as we shall see later, the large-N limit correctly captures the qualitative behavior of the finite N case.

[10] Note that, in contrast with the p-represented regulator (1.70) used in Lorentzian signature, the regulator (2.45) respects all the symmetries of S_D.

2.4.1 Generalizing to $O(N)$ theories

It is straightforward to generalize this analysis to N scalar fields with rotational invariance. The two-point functions now have a tensorial structure in the field indices, for example the statistical correlator is

$$F_{ab} \equiv \frac{1}{2} \langle \Omega_J | \{ \hat{\varphi}_a ; \hat{\varphi}_b \} | \Omega_J \rangle \, . \tag{2.49}$$

In our case there will be no explicit symmetry breaking, so that this tensorial structure can be decomposed as

$$F_{ab} = F_L P^L_{ab} + F_T P^T_{ab}, \tag{2.50}$$

where $P^{L,T}$ are the longitudinal and transverse projectors with repost to the background field:

$$P^L_{ab} = \frac{\phi_a \phi_b}{\phi^2}, \qquad P^T_{ab} = \delta_{ab} - \frac{\phi_a \phi_b}{\phi^2}. \tag{2.51}$$

We have noted $\phi^2 = \phi_a \phi_a$ and summation over repeated indices is to be understood. The two statistical correlators $F_{L,T}$ are constructed with the same one-point function (2.17) where V_k'' must be replaced by the longitudinal and transverse components of $V''_{k,ab}$ respectively. Defining

$$V_k(\phi) = N U_k(\rho) \quad \text{with} \quad \rho = \frac{\phi^2}{2N}, \tag{2.52}$$

we find that

$$V''_{ab}(\phi) = U'_k \delta_{ab} + \frac{\phi_a \phi_b}{N} U''_k(\rho). \tag{2.53}$$

The longitudinal and transverse curvatures are therefore

$$m^2_{l,k}(\rho) = U'_k(\rho) + 2\rho U''_k(\rho) \;\; \text{and} \;\; m^2_{t,k}(\rho) = U'_k(\rho). \tag{2.54}$$

The same generalization concerns of course ρ_k and G_k. To generalize the flow equation, the trace on the right hand side of the Wetterich equation must now also be understood on the field indices, so that

$$N \dot{U}_k(\rho) = \frac{1}{2} \int \frac{d^d p}{(2\pi)^d} \dot{R}_{k,ab}(p) \frac{\hat{F}_{k,ab}(p,p)}{p}, \tag{2.55}$$

Choosing a regulator which preserves the symmetry : $R_{k,ab} = R_k \delta_{ab}$, we obtain the trace of $F_{k,ab}$ in the integrand:

$$N \dot{U}_k(\rho) = \frac{1}{2} \int \frac{d^d p}{(2\pi)^d} \dot{R}_{k,ab}(p) \frac{|\hat{u}^L_k(p)|^2 + (N-1)|\hat{u}^T_k(p)|^2}{p} \tag{2.56}$$

$$= \beta \left(m^2_{l,k}, k \right) + (N-1) \beta \left(m^2_{t,k}, k \right), \tag{2.57}$$

with β given by (2.20). The flow of the potential is simply the sum of one longitudinal and $N-1$ transverse components.

Notice that in Eq. (2.52) we have chosen specific scalings in N for the field and the potential. These allow us to properly discuss the large N limit. For $N \to \infty$, only the transverse modes contribute to the flow equation (2.57), which becomes

$$\dot{U}_k(\rho) = \beta\left(U_k'(\rho), k\right), \tag{2.58}$$

with the beta function given by Eqs. (2.20) and (2.21). A standard trick [107, 108] is to rewrite this equation in terms of the function $\rho_k(W)$ defined by the relation[11] $U_k'\big(\rho_k(W)\big) = W$. One thus has

$$\dot{\rho}_k(W) = -\dot{U}_k'(\rho)/U_k''(\rho)|_{\rho=\rho_k(W)} \tag{2.59}$$

as well as $U_k''\big(\rho_k(W)\big)\rho_k'(W) = 1$ and the flow takes the following explicit expression

$$\dot{\rho}_k(W) = -\partial_W \beta(W, k). \tag{2.60}$$

An important property of this flow equation is that, because the k-dependence of the right-hand side is explicit, the coefficients of the Taylor expansion of $\rho_k(W)$ in W, e.g., around $W = 0$, all have independent RG flows.

2.4.2 Flow of a ϕ^4 theory

A typical initial condition at the UV scale $k = \Lambda$ is $U_\Lambda(\rho) = m_\Lambda^2\rho + \lambda_\Lambda\rho^2/2$, that is, $\rho_k(W) = (W - m_\Lambda^2)/\lambda_\Lambda$. Here, the parameter m_Λ^2 can be of any sign and $\lambda_\Lambda \geq 0$. The flow in the UV regime $k \gtrsim 1$ is described by the Minkowski beta function (2.28) and one gets

$$\rho_k(W) = \rho_\Lambda(W) - \frac{4C_d}{\pi}\int_k^\Lambda du \frac{u^{d+1}}{\left(u^2+W\right)^{3/2}}. \tag{2.61}$$

For theories deep in the symmetric phase, where $U_k'(\rho) \gg 1\ \forall \rho \geq 0$, the flow eventually freezes out in the Minkowski regime at a scale $k^2 \sim U_k'(0)$. More interesting are the cases of theories either close to criticality or deep in the broken phase, for which there exists a significant region in field space where[12] $|U_k'(\rho)| \lesssim 1$ down to scales $k \sim 1$. This is the case where we expect important gravitational effects. In the region $W \ll 1$, the Minkowski flow (2.61) reads

$$\rho_k(W) = \frac{W - m_k^2}{\lambda_k} + \mathcal{O}\left(W^2\right), \tag{2.62}$$

[11] This assumes that the function $U_k'(\rho)$ or, equivalently, $\rho_k(W)$, is invertible. It is easy to check that $\dot{\rho}_k(W)$ in Eq. (2.60) is a decreasing function of W: $\dot{\rho}_k'(W) \leq 0$. Here, we shall consider cases where the initial condition at the scale $k = \Lambda$ is a monotonous—thus invertible—function with $\rho_\Lambda'(W) \geq 0\ \forall W$. It follows that $\rho_{k\leq\Lambda}'(W) \geq 0\ \forall W$ and hence the function $\rho_k(W)$ is invertible for all $k \leq \Lambda$.

[12] This stems from the fact that, unlike the interpolating potential $U_k(\rho)$, the regulated potential $U_k(\rho) + R_k(0)\rho$ is a convex function of φ_a [58, 59]. Indeed, it is the Legendre transform of the generating functional (1.52) for constant sources $W[J = \text{const.}]$, which is a convex function of J_a. Note that this assumes that the infrared regulator $R_k(p)$ indeed completely regulates the theory at all scales k. With the regulator (1.71), this implies that a possibly concave region is such that the negative curvature never exceeds the IR cutoff scale: $k^2 + U_k'(\rho) > 0$.

where

$$\frac{m_k^2}{\lambda_k} = \frac{m_\Lambda^2}{\lambda_\Lambda} + \frac{4C_d}{\pi}\frac{\Lambda^{D-2} - k^{D-2}}{D-2}, \tag{2.63}$$

$$\frac{1}{\lambda_k} = \frac{1}{\lambda_\Lambda} + \frac{6C_d}{\pi}\frac{\Lambda^{D-4} - k^{D-4}}{D-4}. \tag{2.64}$$

For infrared scales $k \ll 1$, the flow of the part of the potential where $|U_k'(\rho)| \ll 1$ is described by the dimensionally reduced beta function (2.32) and one gets

$$\rho_k(W) = \rho_{k_0}(W) + \frac{1}{2\Omega_{D+1}}\left\{\frac{1}{k_0^2+W} - \frac{1}{k^2+W}\right\}, \tag{2.65}$$

where $k_0 \sim 1$ denotes the horizon scale. Using the approximate UV flow (2.62) down to the scale k_0, we have $U_{k_0}(\rho) \approx m_{k_0}^2\rho + \lambda_{k_0}\rho^2/2$ and Eq. (2.65) can be rewritten as

$$\left(U_k' + k_0^2\right)\left(U_k' + k^2\right)\left(U_k' - U_{k_0}'\right) = \frac{\lambda_{k_0}}{2\Omega_{D+1}}\left(k_0^2 - k^2\right). \tag{2.66}$$

Under the above assumptions, we have $U_k'(\rho) \ll k_0^2$ in the relevant region of the potential and Eq. (2.66) becomes a second order polynomial equation for U_k' with positive solution

$$U_k'(\rho) = \frac{m_{k_0}^2 + \lambda_{k_0}\rho - k^2}{2} + \sqrt{\left(\frac{m_{k_0}^2 + \lambda_{k_0}\rho + k^2}{2}\right)^2 + \frac{\lambda_{k_0}}{2\Omega_{D+1}}\left(1 - \frac{k^2}{k_0^2}\right)}. \tag{2.67}$$

After integrating over ρ, we find

$$U_k(\rho) + k^2\rho = U_k(0) + \frac{M_k^4(\rho) - M_k^4(0)}{2\lambda_{k_0}} + \frac{1}{2\Omega_{D+1}}\left(1 - \frac{k^2}{k_0^2}\right)\ln\frac{M_k^2(\rho)}{M_k^2(0)}, \tag{2.68}$$

where the curvature term $M_k^2(\rho) = U_k'(\rho) + k^2$ is, as expected, positive all along the infrared flow[13]. This is directly related to the zero-dimensional Euclidean functional, whose Legendre transform $U_k(\rho) + k^2\rho$ is convex.

For $k = 0$, this reproduces the result of Ref. [70], obtained by a direct calculation of the effective potential in the limit $N \to \infty$. We mention that the above result for the running potential in the infrared regime can equivalently be obtained by a direct calculation of the integral (2.33) using standard large-N techniques (see appendix D).

2.4.3 Symmetry restoration

Let us discuss some consequences of the findings from the previous sections. As pointed out in Ref. [66], an important consequence of the effective dimensional reduction of the RG flow in the infrared regime is the fact that any spontaneously broken symmetry gets radiatively restored. This is easily understood from the fact that the generating function of the effective zero-dimensional field theory given by the ordinary integral Eq. (2.33) is analytic and cannot present a spontaneously broken phase. In the limit $N \to \infty$, this

[13] we recall that the expressions (2.67) and (2.68) are valid provided $M_k^2(\rho) \ll 1$.

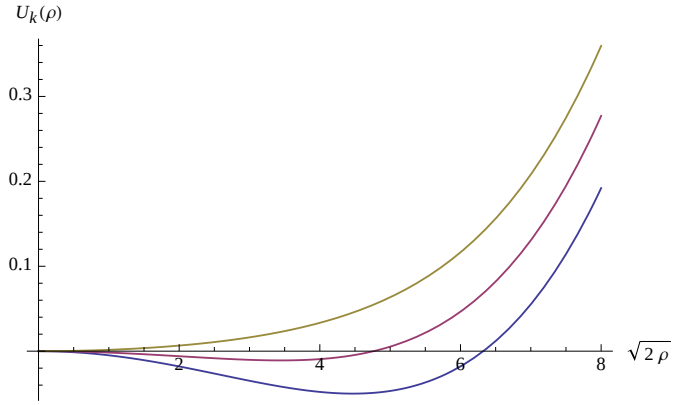


Figure 2.6: The effective potential $U_k(\rho)$ in the limit $N \to \infty$ [see Eq. (2.67)] in $D = 3 + 1$ as a function of the radial variable $\sqrt{2\rho}$ in field space for (from bottom to top) $k = 1, 0.1, 0$. The parameters at the horizon scale $k_0 = 1$ are taken as $m^2_{k_0} = -0.01$, and $\lambda_{k_0} = 0.001$.

phenomenon of symmetry restoration along the flow in the infrared regime can be seen on the exact solution, Eqs. (2.67) and (2.68), as illustrated on Fig. 2.6.

The analysis of Ref. [66] was restricted to the deep infrared regime, where the flow is already dimensionally reduced. Here, we extend this discussion and we consider the complete flow from subhorizon to superhorizon scales. This allows us to study how a possible broken phase in the Minkowski regime gets restored once gravitational effects become important in the infrared regime. We follow the flow of the minimum $\bar{\rho}_k$ of the potential, defined as $U'_k(\bar{\rho}_k) = 0$ or, equivalently, as $\bar{\rho}_k = \rho_k(W = 0)$. As explained above, the RG flow of $\bar{\rho}_k$ is independent of that of other couplings. We have, from Eq. (2.60),

$$\dot{\bar{\rho}}_k = -\,\partial_W \beta(W,k)|_{W=0} \tag{2.69}$$

$$= \frac{\Omega_d}{(2\pi)^d}\frac{\pi}{16d}k^d\left(\frac{B(\nu,k)}{k^2} + \frac{1}{d}\partial_\nu B(\nu,k)\right)_{\nu=d/2} \tag{2.70}$$

The right-hand side can be evaluated in closed form for each dimension d. For this, we give the following result:

$$\begin{aligned}\partial_\nu B_d(\nu,k) = {} & 2d|H_\nu|^2 - 4k\mathrm{Re}[H_\nu H^*_{\nu-1}] + 4(d^2+k^2)\mathrm{Re}[H_\nu \partial_\nu H^*_\nu] \\ & + 4k^2\mathrm{Re}[\partial_\nu H_{\nu-1} H^*_{\nu-1}] - 4kd\mathrm{Re}[\partial_\nu H_\nu H^*_{\nu-1} + H_\nu \partial_\nu H^*_{\nu-1}],\end{aligned} \tag{2.71}$$

where all Hankel functions are evaluated at k.

Case $d = 1$

The relevant funcions are:

$$H_{\frac{1}{2}}(k) = -iH_{-\frac{1}{2}}(k) = -i\sqrt{\frac{2}{\pi k}}e^{ik}, \tag{2.72}$$

$$\partial_\nu H_\nu(k)|_{\nu=\frac{1}{2}} = \sqrt{\frac{2}{\pi k}}\left(-ie^{-ik}\int_{2k}^{\infty}\frac{e^{it}}{t}dt - \frac{\pi}{2}e^{ik}\right), \tag{2.73}$$

$$\partial_\nu H_\nu(k)|_{\nu=-\frac{1}{2}} = \sqrt{\frac{2}{\pi k}}\left(-e^{-ik}\int_{2k}^{\infty}\frac{e^{it}}{t}dt - i\frac{\pi}{2}e^{ik}\right), \tag{2.74}$$

from which we get the flow of the potential minimum:

$$\dot{\bar{\rho}} = \frac{1}{4\pi}\left\{3 + \frac{1}{k^2} + 2g(2k) - 4kf(2k)\right\} \tag{2.75}$$

where the real functions g and f are defined as

$$g(x) + if(x) = \int_0^\infty du\frac{e^{iu}}{u+x} \quad \text{for} \quad x > 0. \tag{2.76}$$

Case $d = 2$

The relevant functions to compute are:

$$\partial_\nu H_\nu(k)|_{\nu=1} = -i\frac{\pi}{2}H_1(k) + \frac{H_0(k)}{k}, \qquad \partial_\nu H_\nu(k)|_{\nu=0} = -i\frac{\pi}{2}H_0(k), \tag{2.77}$$

from which we get

$$\dot{\bar{\rho}} = \frac{1}{32}\left\{\left(2k^2+4\right)|H_1(k)|^2 - k^2|H_0(k)|^2\right\}. \tag{2.78}$$

Case $d = 3$

The relevant functions to compute are:

$$H_{\frac{1}{2}}(k) = -i\sqrt{\frac{2}{\pi k}}e^{ik}, \qquad H_{\frac{3}{2}}(k) = -\sqrt{\frac{2}{\pi k}}\left(1 + \frac{i}{k}\right)e^{ik}, \tag{2.79}$$

and

$$\partial_\nu H_{\frac{3}{2}}(k) = \sqrt{\frac{2}{\pi k}}\left(\left(1 - \frac{i}{k}\right)e^{-ik}\int_{2k}^{\infty}\frac{e^{it}}{t}dt + \left(i - \frac{1}{k}\right)\frac{\pi}{2}e^{ik} - \frac{2i}{k}e^{ik}\right), \tag{2.80}$$

from which we get

$$\dot{\bar{\rho}} = \frac{1}{144\pi^2}\left\{\frac{54}{k^2} + 30 - 2k^2 + g(2k)\big(36 - 64k^2\big) + f(2k)\big(-72k + 16k^3\big)\right\}. \tag{2.81}$$

General case

The functions (2.75, 2.78, 2.81) are plotted in Fig. 2.7 along with their equivalents in Minkowski space. As before, the subhorizon regime is governed by the Minkowski beta function (2.28), which yields, in arbitrary dimension,

$$\dot{\bar{\rho}}_k \approx \frac{4C_d}{\pi} k^{D-2} \quad \text{for} \quad k \gg 1. \tag{2.82}$$

With the asymptotic behaviours

$$x \to \infty : \qquad f(x) \sim \frac{1}{x}, \quad g(x) \sim \frac{1}{x^2}, \quad |H_\nu(x)| \sim \sqrt{\frac{2}{\pi x}} \quad \forall \nu \in \mathbb{R}, \tag{2.83}$$

one easily checks that the functions (2.75, 2.78, 2.81) are indeed given by the above formula in this regime. One sees in Fig. 2.7 that gravitational corrections become significant for $k \sim 1$ and dramatically modify the flow for $k \ll 1$, where the functions (2.75)–(2.81) acquire the same slope in all dimensions. This signals the effective dimensional reduction discussed above. Indeed, inserting the beta function (2.32) in Eq. (2.69), we obtain

$$\dot{\bar{\rho}}_k \approx \frac{1}{\Omega_{D+1} k^2} \quad \text{for} \quad k \ll 1, \tag{2.84}$$

which reproduces the small k behavior of Eqs. (2.75, 2.78, 2.81), given the asymptotic behaviours

$$x \to 0 : \qquad \begin{cases} f(x) \sim \dfrac{\pi}{2}, & g(x) \sim -\ln x, \\ |H_0(x)| \sim \dfrac{2}{\pi} \ln \dfrac{x}{2}, & |H_1(x)| \sim \dfrac{2}{\pi x}. \end{cases} \tag{2.85}$$

In the Minkowski regime, the flow (2.82) integrates to

$$\bar{\rho}_k = \bar{\rho}_\Lambda - \frac{4C_d}{\pi} \frac{\Lambda^{D-2} - k^{D-2}}{D-2} \quad \text{for} \quad 1 \lesssim k \leq \Lambda \tag{2.86}$$

and we recover the following known facts. First, in $D = 2$, the minimum of the potential would reach zero at a finite scale $k = \Lambda \exp(-4\pi\bar{\rho}_\Lambda)$ for any initial condition and the Minkowski theory has no phase of spontaneously broken symmetry. In contrast, in $D > 2$, the Minkowski theory reaches a phase of broken symmetry in the limit $k \to 0$ if $\bar{\rho}_\Lambda > \rho_c = 4C_d\Lambda^{D-2}/[\pi(D-2)]$. For $\bar{\rho}_\Lambda = \rho_c$, the Minkowski theory is critical.

These matters are drastically changed in de Sitter space for $k \lesssim 1$. In that regime, the flow (2.84) integrates to

$$\bar{\rho}_k = \bar{\rho}_{k_0} + \frac{1}{2\Omega_{D+1}} \left(\frac{1}{k_0^2} - \frac{1}{k^2} \right) \quad \text{for} \quad k \leq k_0 \lesssim 1. \tag{2.87}$$

One sees that the minimum of the potential reaches zero at a finite scale so the theory always ends up in the symmetric phase at $k = 0$. The flow of the minimum of the potential is shown in Fig. 2.8 in various dimensions for an initial condition which would result in a broken phase in Minkowski space in both $D = 3$ and $D = 4$. The plain curves

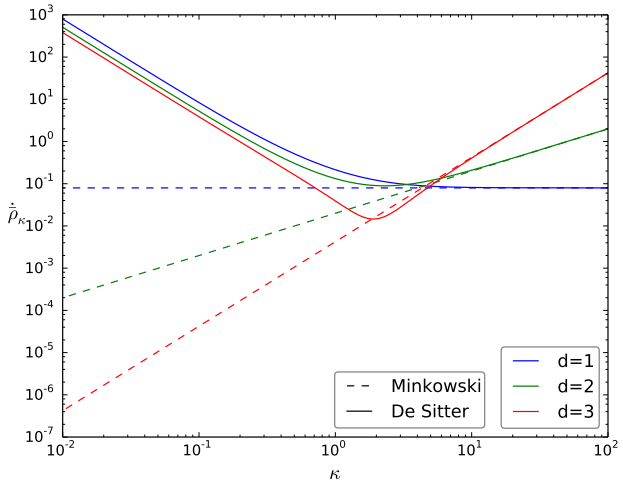


Figure 2.7: The beta functions for the minimum of the potential in the large-N limit in de Sitter (plain lines) and Minkowski (dashed lines) space-times in $D = d + 1$ dimensions. The de Sitter and Minkowski beta functions coincide in the regime of subhorizon scales $k \gg 1$, where they behave as a power law k^{D-2}. Significant deviations occur for scales close to the horizon, $k \sim 1$. As a result of the strong gravitational enhancement of infrared fluctuations, the de Sitter beta functions switch to a common k^{-2} behavior for superhorizon scales, which signals an effective zero-dimensional flow.

are obtained by integrating the complete flow equations (2.75)–(2.81) and are compared to the corresponding flow in Minkowski space. We see that, even in the case $D = 2$, where the Minkowski flow would eventually reach the symmetric phase logarithmically, gravitational effects make a qualitative difference and dramatically speed up symmetry restoration due to the negative power law. Finally, we mention that the result of the numerical integration of Eqs. (2.75)–(2.81) in that case is quantitatively well described by Eqs. (2.86) and (2.87) with a matching point at $k_0 = 1$.

2.4.4 Mass (re)generation

As we have seen previously, a theory with a large mass gap in units of the space-time curvature does not feel any de Sitter effects and is essentially described by the Minkowski flow all the way to the deep infrared. Space-time curvature plays a nontrivial role when there are light excitations $m_{k_0} \lesssim k_0$ at the horizon scale $k_0 \sim 1$. This is the case for theories which are nearly critical ($\bar{\rho}_\Lambda \approx \rho_c$) or in the broken phase ($\bar{\rho}_\Lambda \gtrsim \rho_c$) at subhorizon scales.

We thus consider initial conditions at the UV scale Λ such that $\bar{\rho}_\Lambda \geq \rho_c$. The flow of the minimum of the potential has been described in the previous subsection. As long as it is nonzero, the mass of the transverse Goldstone modes vanish identically $m^2_{t,k} = U'_k(\bar{\rho}_k) = 0$ whereas the mass of the longitudinal mode is given by $m^2_{l,k} = 2\lambda_k \bar{\rho}_k$,

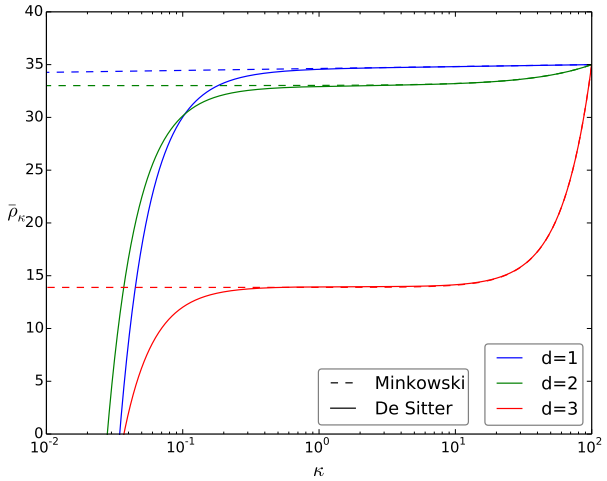


Figure 2.8: The flow of the minimum of the potential in de Sitter (plain lines) and Minkowski (dashed lines) space-times obtained by a direct integration of the beta functions shown in Fig. 2.7. The initial condition $\bar{\rho}_\Lambda$ at the scale $\Lambda = 10^2$ is chosen such that the Minkowski theories in $D > 2$ are in the broken phase. We clearly see the effects of gravitationally amplified infrared modes in de Sitter space which quickly restore the symmetry as soon as $k \lesssim 1$. In the case $D = 2$, the Minkowski flow slowly restores the symmetry with a logarithmic flow. Infrared de Sitter effects lead to a much faster (power law) symmetry restoration.

where $\lambda_k = U_k''(\bar{\rho}_k)$. Once the symmetry gets restored, the minimum of the potential stays at $\bar{\rho}_k = 0$ and the transverse and longitudinal masses become degenerate: $m_{t,k}^2 = m_{l,k}^2 = U_k'(0) \equiv m_k^2$.

The flow of the coupling λ_k in the UV regime is given by Eq. (2.64). In the infrared regime, it can be obtained directly from Eq. (2.65) using $\lambda_k \rho_k'(W = m_{t,k}^2) = 1$:

$$\frac{1}{\lambda_k} = \frac{1}{\lambda_{k_0}} - \frac{1}{2\Omega_{D+1}} \left\{ \frac{1}{\left(k_0^2 + m_{t,k}^2\right)^2} - \frac{1}{\left(k^2 + m_{t,k}^2\right)^2} \right\}. \tag{2.88}$$

Alternatively, it can be computed by evaluating the second derivative of the approximate solution (2.67) for the potential at the minimum. As recalled above, the transverse mass is zero as long as $\bar{\rho}_k \neq 0$. Once the symmetry is restored, the flow of the degenerate mass is obtained from Eq. (2.68) as $m_k^2 = U_k'(0) = M_k^2(0) - k^2$, that is,

$$m_k^2 = \frac{m_{k_0}^2 - k^2}{2} + \sqrt{\left(\frac{m_{k_0}^2 + k^2}{2}\right)^2 + \frac{\lambda_{k_0}}{2\Omega_{D+1}} \left(1 - \frac{k^2}{k_0^2}\right)}. \tag{2.89}$$

In particular, these converge to the final values for $k \to 0$

$$m_{k=0}^2 = \frac{m_{k_0}^2}{2} + \sqrt{\frac{m_{k_0}^4}{4} + \frac{\lambda_{k_0}}{2\Omega_{D+1}}} \tag{2.90}$$

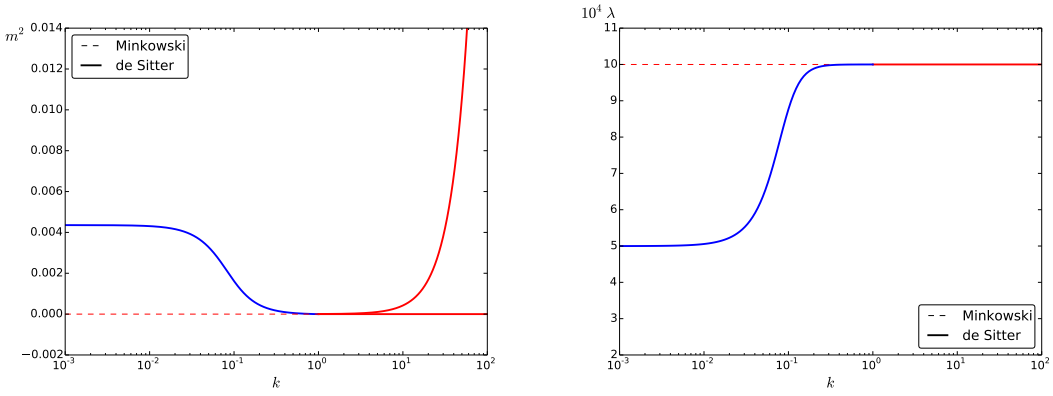


Figure 2.9: Flow of the (would-be) critical theory in $D = 3 + 1$ in the large-N limit (see text). The initial conditions at the scale $\Lambda = 10^2$ are $\rho_\Lambda = \rho_c = 625/(3\pi^2) \approx 21$ and $\lambda_\Lambda = 10^{-3}$. The left panel shows the flow of longitudinal and transverse masses. The transverse Goldstone mass is zero and the longitudinal mass decreases until symmetry restoration at $k = k_0 \sim 1$. For lower scales both masses agree and a nontrivial infrared gap is generated (blue curve). The right panel shows the flow of the coupling constant $\lambda_k = U_k''(\bar{\rho}_k)$. The UV flow is very slow (logarithmic) while we see a rapid transition to the final value $\lambda_{k=0} = \lambda_{k_0}/2 \approx \lambda_\Lambda/2$ in the infrared. In both panels, the dashed lines show the corresponding flows in Minkowski space. The Minkowski theory is critical in that case: the longitudinal and transverse mass vanish at $k = 0$.

and

$$\lambda_{k=0} = \lambda_{k_0} \left(1 + \frac{\lambda_{k_0}}{2\Omega_{D+1} m_{k=0}^4} \right)^{-1}. \tag{2.91}$$

Equation (2.90) reproduces the result of Ref. [70]. The nonanalytic expression of the generated mass and coupling at the scale $k = 0$ in terms of the coupling λ_{k_0} is a signature of the nontrivial infrared physics at work here.

Two cases are of interest. The first one is that of a theory which would be close to critical in Minkowski space, i.e., $\bar{\rho}_\Lambda \approx \rho_c$. In that case, the symmetry gets almost restored already at the horizon scale and the whole infrared flow takes place in the restored symmetry phase. The infrared generated mass and coupling are given by

$$m_{k=0}^2 \approx \sqrt{\frac{\lambda_{k_0}}{2\Omega_{D+1}}} \quad \text{and} \quad \lambda_{k=0} \approx \frac{\lambda_{k_0}}{2}. \tag{2.92}$$

This reproduces the result of the stochastic approach in the large-N limit for the so-called dynamical mass [94]. To quantify the nonperturbative character of the dynamics, we introduce the dimensionless coupling of the dimensionally reduced theory at scale k,

$$\lambda_k^{\text{eff}} \equiv \frac{\lambda_k}{2\Omega_{D+1} m_k^4}. \tag{2.93}$$

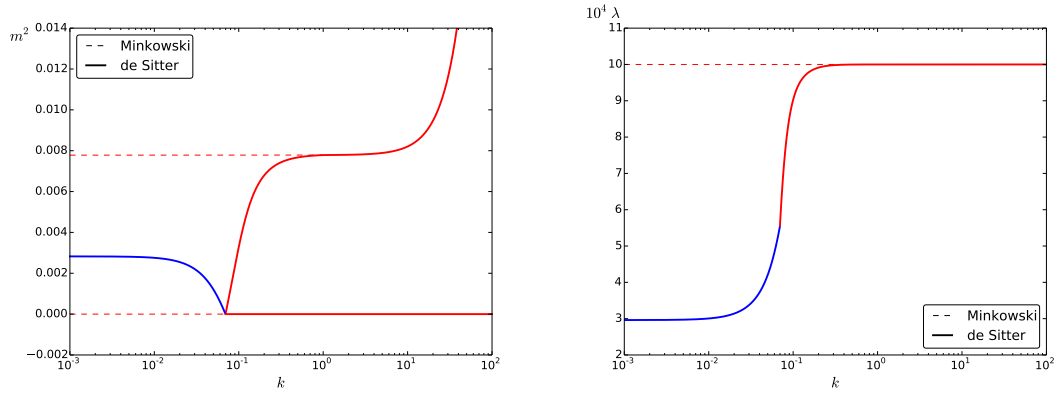


Figure 2.10: Similar to Fig. 2.9 with a UV theory in the broken phase. Here, we chose $\bar{\rho}_\Lambda = 25 > \rho_c$ and $\lambda_\Lambda = 10^{-3}$. The symmetry gets restored deeper in the infrared and the generated mass is thus smaller than in the critical case. The smaller infrared mass implies a smaller infrared coupling as can be seen from Eq. (2.91). The dashed lines show the corresponding flows in Minkowski space. We see that the Minkowski theory is in the broken phase at $k = 0$, with massless Goldstone modes and a massive longitudinal mode.

It is very large at the horizon scale k_0, and of order unity at the end of the flow:

$$\lambda^{\rm eff}_{k=0} = \frac{\lambda_{k=0}}{2\Omega_{D+1} m^4_{k=0}} \approx \frac{1}{2}. \tag{2.94}$$

The other interesting limit is that of a theory which would be deeply in the broken phase in Minkowski space ($\bar{\rho}_\Lambda \gg \rho_c$). In that case, part of the infrared de Sitter flow takes place in the broken phase and the symmetry gets restored in the deep infrared. There remains less RG time to build up a mass and the latter is thus smaller than in the previous critical case. Here, one has $m^2_{k_0} < 0$ and, in the limit where $\lambda^{\rm eff}_{k_0} \ll 1$, we obtain, for the infrared mass and coupling,

$$m^2_{k=0} \approx \lambda^{\rm eff}_{k_0} |m^2_{k_0}| \quad \text{and} \quad \lambda_{k=0} \approx \lambda^{\rm eff}_{k_0} \lambda_{k_0}. \tag{2.95}$$

We note that despite the fact that the effective coupling at the horizon scale $\lambda^{\rm eff}_{k_0} \ll 1$, the resulting zero-dimensional theory is, again, strongly coupled in the deep infrared:

$$\lambda^{\rm eff}_{k=0} = \frac{\lambda_{k=0}}{2\Omega_{D+1} m^4_{k=0}} \approx 1. \tag{2.96}$$

We show in Fig. 2.9 the flow of the longitudinal and transverse masses as well as that of the coupling for the would-be critical theory in $D = 3 + 1$. The case of a theory in the would-be broken phase is shown in Fig. 2.10.

2.4.5 Correlation length

A crucial concept in field theories is the correlation length, which describes the scale at which the system is correlated. In flat space, it is accessed through the exponential

decay of the correlation function, and corresponds to the inverse mass. For a critical theory, the mass is zero and the system is correlated on (infinitely) large scales.

In de Sitter space, it is not obvious that we could generalize this concept; the correlators on large scales are power laws depending on the mass and do not exhibit any exponential decay. We can still define it as the inverse mass by analogy to flat space, and find that it is always finite as we have discussed in the previous section. For a theory which remains in the broken phase in the IR, we have the large N result from (2.95):

$$\frac{1}{m_{k=0}} = \sqrt{4\Omega_{D+1}\bar{\rho}_{k_0}}. \tag{2.97}$$

There is another empirical approach that we may borrow from NPRG in statistical physics: the correlation length should also corresponds to the RG scale at which the symmetry restoration takes place. The idea is that the system finds that it is in the symmetric phase once all fluctuations of scale larger than the correlation length have been integrated on. Indeed, demanding that $\bar{\rho}_{k^*} = 0$ from (2.87), we find that in the large N limit

$$\frac{1}{k^*} = \sqrt{2\Omega_{D+1}\bar{\rho}_{k_0}}, \tag{2.98}$$

which is the same as (2.97) up to a factor of order unity. This is quite remarkable and nurses the idea that concepts of flat space physics can be extended in de Sitter space.

The transition from a Minkowskian regime to a dimensionally reduced flow also tells a story regarding the correlation length. For theories where the symmetry is restored in the Minkowskian regime, everything happens as in flat space; in particular, the correlation length is smaller than the Hubble scale, and the system presents disorder on such scales. For theories that reach the IR regime in the broken phase, the restoration is purely due to the expansion; at the scale of a causal patch, the system is correlated, but at superhorizon scales each patch is uncorrelated from the others, effectively restoring the symmetry. This is illustrated in fig. 2.11.

2.5 Finite N

We now discuss the flow equation (2.57) for N finite. The longitudinal mode plays an increasingly important role as N decreases down to $N = 1$, where there are no transverse modes left. As already discussed, nontrivial gravitational effects occur when the local curvature of the potential at the horizon scale $k_0 \sim 1$ is small, namely, $m^2_{l,k_0}(\rho) \lesssim k_0^2$ and/or $m^2_{t,k_0}(\rho) \lesssim k_0^2$. This is the case for theories which are close to critical or in the broken phase in the UV sense (i.e., theories which would flow toward a critical theory or a broken phase in Minkowski space).

2.5.1 Goldstone contributions

For $N \geq 2$ the condition of small potential curvature in the broken phase is guaranteed by the presence of Goldstone modes, for which $m^2_{t,k} = U'_k(\bar{\rho}_k) = 0$. Indeed, the potential

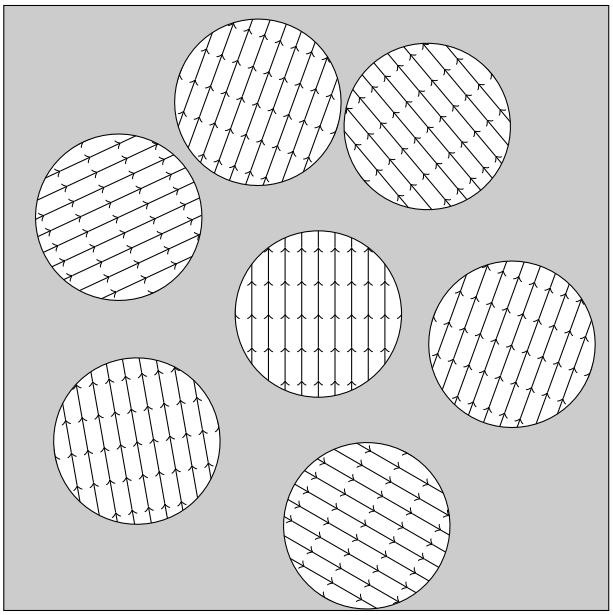


Figure 2.11: Schematic representation of the symmetry restoration on super horizon scales. Even for theories such that the field has an average value on causal (subhorizon) scales, the preferred direction in field space is uncorrelated from one causal patch to another. The symmetry is therefore restored at sufficiently large scale.

minimum defined by this relation has the following flow:

$$\dot{\bar{\rho}}_k = -\frac{\dot{U}'_k(\bar{\rho}_k)}{U''_k(\bar{\rho}_k)}. \tag{2.99}$$

This can be computed directly by deriving the flow function with respect to ρ. In the infrared regime, we find[14]:

$$\dot{\bar{\rho}}_k = \frac{k^2}{N\Omega_{D+1}}\left(\frac{3+g_k}{(k^2+m_k^2)^2}+\frac{N-1}{k^4}\right) \tag{2.100}$$

where $g_k = 2\bar{\rho}_k U_k^{(3)}(\bar{\rho}_k)/U''_k(\bar{\rho}_k)$ and $m_k^2 = m_{t,k}^2(\bar{\rho}_k)$. We see that for $N > 1$, there is still a k^{-2} contribution from the Goldstone modes which ensures symmetry restoration as discussed previously.

2.5.2 Convexification

For $N = 1$, there are no Goldstone contributions and it is not obvious that the potential minimum follows a negative power law. In fact, even for a small mass the flow (2.100)

[14]Here, we have written the flow of the minimum in the case of a small mass $m_k \ll 1$. This is not necessary for this discussion, where we focus on Goldstone contributions, but will be useful in the following section.

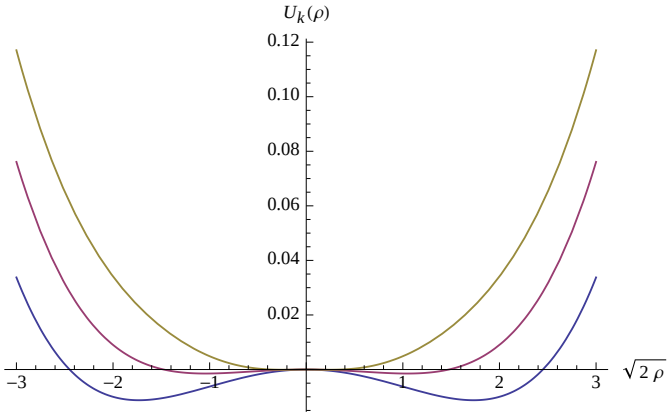


Figure 2.12: The effective potential for the $N = 1$ theory in $D = 3 + 1$ obtained from the complete functional flow equation (2.20) with initial condition $U_\Lambda(\rho) = \lambda_\Lambda(\rho - \bar{\rho}_\Lambda)^2/2$ at the ultraviolet scale $\Lambda = 10$, with $\lambda_\Lambda = 0.01$ and $\bar{\rho}_\Lambda = 1.5$. Curves from bottom to top correspond to $k = 10, 1, 0.1$ One clearly observes the convexification of the potential in the Minkowski regime $k \gtrsim 1$ and the symmetry restoration in the infrared regime $k \lesssim 1$.

describes a non-trivial phase structure for any order in Taylor expansion of the potential. Appendix E shows how taking a polynomial ansatz ($g_k = 0$) results in a line of fixed points. This is an artifact of the Taylor expansion however, and we argue that the dimensional reduction always regenerates the symmetry.

Indeed, there is another mechanism (besides Goldstones modes) which drives the system into the interesting infrared regime, namely the convexification of the potential along the flow [58, 59]. This simply stems from the fact that, if the theory is properly regulated, one has $k^2 + m_{l,k}^2(\rho) > 0$ and $k^2 + m_{t,k}^2(\rho) > 0$ for all scales. In particular, starting the flow in the broken phase at a given ultraviolet scale, the inner region of negative potential curvature between the minima of the potential is brought to a nearly flat profile at the horizon scale, with a (negative) curvature at most of the order of k_0^2. This is a sufficient condition for the flow at superhorizon scales to enter the dimensionally reduced regime mentioned above. We can now conclude by comparing the flow of the inner and outer parts of the potential. The outer part of the potential is by definition convex, its flow is frozen by a positive power law[15] which is at least $\propto k^2$. The inner part necessarily contains an inflection point where the potential flows as $\propto k^0$. Since it will never freeze out, specifically because of the dimensional reduction, there must come a *finite* flow time where the inner region is below the outer region and therefore *strict* convexity is achieved, meaning that the symmetry is restored. A similar discussion can be found in [109], where finite volume/temperature effects also result in a dimensional reduction with the same flow equation.

For $N = 1$, this second convexification mechanism is the only one at work. This is

[15]Specifically, if the local curvature in this region is not small in units of H, but smaller than $d/2$, then the power law is $k^{d+2-2\nu}$. If the mass is larger than $d/2$ then it is as k^{d+2}.

illustrated by numerical integration in Fig. 2.12, where we show the convexification of the potential along the flow in the UV regime and the subsequent symmetry restoration (complete convexification) due to the effective dimensional reduction in the infrared regime[16].

We conclude that the qualitative discussion of the large-N case goes over to finite N: for initial conditions corresponding to the would-be critical or broken phase cases, the flow enters the dimensionally reduced regime in the infrared. It follows that the symmetry gets restored at a finite RG scale and that a nonzero mass is generated. The latter can be exactly computed from the equivalent integral (2.33); see Appendix C. As before, we parametrize the effective potential at the horizon scale as $U_{k_0}(\rho) = m_{k_0}^2\rho + \lambda_{k_0}\rho^2/2$ and we define $\lambda_{k_0}^{\text{eff}} = \lambda_{k_0}/(2\Omega_{D+1}m_{k_0}^4)$.

- For the critical case ($m_{k_0}^2 \approx 0$ and $\lambda_{k_0}^{\text{eff}} \gg 1$), we get

$$m_{k=0}^2 = \mathcal{A}(N)\sqrt{\frac{\lambda_{k_0}}{2\Omega_{D+1}}} \quad \text{and} \quad \frac{\lambda_{k=0}}{\lambda_{k_0}} = \frac{N\mathcal{A}^2(N)}{2}\left(1 - \frac{\mathcal{A}^2(N)}{1+2/N}\right), \tag{2.101}$$

  where we defined[17]

$$\mathcal{A}(N) = \frac{\sqrt{N}}{2}\frac{\Gamma\left(\frac{N}{4}\right)}{\Gamma\left(\frac{N+2}{4}\right)}. \tag{2.102}$$

  In that case, the effective coupling of the dimensionally reduced theory in the infrared is

$$\lambda_{k=0}^{\text{eff}} = \frac{N}{2}\left(1 - \frac{\mathcal{A}^2(N)}{1+2/N}\right) > 0.135. \tag{2.103}$$

  Eq. (2.101) is consistent with the perturbative expansion on Euclidean de Sitter [115].

- In the broken symmetry case ($m_{k_0}^2 < 0$ and $\lambda_{k_0}^{\text{eff}} \ll 1$), we obtain

$$m_{k=0}^2 \approx \lambda_{k_0}^{\text{eff}}|m_{k_0}^2| \quad \text{and} \quad \lambda_{k=0} \approx \frac{N}{N+2}\lambda_{k_0}^{\text{eff}}\lambda_{k_0}, \tag{2.104}$$

  and the effective coupling is

$$\lambda_{k=0}^{\text{eff}} = \frac{N}{N+2} > \frac{1}{3}. \tag{2.105}$$

[16] It is to be mentioned that some studies [110–113] find a possible (de Sitter invariant) broken symmetry phase for finite N. However, for continuous symmetries ($N \geq 2$), the Goldstone modes acquire a nonzero mass, which is rather unphysical. We believe these are artifacts of the various approximation schemes employed in these works. For instance, the Hartree approximation used in Refs. [110–112] is known to produce similar spurious solutions in flat space-time at finite temperature [114].

[17] The large-N results of the previous section are recovered using $\mathcal{A}(N) = 1 + 1/(2N) + \mathcal{O}(N^{-2})$.

Conclusion

We have studied the RG flow of $O(N)$ scalar theories in de Sitter space-time in the Local Potential Approximation. Gravitational effects come into play as one progressively integrates over degrees of freedom from subhorizon to superhorizon momentum scales. At the level of the effective potential, the gravitational enhancement of superhorizon fluctuations results in an effective dimensional reduction of the original D-dimensional Lorentzian action to an effective zero-dimensional Euclidean theory. The latter is equivalent to the late-time equilibrium state of the stochastic approach and to the nonperturbative description of the zero mode on the compact Euclidean de Sitter space. The phenomenon of dimensional reduction thus provides a unifying description of these two approaches and explains their identical results for what concerns the calculation of the effective potential.

This framework provides a number of handles to compute the effective potential, from large N techniques to the equivalent zero-dimensional functional. Using those, we were able to argue that any theory with spontaneous symmetry breaking exhibits radiative restoration in the infrared. Furthermore, we related the effective mass and coupling to the "soft" potential defined at the horizon scale. This is a correction to the stochastic approach, and makes perfect physical sense: the potential for the superhorizon modes in the Langevin equation should already have integrated out the subhorizon modes.

Besides the light infrared regime, we have discussed the heavy UV regime and stated that the flow is then Minkowskian. In the following chapter, we prove this claim by performing a complete flat space analysis. Beyond the de Sitter/Minkowski comparison, this provides a reflexion on the regularization scheme that we have used. To this end, we compute some critical properties of scalar theories and compare them to fully regularized results. Finally, we take this opportunity to introduce the derivative expansion, which generalizes the local potential approximation. We compute the renormalization of the field in a simplified version of the first order derivative expansion, the LPA'. This will serve as a guideline and point of comparison for the same analysis in de Sitter space.

Chapter 3

NPRG in Minkowski space

Normal is an illusion. What is normal for the spider is chaos for the fly.
– Charles Addams, *Drawn and Quartered*

Contents

3.1 Derivative expansion 50
3.1.1 LPA' 50
3.1.2 Flow of the potential 51
3.2 Anomalous dimension 52
3.2.1 Flow of the inverse propagator 52
3.2.2 Flow of Z_k through frequency derivative 54
3.2.3 Flow of Z_k through momentum derivative 55
3.2.4 Critical exponents at the Wilson-Fischer fixed point 56
3.2.5 Concerning regulators 58
3.3 Conclusion 60

The NPRG has been extensively studied in flat Euclidean space with numerous applications to statistical physics, see e.g. [95, 116, 117]. Usual studies employ a regulator which respects all isometries for lack of a reason not to. In this chapter, we are interested in reproducing the limit $H \to 0$ of our de Sitter flow with regulation of spatial momenta only. The Minkowskian analysis we perform is therefore an original one, with prime motivation to complete the discussion on de Sitter space physics. An added value is that this formulation allows us to study flat space RG in Lorentzian signature, which has been little studied in the literature.

This chapter is also an opportunity to improve our approximation scheme. The local potential approximation is placed back in the context of the derivative expansion. We generalize the flow of the potential to include a renormalization of the field, meanwhile reproducing de Sitter results in the limit $H \to 0$. The running of the field raises the issue of broken isometries. As a result, its flow can be computed in two different ways.

With this setup, we study the Wilson-Fischer fixed point in various dimensions. While properties such as the fixed point position depend on the regularization scheme, the value of critical exponents at one loop is universal in some situations. In particular, our approach reproduces these results in the ϵ-expansion. Finally, we discuss the value of the anomalous dimension obtained by our regularization scheme as compared to results in other approaches.

3.1 Derivative expansion

3.1.1 LPA'

The Local Potential Approximation introduced in the previous chapter was based on an expansion of the effective action around constant field configurations. In Minkowsi space, this derivative expansion writes:

$$\Gamma_k[\phi] = -\int_x \big(V_k(\phi) + \frac{Z_k(\phi)}{2}\phi\Box\phi + O(\Box^2)\big), \tag{3.1}$$

where the Laplace-Beltrami operator acting on the field is a small parameter. We stress that all the coefficients of the expansion generally depend both on the RG scale k and the field ϕ. This infinite series must of course be truncated at a finite order. At lowest order, the Local Potential Approximation considers only V_k and a kinetic term to match the bare action at high energy. This is equivalent to setting $Z_k(\phi) = 1$ in the above expression.

To go beyond this approximation, it is necessary to allow for a running of the kinetic term. A frequent approximation scheme is to consider Z_k as a field-independent renormalization parameter. This upgrade of the LPA is often referred to as the LPA'. It captures some interesting features of statistical systems close to criticality at a reduced analytical cost. Indeed, the anomalous dimension

$$\eta \equiv -\left.\frac{\partial \ln Z_k}{\partial \ln k}\right|_{k=0} \tag{3.2}$$

contains some information on the correlation properties of such theories, namely that the propagator is a modified power law [95]

$$G(p) \sim 1/p^{2-\eta}. \tag{3.3}$$

The anomalous dimension is usually small and positive, therefore playing a crucial role in regulating the IR behaviour in this case. Another remarkable case is the Ising model in $d = 2$, $N = 2$. Although the Mermin-Wagner theorem [118] forbids any broken phase for continuous symmetries ($N \geq 2$) with a local order parameter, it is known that there is a phase transition for $N = 2$ governed by topological (non-local) excitations [119]. The LPA' is able to capture the qualitative difference between the $N = 2$ and $N > 2$ cases, the former being characterized by a large anomalous dimension.

3.1.2 Flow of the potential

To reproduce the de Sitter flow in the limit $H \to 0$, we derive the LPA' flow equation for the effective potential in $D = d + 1$ Minkowski space-time using a regulator (on the closed time contour) of the form $R_k(t, t', p) = \delta(t - t')R_k(p)$. Following the procedure outlined in the previous chapter, we get, for $N = 1$ and leaving the field dependence implicit,

$$\dot{V}_k = \frac{1}{2}\int \frac{d^d p}{(2\pi)^d}\dot{R}_k(p)\frac{\left|\chi_k(p,t)\right|^2}{Z_k}, \tag{3.4}$$

where the mode function χ_k is now solution of

$$\left(\partial_t^2 + p^2 + \frac{R_k(p) + V_k''}{Z_k}\right)\chi_k(p,t) = 0. \tag{3.5}$$

The Litim regulator (1.71) must be adapted to the LPA' in order to perform the same advantageous simplifications:

$$R_k(p) = Z_k(k^2 - p^2)\theta(k^2 - p^2), \tag{3.6}$$

leading to the following mode function:

$$\chi_k(p,t) = \frac{e^{-i\omega_k(k)t}}{\sqrt{2\omega_k(k)}} \quad \text{for} \quad p \leq k, \tag{3.7}$$

$$\chi_k(p,t) = \frac{e^{-i\omega_k(p)t}}{\sqrt{2\omega_k(p)}} \quad \text{for} \quad p \geq k, \tag{3.8}$$

where $\omega_k(p) = \sqrt{p^2 + V_k''/Z_k}$, and where we have selected positive frequency solutions in the infinite past corresponding to the Minkowski vacuum. Defining the running anomalous dimension[1] as

$$\eta_k \equiv -\frac{\partial \ln Z_k}{\partial \ln k}, \tag{3.9}$$

[1]The denomination *anomalous dimension* in statistical physics refers to the value of the quantity (3.9) at the end of the flow and at criticality. We use it somewhat loosely here to refer to η_k.

we get

$$\dot{R}_k(p) = Z_k\big[(2-\eta_k)k^2 + \eta_k p^2\big]\theta(k^2-p^2). \tag{3.10}$$

The integrand (3.4) is then a sum of power laws on a finite volume, and the Minkowski flow equation reads

$$\dot{V}_k = \big(1 - \frac{\eta_k}{d+2}\big)\frac{v_d k^{d+2}}{\sqrt{k^2 + V_k''/Z_k}}, \tag{3.11}$$

where $v_d = \Omega_d/[2d(2\pi)^d]$. This result agrees with Eq. (2.28) when $\eta_k = 0$, that is, in the LPA. The flow of the potential is modified by the presence of the anomalous dimension, for which we must find an expression.

3.2 Anomalous dimension

As for the potential, we must provide a prescription for the flow of the field renormalization. In Euclidean signature, the usual prescription writes

$$\eta_k \equiv \partial_{p^2}\dot{\Gamma}_k^{(2)}(p)\Big|_{p^2=0} \tag{3.12}$$

The matter will be slightly different in Lorentzian signature, especially since we have broken the full symmetry due to our choice our regulator. Let us follow this line of thought nonetheless.

3.2.1 Flow of the inverse propagator

Using the LPA' ansatz for the effective action and taking two field derivatives,

$$\tilde{\Gamma}^{(2)}(p,\omega) \equiv \int_C dt'\ e^{i\omega(t-t')}\Gamma^{(2)}(t-t',p) = -[V_k'' + Z_k(-\omega^2+p^2)]. \tag{3.13}$$

The flow of this quantity can be directly derived from the Wetterich equation:

$$\dot{\Gamma}_k[\phi] = \frac{i}{2}\tilde{\partial}_k\big(\operatorname{Tr}\ln(\Gamma_k^{(2)} + R_k)\big), \tag{3.14}$$

$$\dot{\Gamma}_k^{(1)}(x) = \frac{i}{2}\tilde{\partial}_k\int_{a,b}(\Gamma_k^{(2)} + R_k)^{-1}(a,b)\Gamma_k^{(3)}(b,a,x)\big), \tag{3.15}$$

$$\dot{\Gamma}_k^{(2)}(x,y) = \frac{1}{2}\tilde{\partial}_k\int_{a,b}\Big[G_k(a,b)\Gamma_k^{(4)}(b,a,x,y) + i\int_{c,d}G_k(a,b)\Gamma_k^{(3)}(b,c,x)G_k(c,d)\Gamma_k^{(3)}(d,a,y)\Big]. \tag{3.16}$$

The three- and four-point vertex functions in the LPA' are:

$$\Gamma_k^{(3)}(x,y,z) = -V_k^{(3)}(\phi)\delta(x,y)\delta(y,z), \tag{3.17}$$

$$\Gamma_k^{(4)}(w,x,y,z) = -V_k^{(4)}(\phi)\delta(x,y)\delta(y,z)\delta(w,x), \tag{3.18}$$

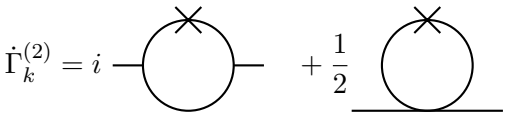


Figure 3.1: Diagrammatic representation for the flow if the inverse correlator. It is governed by 1PI one-loop diagrams, namely the tadpole and sunset contributions. The full line represents the exact propagator, the cross is $\dot{R}_k$ and the loop stands for the trace integral.

After moving to spatial Fourier modes, we get

$$\dot{\Gamma}^{(2)}(p,t-t') = \frac{1}{2}\tilde{\partial}_k\left[-V^{(4)}\int\frac{d^dq}{(2\pi)^d}G(q,t-t')\delta(t-t')+iV^{(3)^2}\int\frac{d^dq}{(2\pi)^d}G(q,t-t')G(p-q,t-t')\right]. \tag{3.19}$$

Frequency modes are obtained by taking the Fourier transform on the closed time path, which gives:

$$\dot{\tilde{\Gamma}}^{(2)}(p,\omega) = \frac{1}{2}\tilde{\partial}_k\int_q\left[-V^{(4)}F(q,t=0)+2V^{(3)^2}\int_{-\infty}^{t}dt'e^{i\omega(t-t')}F(q,t-t')\rho(p-q,t-t')\right] \tag{3.20}$$

Defining the advanced propagator as $G_A(p,t-t') = \rho(p,t-t')\theta(t-t')$ we can complete the time integral and identify the Fourier transform

$$\dot{\tilde{\Gamma}}^{(2)}(p,\omega) = \frac{1}{2}\tilde{\partial}_k\int_Q\big[-V^{(4)}\tilde{F}(q,q_0)+2V^{(3)^2}\tilde{F}(q,q_0)\tilde{G}_A(p-q,\omega-q_0)\big], \tag{3.21}$$

where $\int_Q = \int\frac{d^dqdq_0}{(2\pi)^D}$. The correlators involved are computed from the mode function (3.7–3.8) and found to be:

$$\tilde{F}(q,\omega) = 2\pi\frac{\delta(\omega-\omega_q)+\delta(\omega+\omega_q)}{4Z_k\omega_q}, \qquad \tilde{G}_A(q,\omega) = \frac{1}{Z_k}\frac{1}{(\omega-i\epsilon)^2-\omega_q^2}, \tag{3.22}$$

where

$$\omega_q^2 = q^2+\frac{V_k''+R_k(q)}{Z_k}, \tag{3.23}$$

and the limit $\epsilon\to 0^+$ is understood. There are two remarks concerning this flow in the LPA' ansatz. First, the tadpole contribution $\propto V^{(4)}$ in (3.21) does not depend on the external 4-momentum and therefore does not contribute to the anomalous dimension. Second, the remaining diagram is $\propto V^{(3)^2}$ and therefore vanishes exactly in the symmetric phase. As a consequence, the LPA' is only suited to compute the field renormalization in the broken phase. A better approximation involves $Z_k(\phi)$ as already mentioned.

Isometry breaking

We must now extract the running anomalous dimension from this flow. Notice that the left hand side of (3.21) depends only on the combination ω^2-p^2, but our choice of

regulator breaks this invariance on the right hand side. An ansatz more suited would lead to

$$\tilde{\Gamma}^{(2)}(p,\omega) = -[V_k'' - Z_k^{(\omega)}\omega^2 + Z_k^{(p)}p^2], \tag{3.24}$$

with a regulator $R_k(p) = Z_k^{(p)}(k^2 - p^2)\theta(k^2 - p^2)$ in order to perform the desired cancellations. Following the same steps to get the flow of the potential, we find that

$$\dot{V}_k = \frac{Z_k^{(\omega)}}{Z_k^{(p)}}\left(1 - \frac{\eta_k^{(p)}}{d+2}\right)\frac{v_d k^{d+2}}{\sqrt{k^2 + V_k''/Z_k^{(p)}}}. \tag{3.25}$$

There are two remarks here. First, the occurrences of Z_k and η_k have been replaced by their momentum representant. This suggests that the proper prescription for the anomalous dimension involves the derivation of $\Gamma_k^{(2)}$ with respect to p^2 and not ω^2. The second remark, however, is that a prefactor appears which is the ratio between the two field renormalization. This means that the isometry breaking will have an influence on the LPA' potential flow if these two quantities evolve differently. We should therefore also track the running of $Z_k^{(\omega)}$.

In what follows, we will compute both runnings, although we will not differentiate between $Z_k^{(\omega)}$ and $Z_k^{(p)}$ in the equations. As we will see, it is reasonable to assume that the two quantities are close to each other. Furthermore, we do not wish to focus on the momentum derivative (as suggested above) because it is the least relevant to de Sitter physics. Indeed, as shown in chapter 4, taking a momentum derivative in the equivalent de Sitter space setup fails to isolate the anomalous dimension in the derivative expansion, while it is possible to define a frequency derivative that does so. Computing the frequency derivative of the inverse correlator is therefore also motivated by providing a point of comparison for the $H \to 0$ de Sitter results, as we have done for the flow of the potential.

3.2.2 Flow of Z_k through frequency derivative

Evaluating $\dot{\Gamma}^{(2)}(p,\omega)$ at $p = 0$ yields

$$\dot{V}_k'' - \dot{Z}_k\omega^2 = \frac{1}{2}\tilde{\partial}_k \int_Q \big[- V^{(4)}F(q,q_0) + 2{V^{(3)}}^2 F(q,q_0)G_D(q,\omega - q_0)\big]. \tag{3.26}$$

Let us compute the relevant integrand:

$$\begin{aligned}\int \frac{dq_0}{2\pi}F(q,q_0)G_D(q,\omega - q_0) &= \frac{1}{4Z_k^2\omega_q}\left(\frac{1}{(\omega - \omega_q - i\epsilon)^2 - \omega_q^2} + \frac{1}{(\omega + \omega_q - i\epsilon)^2 - \omega_q^2}\right) \\ &= \frac{1}{2\omega_q Z_k^2}\frac{1}{(\omega - i\epsilon)^2 - 4\omega_q^2}.\end{aligned} \tag{3.27}$$

Therefore, after derivation with respect to ω^2 and taking the frequency (as well as ϵ) to zero, we get

$$\dot{Z}_k = -\frac{{V^{(3)}}^2}{Z_k^2}\tilde{\partial}_k \int_q \frac{1}{32\omega_q^5}. \tag{3.28}$$

Recalling that

$$\tilde{\partial}_k \bullet = \int_q \dot{R}(q) \frac{\delta \bullet}{\delta R(q)}, \tag{3.29}$$

the general expression for any regulator reads

$$\dot{Z}_k = -\frac{5V^{(3)^2}}{64 Z_k^3} \int_q \frac{\dot{R}}{\omega_q^7}. \tag{3.30}$$

The running anomalous dimension with the Litim regulator is therefore

$$\eta_k = \left(1 - \frac{\eta_k}{d+2}\right) \left(\frac{V_k^{(3)}}{Z_k^{3/2}}\right)^2 \frac{5 v_d}{16} \frac{k^{d+2}}{(k^2 + V_k''/Z_k)^{7/2}} \Bigg|_{\phi=\phi_{\min}}. \tag{3.31}$$

3.2.3 Flow of Z_k through momentum derivative

Evaluating $\dot{\Gamma}^{(2)}(p,\omega)$ at $\omega = 0$ yields

$$\dot{V}_k'' + \dot{Z}_k p^2 = \frac{1}{2}\tilde{\partial} \int_Q \left[- V^{(4)} F(q,q_0) + 2V^{(3)^2} F(q,q_0) G_D(p-q,q_0)\right]. \tag{3.32}$$

Let us compute the relevant integrand:

$$\begin{aligned} \int \frac{dq_0}{2\pi} F(q,q_0) G_D(l,q_0) &= \frac{2\pi}{Z_k^2} \frac{1}{4\omega_q} \left(\frac{1}{(\omega_q^2 - i\epsilon)^2 - \omega_l^2} + \frac{1}{(\omega_q^2 + i\epsilon)^2 - \omega_l^2} \right) \\ &= \frac{2\pi}{Z_k^2} \frac{1}{2\omega_q} \frac{\Omega^2}{\Omega^4 + 4\epsilon^2 \omega_q^2}, \end{aligned} \tag{3.33}$$

where $\Omega^2 = \omega_q^2 - \omega_l^2 - \epsilon^2$ and $l = |\mathbf{p} - \mathbf{q}|$. The derivative with respect to p^2 is done using the following identity:

$$\partial_{p^2} \int d^d q f(q) g(|\mathbf{p} - \mathbf{q}|) \Big|_{p=0} = \int d^d q f(q) \big(g'(q) + \frac{2q^2}{d} g''(q) \big), \tag{3.34}$$

where prime denotes a derivative with respect to a momentum squared. We obtain the following expression:

$$\begin{aligned} \dot{Z}_k = \frac{2\pi V^{(3)^2}}{Z_k^2 (2\pi)^d} \tilde{\partial} \int \frac{d^d q}{2\omega_q} \Bigg[&(1 + r_k' + \frac{2q^2}{d} r_k'')(-\frac{1}{A} + \frac{2\Omega^4}{A^2}) \\ &+ \frac{2q^2}{d} \frac{2\Omega^2 (1 + r_k')^2}{A^3} (-3A + 4\Omega^4) \Bigg], \end{aligned} \tag{3.35}$$

where $A = \Omega^4 + 4\epsilon^2 \omega_q^2$ and $r_k = R_k / Z_k$. Having taken $p^2 = 0$ we get that $\Omega^2 = -\epsilon^2$, and it is easy to see that terms in red behave as ϵ^{-2}. Let us check that they cancel out at leading order (that is, taking $A = 4\epsilon^2 \omega_q^2$):

$$\tilde{\partial} \int \frac{d^d q}{\omega_q^3} \left(-(1 + r_k' + \frac{2q^2}{d} r_k'') + \frac{3q^2 (1 + r_k')^2}{d \omega_q^2} \right) = \tilde{\partial} \left[\frac{r' q^d}{\omega_q^3} - \frac{2q^d}{d\omega_q^3} \right]_0^\infty = 0. \tag{3.36}$$

These terms contain ϵ^0 contributions nonetheless, developing $\frac{1}{A} \approx \frac{1}{4\epsilon^2\omega_q^2} - \frac{1}{(4\omega_q^2)^2}$. Taking $\epsilon \to 0$, Eq. (3.35) becomes

$$\dot{Z}_k = \frac{2\pi {V^{(3)}}^2}{Z_k^2(2\pi)^d}\tilde{\partial}\int \frac{d^dq}{2\omega_q}\left[\frac{3}{16\omega_q^4}(1+r_k'+\frac{2q^2}{d}r_k'') - \frac{2q^2}{d}\frac{20(1+r_k')^2}{(4\omega_q^2)^3}\right]. \tag{3.37}$$

Integrating by parts we find

$$\int \frac{d^dq}{2\omega_q}\frac{3}{16\omega_q^4}\frac{2q^2}{d}r_k'' = \int \frac{d^dq}{2\omega_q}\frac{3}{16\omega_q^4}\left(-r_k' + \frac{2q^2}{d}\frac{5r_k'(1+r_k')}{2\omega_q^2}\right). \tag{3.38}$$

After rearranging the terms,

$$\dot{Z}_k = \frac{2\pi {V^{(3)}}^2}{Z_k^2(2\pi)^d}\tilde{\partial}\int \frac{d^dq}{2\omega_q}\left[\frac{3}{16\omega_q^4} + \frac{2q^2}{d}\left(-\frac{15(1+r_k')}{32\omega_q^6} + \frac{5(1+r_k')^2}{16\omega_q^6}\right)\right]. \tag{3.39}$$

The first two terms can be rewritten together as $\propto \tilde{\partial}\int d(q^2)\partial_{q^2}\frac{q^d}{\omega_q^5} = 0$. Finally, we get the general expression for any regulator

$$\dot{Z}_k = \frac{10\pi {V^{(3)}}^2}{16dZ_k^2}\tilde{\partial}\int_q q^2\frac{(1+r_k')^2}{\omega_q^7} \tag{3.40}$$

$$= \frac{10\pi {V^{(3)}}^2}{16dZ_k^3}\int_q q^2\left(\frac{2\dot{R}_k'(1+r_k')}{\omega_q^7} - \frac{5\dot{R}_k(1+r_k')^2}{2\omega_q^9}\right), \tag{3.41}$$

and the running anomalous dimension with the Litim regulator is

$$\eta_k = \left(1-\frac{\eta_k}{d+4}\right)\left(\frac{V_k^{(3)}}{Z_k^{3/2}}\right)^2\frac{5v_d}{4(d+2)}\frac{k^{d+2}}{(k^2+V_k''/Z_k)^{7/2}}\bigg|_{\phi=\phi_{\min}} \tag{3.42}$$

3.2.4 Critical exponents at the Wilson-Fischer fixed point

As we have mentioned several times, the NPRG is a powerful tool to capture critical properties. We illustrate this here by reproducing some properties of the Wilson-Fischer fixed point. The generalization to $N \geq 1$ of the flow of the potential is straightforward; see section 2.4.1. Introducing the $O(N)$ invariant potential

$$V_k(\phi) = NU_k(\rho), \quad \text{with} \quad \rho = \frac{Z_k\phi^2}{2N}, \tag{3.43}$$

the flow $\dot{V}(\phi) = \beta(k, V_k'')$ given by (3.11) generalizes as

$$\dot{V}_k = N(\dot{U}_k - \eta_k\rho U_k') = \beta(k, U_k' + 2\rho U_k'') + (N-1)\beta(k, U_k'). \tag{3.44}$$

To capture the features of the fixed point, it is sufficient to consider a polynomial ansatz

$$U_k(\rho) = \frac{\lambda_k}{2}\left(\rho - \bar{\rho}_k\right)^2. \tag{3.45}$$

In the broken phase ($\bar{\rho}_k > 0$), the parameters $\bar{\rho}_k$ and λ_k are defined as

$$U_k'(\bar{\rho}_k) = 0\,, \quad U_k''(\bar{\rho}_k) = \lambda_k, \tag{3.46}$$

and, therefore, have the following flows:

$$\dot{\bar{\rho}}_k = -\frac{\dot{U}_k'(\bar{\rho})}{U_k''(\bar{\rho})}, \quad \dot{\lambda}_k = \dot{U}_k''(\bar{\rho}_k). \tag{3.47}$$

Using Eq. (3.44), we find

$$\dot{\bar{\rho}}_k = -\eta_k\bar{\rho}_k + \big(1 - \frac{\eta_k}{d+2}\big)\frac{v_d}{2N}k^{d+2}\left[\frac{3}{(k^2 + 2\lambda_k\bar{\rho}_k)^{\frac{3}{2}}} + \frac{N-1}{k^3}\right], \tag{3.48}$$

$$\dot{\lambda}_k = 2\eta_k\lambda_k + \big(1 - \frac{\eta_k}{d+2}\big)\frac{3v_d}{4N}k^{d+2}\lambda_k^2\left[\frac{9}{(k^2 + 2\lambda_k\bar{\rho}_k)^{\frac{5}{2}}} + \frac{N-1}{k^5}\right], \tag{3.49}$$

where $v_d = \Omega_d/[2d(2\pi)^d]$. Introducing the dimensionless parameters

$$r_k = \bar{\rho}_k k^{2-D} \quad \text{and} \quad \ell_k = \lambda_k k^{D-4}, \tag{3.50}$$

we get the autonomous flows

$$\dot{r}_k = (2 - D - \eta_k)r_k + \big(1 - \frac{\eta_k}{d+2}\big)\frac{v_d}{2N}\left[\frac{3}{(1 + 2l_k r_k)^{\frac{3}{2}}} + N - 1\right], \tag{3.51}$$

$$\dot{l}_k = (D - 4 + 2\eta_k)l_k + \big(1 - \frac{\eta_k}{d+2}\big)\frac{3v_d}{4N}l_k^2\left[\frac{9}{(1 + 2l_k r_k)^{\frac{5}{2}}} + N - 1\right], \tag{3.52}$$

along with the expression for the anomalous dimension given either by frequency or by momentum derivative, respectively,

$$\partial_{\omega^2} \to \quad \eta_k = \big(1 - \frac{\eta_k}{d+2}\big)\frac{45v_d l_k^2 r_k}{8(1 + 2l_k r_k)^{7/2}} \tag{3.53}$$

$$\partial_{p^2} \to \quad \eta_k = \big(1 - \frac{\eta_k}{d+4}\big)\frac{45v_d l_k^2 r_k}{2(d+2)(1 + 2l_k r_k)^{7/2}} \tag{3.54}$$

These expressions are only valid for $N = 1$. We do not generalize the anomalous dimension for $N > 1$ here because it is not straightforward and unnecessary to this discussion.

Fixed points are solutions of $\dot{l}_k = \dot{r}_k = 0$. At a fixed point, the theory is critical and the minimum of the potential is a power law k^{D-2} that reaches zero only at the end of the flow. An obvious solution to $\dot{l}_k = 0$ is $l_k = 0$, corresponding to the Gaussian fixed point[2]. We now study the non-trivial Wilson-Fischer fixed point in various dimensions.

[2]The expression (3.51) is incorrect for a Gaussian theory. In this case, $\dot{r}_k = (2 - D)r_k$, and the Gaussian fixed point corresponds to $l = r = 0$.

Dimension $4-\epsilon$

It is interesting to study the Wilson-Fischer fixed point in dimension $D = 4 - \epsilon$ for ϵ small. As is well known, the coupling is of order $\ell_k \sim \mathcal{O}(\epsilon)$, and the anomalous dimension $\eta_k \sim \mathcal{O}(\epsilon^2)$ does not contribute at leading order. We can therefore study this fixed point for any N in perturbation theory. Expanding the flow equations (3.51), (3.52) at leading order in ϵ close to the Wilson-Fisher fixed point, we have

$$\dot{r}_k = -\left(2 - \epsilon + \frac{9v_d}{2N}\ell_k\right) r_k + \frac{v_d(N+2)}{2N} + \mathcal{O}(\epsilon^2) \tag{3.55}$$

$$\dot{\ell}_k = -\epsilon\ell_k + \frac{3v_d(N+8)}{4N}\ell_k^2 + \mathcal{O}(\epsilon^3). \tag{3.56}$$

The fixed point is located at

$$r^* = \frac{v_d(N+2)}{4N} \quad \text{and} \quad \ell^* = \frac{4N\epsilon}{3v_d(N+8)}. \tag{3.57}$$

Critical exponents are obtained from the linearized flow around the fixed point. For instance, the correlation-length exponent ν is obtained as minus the inverse of the smallest (negative) eigenvalue of the Jacobian matrix of the linearized flow [59]. It is particularly interesting to compute since the leading and next-to-leading (one-loop) orders are universal and therefore regulator independent. Here, we get

$$\nu = \frac{1}{2} + \frac{\epsilon}{4}\frac{N+2}{N+8} + O(\epsilon^2), \tag{3.58}$$

which reproduces the well-known perturbative result [95]. For $N = 1$, the fixed point solution (3.57) gives the following results for the anomalous dimension at leading order

$$\eta_k^{\text{freq}} = \frac{5}{54}\epsilon^2, \qquad \eta_k^{\text{mom}} = \frac{4}{54}\epsilon^2. \tag{3.59}$$

It is possible to perform the same analysis in other dimensions, this time including the anomalous dimension in the computation of the fixed point. Table 3.1 sums our findings in dimensions 2,3 and $4 - \epsilon$.

3.2.5 Concerning regulators

The ability to produce a viable flow without regulating frequencies is a remarkable fact which raises some questions. It is obvious that the usual denominator $k^2 + V_k''$, which is crucial to the convexification and symmetry restoration, is affected by unregulated directions. To see this clearly it is interesting to work in the LPA with Euclidean signature and unregulate directions one by one. For any regulator, the general form of the potential flow is

$$\dot{V}_k = \frac{1}{2}\int \frac{d^Dq}{(2\pi)^D}\frac{\dot{R}_k(q)}{q^2 + R_k(q) + V_k''}, \tag{3.60}$$

	$D=2$	$D=3$	$D=4-\epsilon$
momentum derivative	0.508	0.1053	$\frac{4}{54}\epsilon^2$
frequency derivative	no fixed point	0.1047	$\frac{5}{54}\epsilon^2$
best known	$0.25^{(a)}$	$0.0362^{(b)}$	$\frac{1}{54}\epsilon^2$ $^{(c)}$

Table 3.1: Anomalous dimension η for the phase transition of the $\mathcal{Z}_2$ Ising model in dimensions $2, 3$ and ϵ-expansion. We compare our results with the two expressions for the anomalous dimension (frequency or momentum derivative) to best known results. Our approach systematically overestimates by a factor of 2 to 5. While this is not very quantitative, it is still a correct quantitative picture. The only case where we fail to capture the fixed point is in $D = 2$ using the frequency derivative prescription. In this case, the anomalous dimension plays a crucial role in finding a fixed point and is quite large. It is therefore not surprising that the frequency prescription, whose shortcomings we have discussed, could fail. (a) : exact value (b) : Monte Carlo simulation [120] (c) : ϵ-expansion [95].

so that taking $R_k(q) = (k^2 - q^2)\theta(k^2 - q^2)$ yields the usual result:

$$\dot{V}_k = \frac{\Omega_D}{(2\pi)^D} \int_0^k dq \frac{q^{D-1}}{k^2 + V_k''} \tag{3.61}$$

$$= \frac{\Omega_D}{D(2\pi)^D} \frac{k^{D+2}}{k^2 + V_k''} \tag{3.62}$$

To leave one direction unregulated, we replace $q^2 = q_0^2 + \cdots + q_d^2$ by $q_1^2 + \cdots + q_d^2$ in the regulator. Using the same Litim-like regulator, we now get

$$\dot{V}_k = \frac{\Omega_{D-1}}{d(2\pi)^D} \int_0^k dq\, q^{D-2} \int_{-\infty}^{+\infty} dq_0 \frac{k^2}{q_0^2 + k^2 + V_k''} \tag{3.63}$$

$$= \frac{\pi\Omega_{D-1}}{d(2\pi)^D} \frac{k^{D+1}}{\sqrt{k^2 + V_k''}} \tag{3.64}$$

which is precisely the result obtained in Minkowski, see (3.11). This is no surprise as it is possible to pass from one computation to the other by a Wick rotation.

What happens when we leave more directions unregulated? If the same regulator acts on $q_2^2 + \cdots + q_d^2$, the computation becomes

$$\dot{V}_k = \frac{\Omega_{D-2}}{(2\pi)^D} \int_0^k dq\, q^{D-3} \int_{-\infty}^{+\infty} dq_0 \int_{-\infty}^{+\infty} dq_1 \frac{k^2}{q_0^2 + q_1^2 + k^2 + V_k''} \tag{3.65}$$

$$= \frac{\pi\Omega_{D-2} k^D}{(2\pi)^D} \int_0^\infty \frac{du}{u + k^2 + V_k''} \tag{3.66}$$

which is divergent, as could have been expected from dimensional arguments. This result is not specific to the Litim-like regulator; this divergence appears for any form of the regulator function because its asymptotic behaviour is to vanish at large momentum. This result can also be generalized to more unregulated directions, and we conclude that it is not possible to leave more than one space-time direction unregulated.

3.3 Conclusion

Our formalism in de Sitter space has led us to consider an unusual regulation scheme, for which frequencies are unregulated. It is important to study such a scheme in flat space, both to understand the $H \to 0$ limit of our de Sitter expressions and to check wether this indeed regulates the theory in known situations. We have demonstrated here that this scheme admits a valid flat space limit, capable of reproducing qualitative results of scalar theories.

Anticipating on the next chapter of this thesis, we have introduced an extension of the Local Potential Approximation that captures the renormalization of the field. In what follows, we will adapt the derivative expansion to curved space-time and discuss the role of the anomalous dimension in the flow of the potential.

Chapter 4

Beyond the LPA

You're not thinking four-dimensionaly, Marty!
– Christopher Lloyd as Emett Brown, *Back to the future III*

Contents

4.1 Derivative expansion in de Sitter space 62
4.1.1 Derivative couplings in curved space-time 62
4.1.2 Prescription for the anomalous dimension 63
4.1.3 Correlators in the LPA' 65
4.2 Anomalous dimension of a single field 67
4.2.1 General expression 67
4.2.2 Heavy UV regime 70
4.2.3 Light IR regime 71
4.3 Anomalous dimension in $N > 1$ 71
4.3.1 Generalizing to $O(N)$ theories 71
4.3.2 Light IR regime 74
4.4 Influence on the flow of the potential 74
4.4.1 Dimensional reduction and modified RG scale 74
4.4.2 Field expansion 76
Conclusion 78
4.4.3 Heavy UV regime 80
4.5 first order derivative expansion and anomalous dimension in the symmetric phase 81

4.1 Derivative expansion in de Sitter space

In Chapter 3 we described the derivative expansion as an approximation scheme to compute large scale physics. In flat Euclidean space, it writes

$$\Gamma_k[\phi] = \int_x \big(V_k(\phi) + Z_k(\phi)\phi\Delta\phi + O(\Delta^2)\big). \tag{4.1}$$

The point of course is to truncate this series at a finite order. Inserting this ansatz in the Wetterich equation (1.63) we get a closed system of flow equations for our parameters. The zero order term is the local potential, whose flow is defined as

$$\dot{V}_k(\phi) \equiv \frac{1}{\Omega}\dot{\Gamma}_k(\phi), \tag{4.2}$$

where Ω is the volume factor. The second term is the field renormalisation. The flow of its logarithm, referred to as the running anomalous dimension[1], is defined from the two-point vertex function in momentum space as follows:

$$\eta_k(\phi) \equiv -\dot{Z}_k(\phi)/Z_k(\phi) \equiv \frac{1}{Z_k}\partial_{p^2}\dot{\Gamma}_k^{(2)}(\phi, p)\Big|_{p^2=0} \tag{4.3}$$

Our goal in this chapter is to formulate the derivative expansion in curved space-time and adapt the prescription for the running anomalous dimension.

4.1.1 Derivative couplings in curved space-time

A derivative expansion in curved space-time contains many more terms because of possible couplings to the Riemann tensor. The simple ansatz we wish to write is:

$$\Gamma_k[\phi] = -\int_x \left(V_k(\phi) - \frac{Z_k(\phi)}{2}\phi\Box\phi + ...\right), \tag{4.4}$$

where we remind that $\int_x = \int d^D x\sqrt{-g}$ and $\Box = \nabla_\mu\nabla^\mu$ is the Laplace-Beltrami operator. The first point we wish to stress is that all coefficients $V_k, Z_k, \ldots$ now depend also on the local curvature R. This non-trivial result can lead to large contributions that could possibly alter the hierarchy of terms in this expansion. We remind that the effective potential is saturated with such contributions: for example, the generated mass of a ϕ^4 theory is $m^2 \propto H^D\sqrt{\lambda}$.

Furthermore, at the same order in the expansion we should also consider terms such as $f_k(\phi)R_{\mu\nu}\nabla^\mu\nabla^\nu\phi$ which has the same number of derivatives acting on the field, and $g_k(\phi)\nabla_\mu R\nabla^\mu\phi$ which has one derivative fewer. To make matters even more complicated, an apparently fourth order term such as $\nabla_\mu\nabla_\nu\nabla^\mu\nabla^\nu\phi$ is in fact equal to $\Box^2\phi + \frac{1}{2}\nabla_\mu R\nabla^\mu\phi + R^{\mu\nu}\nabla_\mu\nabla_\nu\phi$, and thus appears to contain second and first order contributions.

This serves to show that successive covariant derivatives acting on the field may not build powers of our desired small parameter if we are not careful. In a general curved

[1]The denomination *anomalous dimension* in statistical physics refers to the value of the quantity (4.3) at the end of the flow and at criticality. We use it somewhat loosely here to refer to η_k.

background, it is not surprising that it would prove difficult (if not impossible) to define large scale physics, given the presence of a local curvature scale at every point in space-time. In de Sitter space, this scale is constant and the derivative expansion is not only meaningful but also quite simple. Due to the maximal degree of symmetry, the Riemann tensor is trivially expressed in terms of the metric:

$$R^{\mu\nu} = dH^2 g^{\mu\nu} \quad \text{and} \quad R = d(d+1)H^2. \tag{4.5}$$

The derivative expansion indeed contains only powers of the Laplace-Beltrami operator. For example,

$$\nabla_\mu \nabla_\nu \nabla^\mu \nabla^\nu \phi = \Box^2 \phi + dH^2 \Box \phi, \tag{4.6}$$

which justifies the use of the ansatz (4.4). Even so, since the generators of the space-time isometries do not commute, we will have to build a limit of constant field configurations such that the derivative expansion coincides with a small parameter expansion.

4.1.2 Prescription for the anomalous dimension

To derive a flow equation for the field renormalization generalizing the flat space prescription (4.3), we compute the two point vertex function by taking two covariant field derivatives on the effective action:

$$\Gamma_k^{(2)}[\phi](x,x') = -\big[V_k''(\phi) - Z_k(\phi)\Box_x + O(\Box_x^2)\big]\delta(x,x'). \tag{4.7}$$

After evaluating at constant field and exploiting spatial translation invariance in comoving Fourier space,

$$\Gamma_k^{(2)}(\phi, K, \eta, \eta') = -\Big(V_k''(\phi) - Z_k(\phi)\Box_{\eta,K} + O(\Box_{K,\eta}^2)\Big)\frac{\delta(\eta-\eta')}{a^D(\eta)}, \tag{4.8}$$

where we have noted $\Box_{K,\eta} = -\eta^2\partial_\eta^2 + (d-1)\eta\partial_\eta - K^2\eta^2$. A procedure similar to that in flat space would be to derive this quantity with respect to K^2 and evaluate at $K = 0$, since Z_k is the coefficient in front of the second order term in the derivative expansion. In de Sitter space, however, we have yet to choose a representation which diagonalizes the Laplace-Beltrami operator. Indeed, because the isometry generators do not commute, we see that

$$\Box^2 = (-\partial_t^2 + d\partial_t)^2 - \big\{-\partial_t^2 + d\partial_t; p^2\big\} + p^4 \tag{4.9}$$

contains $p^2 = K^2\eta^2$ terms, where $t = -\ln(-\eta)$ is the cosmological time. Deriving with respect to K^2 at $K = 0$ will therefore fail to isolate the coefficient of $\phi\Box\phi$, capturing instead contributions from all the $\Box^n$ terms. Our approach is therefore to focus on the time direction; taking spatial modes $K = 0$, $\Box = -\partial_t^2 + d\partial_t$ is now diagonalized by (complex) power laws in conformal time

$$\Box_{K=0,\eta}\eta^\omega = \omega(d-\omega)\eta^\omega. \tag{4.10}$$

We therefore define the Laplace-like transform along the time contour:

$$\Gamma_k^{(2)}(\phi,\omega) \equiv \int_{\mathcal{C}} d\eta' a^D(\eta') \left(\frac{\eta'}{\eta}\right)^{\omega} \Gamma_k^{(2)}(K=0,\eta,\eta'), \tag{4.11}$$

with $\omega \in i\mathbb{R}$. A number of comments are in order:

- This operation is directly related to the Fourier transform in Minkowski space in the limit $H \to 0$. Indeed, adding back H explicitly, we have that

$$\eta = -e^{-Ht}, \quad \eta' = -e^{-Ht'} \quad \text{and} \quad \left(\frac{\eta'}{\eta}\right)^{\frac{\omega}{H}} = e^{\omega(t-t')}. \tag{4.12}$$

  The flat space limit then writes

$$\Gamma_k^{(2)}(\phi,\omega) \equiv \int_{\mathcal{C}} dt' e^{\omega(t-t')} \Gamma_k^{(2)}(K=0,t,t'), \tag{4.13}$$

  which is exactly the time Fourier transform (at vanishing spatial momentum) for $\omega \in i\mathbb{R}$.

- The left hand side of Eq. (4.11) does not depend on the time η due to the de Sitter symmetries[2]. Let us check this with the scaling relation[3]

$$\Gamma_k^{(2)}(\alpha K,\eta,\eta') = \alpha^{-d}\Gamma_k^{(2)}(K,\alpha\eta,\alpha\eta'). \tag{4.14}$$

  Injecting it in (4.11), we get that

$$\Gamma_k^{(2)}(\phi,\omega) = \int_{\mathcal{C}} d\eta' \frac{a^D(\eta')}{\alpha^d} \left(\frac{\eta'}{\eta}\right)^{\omega} \Gamma_k^{(2)}(K=0,\alpha\eta,\alpha\eta') \tag{4.15}$$

$$= \int_{\mathcal{C}} d\eta' a^D(\eta') \left(\frac{\eta'}{\alpha\eta}\right)^{\omega} \Gamma_k^{(2)}(K=0,\alpha\eta,\eta') \tag{4.16}$$

  by change of variable $\eta' \to \eta'/\alpha$. It is therefore obvious that rescaling η does not affect this quantity.

- This approach is related to the mode functions constructed in [84]. There, the authors present an alternative to the physical momentum representation by working with the Lemaître-Painlevé-Gulstrand coordinates $\mathbf{X} = a(t)\mathbf{x}$. Taking the Fourier transform with respect to these coordinates, and to cosmological time, the mode function

$$\Phi(\bar{\omega},\mathbf{P}) = \int_{\mathbf{X},t} e^{-i\bar{\omega}t - i\mathbf{P}\cdot\mathbf{X}} \Phi(\mathbf{X},t) \tag{4.17}$$

  is governed by the equation

$$-(\bar{\omega} - i\mathbf{P}\cdot\partial_{\mathbf{P}})(\bar{\omega} - i\partial_{\mathbf{P}}\cdot\mathbf{P})\Phi(\bar{\omega},\mathbf{P}) = 0. \tag{4.18}$$

  In particular, for $P \to 0$,

$$(-\bar{\omega}^2 + di\bar{\omega})\Phi(\bar{\omega},\mathbf{P}=0) = 0 \tag{4.19}$$

  which is related to (4.10) with $\bar{\omega} = i\omega$. Indeed, both representations coincide for $K = P = 0$.

[2] This is obvious in the flat space limit (4.13) due to time translation invariance.

[3] This relation is a consequence of the p-representation (1.23).

- As we have discussed in chapter 3, a consequence of our regulation scheme is that flow prescriptions involving frequency and momentum derivatives do not give the same result. Although momentum derivatives seem more appropriate for a momentum-regulated theory, we do not have an appropriate prescription and we must resort to frequency derivatives. Again, we rely on the fact that both results should be very close.

Applying this transformation to the ansatz of the derivative expansion, we obtain a series in terms of the eigenvalue $\alpha_\omega \equiv \omega(\omega - d)$, which is indeed a small parameter as $\omega \to 0$:

$$\Gamma_k^{(2)}(\phi, \omega) = -\Big(V_k''(\phi) + Z_k(\phi)\alpha_\omega + O(\alpha_\omega^2)\Big). \tag{4.20}$$

We can now define a prescription for all terms of the derivative expansion. In particular, the running anomalous dimension is defined as

$$\eta_k(\phi) = \frac{1}{Z_k} \frac{d\dot{\Gamma}_k^{(2)}(\phi, \omega)}{d\alpha_\omega}\bigg|_{\omega=0} \tag{4.21}$$

As a first implementation of the derivative expansion, we will consider this additional running quantity. For simplicity however, we discard its field dependency. This approximation, referred to as the LPA', provides an interesting extension of the local potential approximation (see chapter 3). We must then specify the value of the field in the prescription (4.21), for which we choose the minimum of the running potential.

4.1.3 Correlators in the LPA'

Generalizing the computation of the correlators from the LPA to the LPA' is quite straightforward. The ansatz

$$\Gamma_k[\phi] = -\int_x \left(V_k(\phi) - \frac{Z_k}{2}\phi\Box\phi\right) \tag{4.22}$$

defines the correlator through the inverse relation

$$\big(-V''(\phi) + Z_k\Box_{K,\eta} - R(-K\eta)\big)\tilde{G}(K, \eta, \eta') = i\frac{\delta_{\mathcal{C}}(\eta - \eta')}{a^D(\eta)}, \tag{4.23}$$

which we can rewrite

$$\big(-\frac{V''(\phi)}{Z_k} + \Box_{K,\eta} - \frac{R(-K\eta)}{Z_k}\big)\tilde{G}(K, \eta, \eta') = i\frac{\delta_{\mathcal{C}}(\eta - \eta')}{Z_k a^D(\eta)}. \tag{4.24}$$

The regulator is divided by Z_k, but is also conveniently redefined as $R_{\mathrm{LPA}'} = Z_k R_{\mathrm{LPA}}$ in order to perform the desired simplification, so that this term has not changed in the equation. We must solve this modified equation with updated boundary conditions: the

Bunch-Davies vacuum in the infinite past now selects[4]

$$\hat{F}_k(p,p')|_{p=p'\to\infty} = \frac{1}{2Z_k}, \tag{4.25}$$

$$\partial_p \hat{F}_k(p,p')|_{p=p'\to\infty} = 0, \tag{4.26}$$

$$\partial_p\partial_{p'} \hat{F}_k(p,p')|_{p=p'\to\infty} = \frac{1}{2Z_k}. \tag{4.27}$$

The commutation relation also changes the normalization of the spectral correlator: In the LPA, as in a free theory, $\Pi = \dot{\phi}$ and the commutation relation

$$[\phi(x), \Pi(x')] = i\delta(x,x') \tag{4.28}$$

implies that $\partial_p \rho_k(p,p')|_{p=p'} = -1$. In the presence of a field renormalization, $\Pi = Z_k\dot{\phi}$, so that

$$[\phi(x), \dot{\phi}(x')] = i\frac{\delta(x,x')}{Z_k}, \quad \text{and} \quad \partial_p \rho_k(p,p')|_{p=p'} = -\frac{1}{Z_k}. \tag{4.29}$$

In the end, the correlator in the LPA' is related to its LPA equivalent by

$$G_{\mathrm{LPA}'}(V_k'') = \frac{1}{Z_k} G_{\mathrm{LPA}}\left(\frac{V_k''}{Z_k}\right). \tag{4.30}$$

Appendix F gives a summary on the correlation functions, as well as the relevant asymptotic behaviours. Before moving on, we say a word on the flow of the potential in the LPA'. From the Wetterich equation,

$$\dot{V}_k = \frac{1}{2}\int \frac{d^dp}{(2\pi)^d}\dot{R}_k(p)\frac{|\hat{u}_k(p)|^2}{Z_k p}, \tag{4.31}$$

where now $\dot{R}_k(p) = Z_k\big[(2-\eta_k)k^2 + \eta_k p^2\big]\theta(k^2-p^2)$, and, as discussed above, V_k'' now appears divided by Z_k in the mode function. The resulting flow is

$$\dot{V}_k(\phi) = A_d k^{d+2}\big[(2-\eta_k)B(\nu_k,k,d) + \eta_k B(\nu_k,k,d+2)\big], \tag{4.32}$$

where

$$B(\nu,k,x) = \frac{e^{i\pi\nu_i}}{x(x^2-4\bar{\nu}^2)}\Big[(x^2-2\nu^2+2k^2)|H_\nu|^2 + 2k^2|H_\nu'|^2 - 2xkRe[H_\nu^* H_\nu']\Big], \tag{4.33}$$

see appendix B for explicit calculation.

We are now set to compute the running anomalous dimension. In what follows, we extract the expression (4.21) from the Wetterich equation and discuss the usual limits of interest. We start with the case of a single scalar field, then extend the formalism to $O(N)$ theories. Finally, we discuss the physical implications, in particular concerning the effective potential.

[4]We recall that this is a result of an adiabatic switch on of the interactions in the infinite past; see the discussion in chapter 2.

4.2 Anomalous dimension of a single field

4.2.1 General expression

To compute the flow of the inverse correlator, we must take two covariant derivatives of the Wetterich equation:

$$\dot{\Gamma}_k[\phi] = \frac{i}{2}\tilde{\partial}_k\big(\operatorname{Tr}\ln(\Gamma_k^{(2)} + R_k)\big), \tag{4.34}$$

$$\dot{\Gamma}_k^{(1)}(x) = \frac{i}{2}\tilde{\partial}_k \int_{a,b} (\Gamma_k^{(2)} + R_k)^{-1}(a,b)\Gamma_k^{(3)}(b,a,x)\big), \tag{4.35}$$

$$\dot{\Gamma}_k^{(2)}(x,y) = \frac{1}{2}\tilde{\partial}_k \int_{a,b} \Big[G_k(a,b)\Gamma_k^{(4)}(b,a,x,y) + i\int_{c,d} G_k(a,b)\Gamma_k^{(3)}(b,c,x)G_k(c,d)\Gamma_k^{(3)}(d,a,y)\Big]. \tag{4.36}$$

In the LPA' (4.22), the three and four-point vertex functions are simply

$$\Gamma_k^{(3)}(x,y,z) = -V_k^{(3)}(\phi)\delta(x,y)\delta(y,z), \tag{4.37}$$

$$\Gamma_k^{(4)}(w,x,y,z) = -V_k^{(4)}(\phi)\delta(x,y)\delta(y,z)\delta(w,x), \tag{4.38}$$

so that

$$\dot{\Gamma}_k^{(2)}(x,y) = \frac{1}{2}\tilde{\partial}_k\big[-G_k(x,y)V_k^{(4)}\delta(x,y) + i{V_k^{(3)}}^2 G_k(x,y)G_k(x,y)\big]. \tag{4.39}$$

Exploiting spatial homogeneity and moving to Fourier spatial coordinates,

$$\dot{\Gamma}_k^{(2)}(K,\eta,\eta') = \frac{1}{2}\tilde{\partial}_k \int_{\mathbf{q}} G_k(q,\eta,\eta')\Big[-V_k^{(4)}\delta_c(\eta,\eta') + i{V_k^{(3)}}^2 G_k(|\mathbf{K}-\mathbf{q}|,\eta,\eta')\Big]. \tag{4.40}$$

We can now take the transform (4.11). Moving to the p-representation (1.22), it is straightforward to show that

$$\dot{\Gamma}_k^{(2)}(\omega) = \frac{\Omega_d}{2(2\pi)^d}\tilde{\partial}_k \int_0^\infty dp\; p^{d-2}\left[-V_k^{(4)}\hat{F}(p,p) + 2{V_k^{(3)}}^2\int_p^\infty \frac{dp'}{p'^2}\left(\frac{p'}{p}\right)^\omega \hat{F}(p,p')\hat{\rho}(p,p')\right], \tag{4.41}$$

where we have omitted the field dependence for simplicity. We now explicit $\tilde{\partial}_k$, defined by the functional derivative

$$\tilde{\partial}_k \bullet = \int_0^\infty dp \dot{R}_k(p)\frac{\delta \bullet}{\delta R_k(p)}. \tag{4.42}$$

For practical purposes, this operation consists in taking a derivative with respect to k in R_k only, that is, at fixed $\Gamma_k^{(2)}$. To do this, we consider the variation $R_k \to R_k + \delta R_k$ in the following relation:

$$(\hat{\Gamma}_k^{(2)} + R_k)\hat{G}_k = i \implies \tilde{\partial}_k \hat{G}_k = i\hat{G}_k\dot{R}_k\hat{G}_k \tag{4.43}$$

This product relation reads, in its expanded form,

$$\int_{\hat{\mathcal{C}}} dp'' \left(\hat{\Gamma}_k^{(2)}(p,p'') + \frac{\hat{R}_k(p'')}{p''^2}\delta(p-p'') \right) \hat{G}_k(p'',p') = i\delta_{\hat{\mathcal{C}}}(p-p'). \tag{4.44}$$

Therefore,

$$\begin{aligned}
\tilde{\partial}_k G_k(p,p') =& + \frac{1}{2}\int_{\hat{\mathcal{C}}} dp'' \mathrm{sign}_{\hat{\mathcal{C}}}(p-p'')\hat{\rho}_k(p,p'')\frac{\dot{\hat{R}}_k(p'')}{p''^2}\hat{F}_k(p'',p') \\
&+ \frac{1}{2}\int_{\hat{\mathcal{C}}} dp'' \hat{F}_k(p,p'')\frac{\dot{\hat{R}}_k(p'')}{p''^2}\mathrm{sign}_{\hat{\mathcal{C}}}(p''-p')\hat{\rho}_k(p'',p') \qquad (4.45) \\
&- \frac{i}{4}\int_{\hat{\mathcal{C}}} dp'' \mathrm{sign}_{\hat{\mathcal{C}}}(p-p'')\hat{\rho}_k(p,p'')\frac{\dot{\hat{R}}_k(p'')}{p''^2}\mathrm{sign}_{\hat{\mathcal{C}}}(p''-p')\hat{\rho}_k(p'',p') \\
=& - \int_p^{+\infty} dp'' \hat{\rho}_k(p,p'')\frac{\dot{\hat{R}}_k(p'')}{p''^2}\hat{F}_k(p'',p') \\
&+ \int_{p'}^{+\infty} dp'' \hat{F}_k(p,p'')\frac{\dot{\hat{R}}_k(p'')}{p''^2}\hat{\rho}_k(p'',p') \qquad (4.46) \\
&- \frac{i}{2}\mathrm{sign}_{\hat{\mathcal{C}}}(p-p')\left(- \int_p^{p'} dp'' \hat{\rho}_k(p,p'')\frac{\dot{\hat{R}}_k(p'')}{p''^2}\hat{\rho}_k(p'',p') \right) \\
=& \tilde{\partial}_k \hat{F}_k(p,p') - \frac{i}{2}\mathrm{sign}_{\hat{\mathcal{C}}}(p-p')\tilde{\partial}_k\hat{\rho}_k(p,p'). \qquad (4.47)
\end{aligned}$$

By identifying the statistical and spectral parts[5],

$$\begin{aligned}
\tilde{\partial}_k \hat{F}_k(p,p') =& - \int_p^{+\infty} dp'' \hat{\rho}_k(p,p'')\frac{\dot{\hat{R}}_k(p'')}{p''^2}\hat{F}_k(p'',p') \qquad (4.48) \\
&+ \int_{p'}^{+\infty} dp'' \hat{F}_k(p,p'')\frac{\dot{\hat{R}}_k(p'')}{p''^2}\hat{\rho}_k(p'',p') \\
\tilde{\partial}_k \hat{\rho}_k(p,p') =& - \int_p^{p'} dp'' \hat{\rho}_k(p,p'')\frac{\dot{\hat{R}}_k(p'')}{p''^2}\hat{\rho}_k(p'',p') \qquad (4.49)
\end{aligned}$$

Taking this in the flow equation (4.41), we get

$$\begin{aligned}
\dot{\Gamma}_k^{(2)}(\phi,\omega) =& \frac{V_k^{(4)}\Omega_d}{(2\pi)^d}\int_0^\infty dp p^{d-2}\int_p^\infty dp'' \hat{F}(p,p'')\frac{\dot{\hat{R}}(p'')}{p''^2}\hat{\rho}(p'',p) \qquad (4.50) \\
&\frac{{V_k^{(3)}}^2\Omega_d}{(2\pi)^d}\int_{p,p'}\Big[- \int_p^\infty dp'' \hat{\rho}(p,p'')\frac{\dot{\hat{R}}(p'')}{p''^2}\hat{F}(p'',p')\hat{\rho}(p,p') \\
&\qquad + \int_{p'}^\infty dp'' \hat{F}(p,p'')\frac{\dot{\hat{R}}(p'')}{p''^2}\hat{\rho}(p'',p')\hat{\rho}(p,p') \\
&\qquad - \int_p^{p'} dp'' \hat{\rho}(p,p'')\frac{\dot{\hat{R}}(p'')}{p''^2}\hat{\rho}(p,p')\hat{F}(p,p')\Big],
\end{aligned}$$

[5]These expressions are closely linked to the Schwinger-Dyson equations; see [121] and references therein for a discussion on the link between 2PI and NPRG formalisms.

where

$$\int_{p,p'} = \int_0^\infty dp \int_p^\infty dp' \frac{p^d}{(pp')^2} \left(\frac{p'}{p}\right)^\omega . \tag{4.51}$$

This result is valid for any regulator of the form (1.70). Using the Litim regulator (3.6) and after taking care of the integral domains, we get

$$\dot{\Gamma}_k^{(2)}(\phi,\omega) = \frac{Z_k \Omega_d}{(2\pi)^d} \left(V_k^{(4)} J + {V_k^{(3)}}^2 \sum_{j=0}^{4} I_j \right), \tag{4.52}$$

where we have defined

$$J = \int_0^k dp\, p^{d-2} \int_p^k ds\, \hat{\rho}_k(p,s) \frac{(2-\eta_k)k^2 + \eta_k s^2}{s^2} \hat{F}_k(s,p) \tag{4.53}$$

and

$$I_0 = -\int_0^k dp \int_p^k dq \int_p^k dr\, A_k(p,q,r) \hat{\rho}_k(p,r) \hat{F}_k(r,q) \hat{\rho}_k(p,q), \tag{4.54}$$

$$I_1 = -\int_0^k dp \int_k^\infty dq \int_p^k dr\, A_k(p,q,r) \hat{\rho}_k(p,r) \hat{F}_k(r,q) \hat{\rho}_k(p,q), \tag{4.55}$$

$$I_2 = \int_0^k dp \int_p^k dq \int_q^k dr\, A_k(p,q,r) \hat{F}_k(p,r) \hat{\rho}_k(r,q) \hat{\rho}_k(p,q), \tag{4.56}$$

$$I_3 = -\int_0^k dp \int_p^k dq \int_p^q dr\, A_k(p,q,r) \hat{\rho}_k(p,r) \hat{\rho}_k(r,q) \hat{F}_k(p,q), \tag{4.57}$$

$$I_4 = -\int_0^k dp \int_k^\infty dq \int_p^k dr\, A_k(p,q,r) \hat{\rho}_k(p,r) \hat{\rho}_k(r,q) \hat{F}_k(p,q), \tag{4.58}$$

with the integration measure

$$A_k(p,q,r) = p^d \left(\frac{q}{p}\right)^\omega \frac{(2-\eta_k)k^2 + \eta_k r^2}{(pqr)^2}. \tag{4.59}$$

There is much to discuss about these integrals in relation with de Sitter symmetries and flat space limit. To this end, it is enlightening to move back to a representation in terms of comoving momentum and cosmological time. For example[6],

$$I_0 = -\int_0^{ke^{Ht}} dK K^{d-1} \int_{-\frac{\tau}{H}}^t dt' \int_{-\frac{\tau}{H}}^t dt'' \tilde{\rho}_k(K,t,t'') \tilde{F}_k(K,t'',t') \tilde{\rho}_k(K,t,t'), \tag{4.60}$$

where $\tau = \ln k/K$, and we have made occurrences of H explicit.

- Each integration over a physical momentum in the p-representation stems from either comoving momentum integration or time integration. Because in de Sitter space the two are related through redshift, these integrals come to play an equivalent role in the end. Furthermore, because physical momenta are regulated, the time integrals end up being bounded as well: in a way, we find that the time direction is also regulated in de Sitter space.

[6] Of course, as is clear from the p-representation, this expression is independent of t.

- In the flat space limit $H \to 0$, time and momentum decouple. This translates into a time-independent cutoff k for K, and the lower boundary in time moving to the infinite past. The time direction is no longer "regulated" in the sense given above, and by gathering $I_0 + I_2 + I_3$ we recover the expression (3.20), where $\tilde{\partial}_k$ must be made explicit.

- This leaves us with the terms $I_1 + I_4$, which have an unbounded physical momentum q. In the (K, t) representation, this means that t' is integrated over in the range $]-\infty; t - \frac{\tau}{H}[$. This interval vanishes as $H \to 0$, so that these terms do not contribute to the flat space limit. Furthermore, they are also degligeable in the light IR regime, see app. H for a proof.

As in flat space, an important remark is that by choosing Z_k independent of ϕ, only the sunset diagram depends on the frequency ω and contribute to η_k. Furthermore, because we are interested in evaluating Eq. (4.52) at the potential minimum, this contribution is zero if the latter vanishes (symmetric phase). As a consequence, we will be computing the anomalous dimension in the case of (UV) spontaneous symmetry breaking, and address the issue of symmetry restoration with this additional parameter in our model.

4.2.2 Heavy UV regime

As in Chapter 2, it is interesting to study the regime where all dimensionful scales are large in units of the space-time curvature H, because this effectively sends $H \to 0$. We thus recover the results from the equivalent analysis in Minkowski space. A subtle point here is that, because ω is in units of H, the limits $H \to 0$ and $\omega \to 0$ do not commute. We must take the flat space limit first in order to recover the results from the Minkowskian analysis. The details of this lengthy computation are shown in appendix G. The resulting flow is

$$\dot{\Gamma}_k^{(2)}(\omega) = \left(1 - \frac{\eta_k}{d+2}\right) \frac{v_d}{2} k^{d+2} \left(\frac{\tilde{V}^{(4)}}{M_k^3} - \frac{\tilde{V}_k^{(3)^2}}{M_k^3} \frac{2\omega^2 + 24M_k^2}{(\omega^2 + 4M_k^2)^2} \right) \tag{4.61}$$

We have introduced the renormalized field $\tilde{\phi} = \sqrt{Z_k}\phi$ with $\tilde{V}_k(\tilde{\phi}) = V_k(\phi)$. The regulated curvature is $M_k^2(\tilde{\phi}) = \tilde{V}_k''(\tilde{\phi}) + k^2$. The behavior around $\omega = 0$ reproduces the flow for V_k'' and η_k as in Minkowski space:

$$\dot{V}_k'' = \left(1 - \frac{\eta_k}{d+2}\right) \frac{v_d}{2} k^{d+2} \left(-\frac{\tilde{V}_k^{(4)}}{M_k^3} + \frac{3\tilde{V}_k^{(3)^2}}{2M_k^5} \right), \tag{4.62}$$

$$\eta_k = \left(1 - \frac{\eta_k}{d+2}\right) \tilde{V}_k^{(3)^2} \frac{5v_d}{16} \frac{k^{d+2}}{M_k^7} \bigg|_{\phi=\phi_{\min}}. \tag{4.63}$$

We remind that our prescription in the LPA' is to define the running anomalous dimension at the minimum of the potential. The constant $C_d = \pi\Omega_d/[16d(2\pi)^d]$ is the same as in chapter 2. The fact that we recover flat space results (3.11) and (3.31) is

an interesting check of our prescription (4.21). However, the effects of curvature on the flow occur when k and m_k are small in units of H. This is the light IR regime that we consider now.

4.2.3 Light IR regime

Taking $m_k, k \ll 1$, the integrals (4.53-4.58) have the following leading behavior (see appendix H):

$$J = \frac{\Gamma^2(d/2)2^d}{4\pi d Z_k^2}\frac{(2-\eta)k^{d-2\bar{\nu}_k+2}}{(d-2\bar{\nu}_k)^2}, \tag{4.64}$$

$$I_0 + I_2 + I_3 = \frac{2^d\Gamma^2(d/2)}{8\pi\bar{\nu}_\kappa^2 Z_\kappa^3}\frac{(2-\eta_\kappa)k^{2+d-2\bar{\nu}_\kappa}}{\omega}\left(\frac{1}{(d-2\bar{\nu}_\kappa)^2} - \frac{1}{(d-2\bar{\nu}_\kappa-\omega)^2}\right), \tag{4.65}$$

$$I_1 + I_4 \ll I_0 + I_2 + I_3, \tag{4.66}$$

so that the flow of the two-point function writes

$$\dot{\Gamma}_k^{(2)}(\omega) = \frac{(2-\eta_k)k^2}{2\Omega_{D+1}}\left(\frac{\tilde{V}_k^{(4)}}{M_k^4} - \frac{\tilde{V}_k^{(3)^2}}{2M_k^6}\frac{4-2\epsilon}{(1-\epsilon)^2}\right), \quad \text{where} \quad \epsilon = \frac{d\omega}{2M_k^2}. \tag{4.67}$$

It is an interesting check to evaluate these expressions at $\omega = 0$, since $\dot{\Gamma}_k^{(2)}(\omega = 0)$ is the flow of the potential curvature. We indeed retrieve the same IR limit as in Eq. (2.32), generalized in the LPA' ansatz [66]

$$\dot{V}_k''(\phi) = \frac{(2-\eta_k)k^2}{2\Omega_{D+1}}\left(-\frac{\tilde{V}_k^{(4)}}{M_k^4} + \frac{2\tilde{V}_k^{(3)^2}}{M_k^6}\right). \tag{4.68}$$

The anomalous dimension is similarly obtained by deriving once with respect to α_ω and taking $\omega = 0$, $\phi = \phi_{\min}$. One finds

$$\eta_k = \left.\frac{3(2-\eta_k)}{4\Omega_{D+1}}\frac{\tilde{V}_k^{(3)^2}k^2}{M_k^8}\right|_{\phi=\phi_{\min}}. \tag{4.69}$$

There is much to discuss about this result. Before doing so, we develop the analog procedure for $O(N)$ theories in order to have a more general discussion on all cases.

4.3 Anomalous dimension in $N > 1$

4.3.1 Generalizing to $O(N)$ theories

In order to generalize the prescription (4.21) to $O(N)$ theories, we must recall that there are more than one invariants at the first order derivative expansion:

$$\Gamma_k[\phi] = -\int d\eta d^dx\sqrt{-g}\left(V_k(\phi) + \frac{Z_k(\phi)}{2}(\nabla\phi)^2 + \frac{Y_k(\phi)}{2}(\phi_a\nabla\phi_a)^2\right), \tag{4.70}$$

so that after two covariant field derivatives and evaluation at constant field, we get

$$\Gamma^{(2)}_{k,ab}(\phi,x,y) = -(V''_{k,ab}(\phi) - Z_k(\phi)\Box_x\delta_{ab} - Y_k(\phi)\phi_a\phi_b\Box_x)\delta(x,y). \tag{4.71}$$

As explained in section 2.4.1, the inverse correlator admits the following decomposition:

$$\Gamma^{(2)}_{ab} = \Gamma^{(2)}_L P^L_{ab} + \Gamma^{(2)}_T P^T_{ab}, \tag{4.72}$$

where

$$P^L_{ab} = \frac{\phi_a\phi_b}{\phi^2}, \qquad P^T_{ab} = \delta_{ab} - \frac{\phi_a\phi_b}{\phi^2}. \tag{4.73}$$

In this case[7],

$$\Gamma^{(2)}_{k,L} = -(V''_{k,L}(\phi) - Z_k(\phi)\Box_x - Y_k(\phi)\phi^2\Box_x)\delta(x,y), \tag{4.74}$$

$$\Gamma^{(2)}_{k,T} = -(V''_{k,T}(\phi) - Z_k(\phi)\Box_x)\delta(x,y). \tag{4.75}$$

In the LPA' scheme, we neglect this additional term[8], so that we may follow the flow of either component. For consistency however, we select the transverse part to isolate Z_k from Y_k. The prescription for η_k therefore becomes

$$\eta_k(\phi) = \frac{1}{Z_k}\frac{d\dot{\Gamma}^{(2)}_{k,T}(\phi,\omega)}{d\alpha_\omega}\bigg|_{\omega=0}. \tag{4.76}$$

As for the $N=1$ case, we get the following flow from the Wetterich equation

$$\dot{\Gamma}^{(2)}_{k,ij}(K,\eta,\eta') = \frac{1}{2}\tilde{\partial}_k\Big[- V^{(4)}_{k,abij}\int\frac{d^dq}{(2\pi)^d}G_{k,ba}(q,\eta,\eta')\delta_c(\eta-\eta') + iV^{(3)}_{k,bci}V^{(3)}_{k,adj}\int\frac{d^dq}{(2\pi)^d}G_{k,ab}(q,\eta,\eta')G_{k,cd}(|\mathbf{K}-\mathbf{q}|,\eta,\eta')\Big], \tag{4.77}$$

where we have added the field indices and summation over repeated indices is understood. Let us introduce the $O(N)$ invariant potential and its derivatives as

$$V_k(\phi) = NU_k(\rho), \qquad \rho = \frac{Z_k\phi^2}{2N}, \tag{4.78}$$

$$V'_{k,a}(\phi) = Z_k\phi_aU'_k, \tag{4.79}$$

$$V''_{k,ab}(\phi) = Z_kU'_k\delta_{ab} + \frac{Z_k^2}{N}\phi_a\phi_bU''_k, \tag{4.80}$$

$$V^{(3)}_{k,abc}(\phi) = \left(\frac{Z_k^2}{N}U''_k\delta_{ab}\phi_c + 2\circlearrowright\right) + \frac{Z_k^3}{N^2}U^{(3)}_k\phi_a\phi_b\phi_c, \tag{4.81}$$

$$V^{(4)}_{k,abcd}(\phi) = \left(\frac{Z_k^2}{N}U''_k\delta_{ab}\delta_{cd}+2\circlearrowright\right) + \left(\frac{Z_k^3}{N^2}U^{(3)}_k\delta_{ab}\phi_c\phi_d+5\circlearrowright\right) + \frac{Z_k^4}{N^3}U^{(4)}_k\phi_a\phi_b\phi_c\phi_d. \tag{4.82}$$

[7] We give $V''_{k,L}(\phi)$ and $V''_{k,T}(\phi)$ below.

[8] Notice that if we write the same ansatz (4.70) for a single field, Y_k can be reabsorbed as field dependencies of Z_k which we neglect in the LPA'.

Here, $\circlearrowleft$ indicates the non equivalent permutations of indices. Injecting this in the flow (4.77) and taking a transverse projection,

$$\dot{\Gamma}^{(2)}_{T,k}(K,\eta,\eta') = \frac{Z_k^2}{2N}\tilde{\partial}_k \int_{\mathbf{q}} \Bigg[-\Big\{(N+1)U_k'' G_k^T(q,\eta,\eta') + (U_k'' + 2\rho U_k^{(3)}) G_k^L(q,\eta,\eta')\Big\}\delta_c(\eta,\eta') + 4iZ_k\rho U_k''^2 G_k^T(q,\eta,\eta') G_k^L(|\mathbf{K}-\mathbf{q}|,\eta,\eta')\Bigg]. \tag{4.83}$$

Taking the transform (4.11) and with the Litim regulator,

$$\dot{\Gamma}^{(2)}_{k,T}(\phi,\omega) = \frac{Z_k^2\Omega_d}{N(2\pi)^d}\left((N+1)U_k'' J^T + (U_k'' + 2\rho U_k^{(3)})J^L + 2Z_k\rho U_k''^2 \sum_{j=0}^{4} I_j\right) \tag{4.84}$$

$$= -Z_k\Big(\dot{U}_k'(\rho) - \eta_k(U_k' + \rho U_k'') - \eta_k\alpha_\omega + O(\alpha_\omega^2)\Big), \tag{4.85}$$

where $J^{T,L}$ and I_j have similar expressions as for $N = 1$, explicitly

$$J^{T,L} = -\int_0^k dp\, p^{d-2}\int_p^k ds\, \hat{F}_k^{T,L}(p,s)\frac{(2-\eta_k)k^2 + \eta_k s^2}{s^2}\hat{\rho}_k^{T,L}(s,p), \tag{4.86}$$

$$\begin{aligned} I_0 = &-\int_0^k dp\int_p^k dq\int_p^k dr\, A(p,q,r)\hat{\rho}_k^T(p,r)\hat{F}_k^T(r,q)\hat{\rho}_k^L(p,q) \\ &-\int_0^k dp\int_p^k dq\int_p^k dr\, A(p,q,r)\hat{\rho}_k^L(p,r)\hat{F}_k^L(r,q)\hat{\rho}_k^T(p,q), \end{aligned} \tag{4.87}$$

$$\begin{aligned} I_1 = &-\int_0^k dp\int_k^\infty dq\int_p^k dr\, A_k(p,q,r)\hat{\rho}_k^T(p,r)\hat{F}_k^T(r,q)\hat{\rho}_k^L(p,q) \\ &-\int_0^k dp\int_k^\infty dq\int_p^k dr\, A_k(p,q,r)\hat{\rho}_k^L(p,r)\hat{F}_k^L(r,q)\hat{\rho}_k^T(p,q), \end{aligned} \tag{4.88}$$

$$\begin{aligned} I_2 = &+\int_0^k dp\int_p^k dq\int_q^k dr\, A_k(p,q,r)\hat{F}_k^T(p,r)\hat{\rho}_k^T(r,q)\hat{\rho}_k^L(p,q) \\ &+\int_0^k dp\int_p^k dq\int_q^k dr\, A_k(p,q,r)\hat{F}_k^L(p,r)\hat{\rho}_k^L(r,q)\hat{\rho}_k^T(p,q), \end{aligned} \tag{4.89}$$

$$\begin{aligned} I_3 = &-\int_0^k dp\int_p^k dq\int_p^q dr\, A_k(p,q,r)\hat{\rho}_k^T(p,r)\hat{\rho}_k^T(r,q)\hat{F}_k^L(p,q) \\ &-\int_0^k dp\int_p^k dq\int_p^q dr\, A_k(p,q,r)\hat{\rho}_k^L(p,r)\hat{\rho}_k^L(r,q)\hat{F}_k^T(p,q), \end{aligned} \tag{4.90}$$

$$\begin{aligned} I_4 = &-\int_0^k dp\int_k^\infty dq\int_p^k dr\, A_k(p,q,r)\hat{\rho}_k^T(p,r)\hat{\rho}_k^T(r,q)\hat{F}_k^L(p,q) \\ &-\int_0^k dp\int_k^\infty dq\int_p^k dr\, A_k(p,q,r)\hat{\rho}_k^L(p,r)\hat{\rho}_k^L(r,q)\hat{F}_k^T(p,q). \end{aligned} \tag{4.91}$$

Taking the flat space limit $H \to 0$ as in the $N = 1$ case allows us to recover the flow of the potential from the equivalent Minkowskian analysis. The running anomalous dimension

has the following expression

$$\eta_k = \left(1 - \frac{\eta_k}{d+2}\right) \frac{v_d \rho U_k''^2 k^{d+1}}{M_k (k+M_k)^3} \left[\left(\frac{1}{k} + \frac{1}{M_k}\right) \frac{3}{k+M_k} - \frac{1}{k^2} - \frac{1}{M_k^2}\right]\Bigg|_{\phi=\phi_{\min}}. \quad (4.92)$$

This result is expected to match the expression from the Minkowskian analysis of an $O(N)$ theory. We now move on to the light IR regime which is the one of interest to discuss de Sitter physics.

4.3.2 Light IR regime

Taking all masses and the RG scale small in units of H, we find

$$\dot{\Gamma}^{(2)}_{k,T}(\phi,\omega) = \frac{Z_k(2-\eta_k)k^2}{2N\Omega_{D+1}} \Bigg\{ \frac{(N+1)U_k''}{M_T^4} + \frac{U'' + 2\rho U^{(3)}}{M_L^4} + \frac{4\rho U_k''^2}{(d\omega + 2\rho U_k'')M_T^4} + \frac{4\rho U''^2}{(d\omega - 2\rho U_k'')M_L^4} - \frac{16\rho U''^2}{(d\omega + M_T^2 + M_L^2)^2} \left(\frac{2d\omega}{(d\omega)^2 - (M_T^2 - M_L^2)^2}\right) \Bigg\}, \quad (4.93)$$

where the longitudinal and transverse regulated curvatures are, respectively,

$$M_T^2 = k^2 + U_k'(\rho), \quad M_L^2 = k^2 + U_k'(\rho) + 2\rho U_k''(\rho). \quad (4.94)$$

From Eq. (4.93) we recover once again the flow of the transverse mass in the appropriate regime. It writes

$$\dot{U}_k' = \eta_k (U_k' + \rho U_k'') - \frac{1 - \frac{\eta_k}{2}}{N\Omega_{D+1}} \left(\frac{3U_k'' + 2\rho U_k^{(3)}}{(k^2 + U_k' + 2\rho U_k'')^2} + (N-1) \frac{U_k''}{(k^2 + U_k')^2} \right). \quad (4.95)$$

We also extract the expression of the anomalous dimension and find

$$\eta_k = \frac{(2-\eta_k)\rho U_k''}{2N\Omega_{D+1}} \left(\frac{k^4 + 4k^2 M_k^2 + M_k^4}{k^2 M_k^4 (k^2 + M_k^2)^2} \right)\Bigg|_{\phi=\phi_{\min}} \quad (4.96)$$

In both the UV and light IR limits, we find an expression for the running anomalous dimension that differs from the $N = 1$ calculation. This is because, having projected on the transverse component of the inverse correlator, we compute an original quantity which has no equivalent in $N = 1$.

Let us now discuss these infrared expressions, both in $N = 1$ and $N > 1$, in relation with our previous findings regarding the effective potential.

4.4 Influence on the flow of the potential

4.4.1 Dimensional reduction and modified RG scale

In chapter 2 we have made a number of remarks on the flow of the potential, chief of which is the dimensional reduction which takes place in the light infrared regime. It is

interesting to notice that this is still the case: the de Sitter flow

$$\dot{V} = \frac{2-\eta_k}{2\Omega_{D+1}} \frac{k^2}{k^2 + V_k''/Z_k}, \tag{4.97}$$

has the same η_k-dependency as the flow of a (fully regularized) Euclidean theory,

$$\dot{V} = \left(\frac{2-\eta_k}{D} + \frac{\eta_k}{D+2} \right) \frac{v_d k^2}{k^2 + V_k''/Z_k}, \tag{4.98}$$

in the limit where $D \to 0$ (numerical prefactors aside). This is achieved in the de Sitter calculation (4.32 - 4.33) because the $2-\eta_k$ term is enhanced by a denominator $d^2 - 4\bar{\nu}_k^2 \sim M_k^2$, whereas the η_k term receives $(d+2)^2 - 4\bar{\nu}_k^2 \sim 1$ and is therefore negligible.

Although it is odd to consider the LPA' of a zero-dimensional theory, we can find a generating functional for this regularized theory in the same spirit as (2.33):

$$e^{-\Omega_{D+1}\mathcal{W}_k(J)} = \int d\varphi \, e^{-\Omega_{D+1}\left[V_{\text{eff}}(\varphi) + J\varphi + Z_k \frac{k^2}{2}\varphi^2\right]}. \tag{4.99}$$

One easily checks that the flow of the effective potential for this theory is indeed given by (4.97). In the absence of a kinetic term, the only occurrence of Z_k is in front of the regulator (as should be done in the LPA'). This shows that the field renormalization can be reabsorbed in a redefinition of the RG scale, as we now discuss.

In computing the flow of the inverse correlator, we have introduced the renormalized field $\tilde{\phi} = \sqrt{Z_k}\phi$, or equivalently $\rho = Z_k\phi^2/2N$. This is the usual reparameterization thanks to which Z_k disappears from all flow equations, though η_k remains of course. The dimensional reduction offers us an alternative, stemming from the additional symmetry of the β-function:

$$\beta(V'', k^2) = \beta(\alpha V'', \alpha k^2) \tag{4.100}$$

for any number α. Choosing $\alpha = Z_k$ therefore also absorbs all occurrences of Z_k in the flow of the potential. The truly remarkable point is that by introducing this new RG scale $\tilde{k} = \sqrt{Z_k}k$, we have

$$k\partial_k V_k(\phi) = (1 - \eta_k/2)\tilde{k}\partial_{\tilde{k}} V_{\tilde{k}}(\phi), \tag{4.101}$$

so that, for example, the $N = 1$ flow

$$k\partial_k V_k(\phi) = \frac{(2-\eta_k)}{2\Omega_{D+1}} \frac{k^2}{k^2 + V_k''/Z_k} \tag{4.102}$$

can be traded for

$$\tilde{k}\partial_{\tilde{k}} V_{\tilde{k}}(\phi) = \frac{1}{\Omega_{D+1}} \frac{\tilde{k}^2}{\tilde{k}^2 + V_{\tilde{k}}''} \tag{4.103}$$

and similarly for $N > 1$. This is precisely the LPA flow. Assuming we start the flow with $Z_k = 1$, both k and $\tilde{k}$ have the same value. Therefore, the LPA and LPA' flows are the same in their respective scales k and $\tilde{k}$ and will give the same effective potential

(starting with the same initial condition) at the end of the flow when both scales are equal again[9].

The consequence of this rescaling is that the anomalous dimension has strictly no influence on the effective potential. In particular, this means that the LPA' brings no corrections to stochastic results such as

$$\left\langle \phi^2(t) \right\rangle \underset{t\to\infty}{\to} \frac{1}{\Omega_{D+1} V''_{\rm eff}}. \tag{4.104}$$

This result is also true in the LPA. Because the effective potential is the same, using Eq. (4.30), we find[10] in the LPA'

$$\left\langle \phi^2(t) \right\rangle \underset{t\to\infty}{\to} \frac{1}{Z_{\rm k=0}} \frac{1}{\Omega_{D+1} V''_{\rm eff}/Z_{\rm k=0}} = \frac{1}{\Omega_{D+1} V''_{\rm eff}}. \tag{4.105}$$

At finite RG scale, however, the running potential is changed in the presence of η_k. Its effect is to slow the flow down or, in other words, to make the RG time tick faster. This may be of interest if one is to interpret $V_k(\phi)$ as an approximation of the effective potential relevant for dynamics at scale k. It is therefore necessary to quantify this effect; to this end, we evaluate the expressions (4.69,4.96) along the flow using a field expansion.

4.4.2 Field expansion

For $N > 1$, the Goldstone modes dominate and yield a somewhat simpler flow which is well captured by an expansion in powers of the field around the minimum[11]. Here we take the lowest nontrivial order

$$U_k(\rho) = \frac{\lambda_k}{2}(\rho - \bar\rho_k)^2 + \dots \tag{4.106}$$

The flow of these two parameters can be extracted from the flow of the potential (see Eq. (3.47)). In the light IR regime, these are:

$$\dot{\bar\rho}_k = -\eta_k \bar\rho_k + \frac{(2-\eta_k)k^2}{2N\Omega_{D+1}} \left(\frac{3}{(k^2+m_k^2)^2} + \frac{N-1}{k^4} \right), \tag{4.107}$$

$$\dot\lambda = 2\eta_k \lambda_k + \frac{(2-\eta_k)k^2\lambda_k^2}{N\Omega_{D+1}} \left(\frac{9}{(k^2+m_k^2)^3} + \frac{N-1}{k^6} \right), \tag{4.108}$$

where $m_k^2 = 2\lambda_k\bar\rho_k$. Figure (4.1) shows the numerical integration of these equations, followed by the symmetric phase integration, as compared to their LPA equivalents. As predicted, we find that the effective mass and coupling are the same.

To find when the slowing of the flow is maximal, we consider the regime where $m_k^2 \gg k^2$. Indeed, in the opposite case we are close to symmetry restoration where η_k

[9] This argument requires that $\tilde k$ is well defined: if $\eta_k = 2$, $\tilde k$ is infinitely slowed with respect to k. This is never the case however, because the symmetry is eventually restored so that $\eta_k = 0$.

[10] This is because $\left\langle \phi^2(t) \right\rangle$ is the equal-time correlator function averaged on superhorizon modes.

[11] This is not the case for N=1 where such a truncation wrongly produces a phase transition, see appendix E.

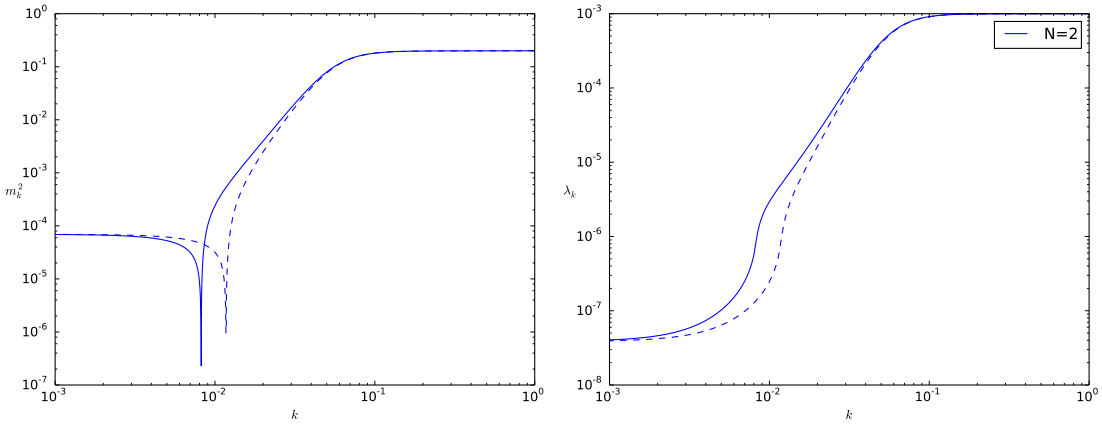


Figure 4.1: flow of the squared mass (left) and coupling (right) in the LPA' (full) and LPA (dashed) ansatz. The value at the end of the flow is the same in both cases, though the anomalous dimension slows the flow. Plotting the LPA' flow as a function of $\tilde{k} = \sqrt{Z_k}k$ would coincide exactly with the dashed line.

vanishes. The running anomalous dimension (4.96) therefore reduces to

$$\eta_k = \frac{2 - \eta_k}{2N\Omega_{D+1}\bar{\rho}_k k^2}, \tag{4.109}$$

and (4.107) approximates to

$$\dot{\bar{\rho}}_k = \frac{(2 - \eta_k)}{2N\Omega_{D+1}k^2}\left[N - 2 + O\left(\frac{k^2}{m_k^2}\right)\right]. \tag{4.110}$$

This has the same form as the contribution from Goldstone modes in (4.107), however, with $N-1$ replaced by $N-2$ in the presence of the running anomalous dimension (4.109). This is due to the $1/\bar{\rho}_k$ in η_k, and is reminiscent of the $d = 2$ XY model[12]. This suppression of the $N = 2$ flow is clear on figure (4.2) where this flow is frozen at first.

Exiting this regime is controlled by the flow of the coupling constant (or, equivalently, the mass)

$$\frac{\dot{\lambda}_k}{\lambda_k^2} = \frac{1}{\Omega_{D+1}k^4}. \tag{4.111}$$

Integrating and neglecting initial values, we get

$$\lambda_k = 4\Omega_{D+1}k^4, \tag{4.112}$$

from which we can extract the scale at which this regime breaks down, by demanding that $2\lambda_k\bar{\rho}_k = k^2$:

$$k^2 = \frac{1}{8\Omega_{D+1}\bar{\rho}_k}. \tag{4.113}$$

[12]There, the same effect together with the appropriate dimensionality generates a line of fixed points. This signals the Kosterlitz-Thouless transition [119]. This does not happen here because the effective dimension is zero.

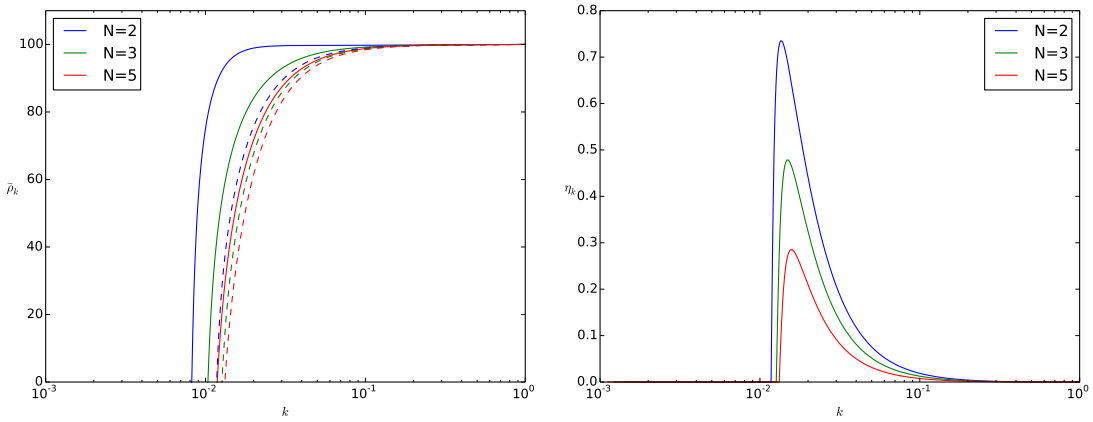


Figure 4.2: Left : IR Flow of the potential minimum $\bar{\rho}_k$ in the LPA (dashed) and LPA' (full line) using the polynomial ansatz. We see that for $N = 2$ fields the flow is suppressed at leading order, delaying the symmetry restoration. For any N, the symmetry restoration is preceded by a spike of the anomalous dimension (right). The anomalous dimension scales as $1/N$, so that the difference between LPA and LPA' decreases with N.

This corresponds to η_k of order one, as we can see on figure (4.2), after which the symmetry is rapidly restored.

We conclude by noting that the running anomalous dimension scales as $1/N$, and therefore vanishes at leading order of the large N approximation. This is already observable in figure (4.2). We illustrate it further by computing the renormalization of the field with same initial conditions but different values of N. Figure (4.3) confirms this expected behaviour.

Conclusion

In this last chapter we have aimed at going beyond the local potential approximation by means of the derivative expansion. We have met a number of obstacles along the way: first, such an expansion takes a much more complicated form in generally curved space-time. Although this does not play a role for de Sitter space, which is maximally symmetric, it is not excluded that difficulties may arise e.g. in considering quasi-de Sitter or FRW space-times. Second, the formulation of the derivative expansion in terms of a small parameter expansion is a complex task. This is by far the most tricky part, and relates directly to the non-commutation of Killing vectors in de Sitter space. As a consequence, we are unable to express this expansion in terms of the physical momentum. The solution we construct is to focus on the time Killing instead, taking the limit of homogeneous field configuration. We are then able to define a prescription for the running parameters of the derivative expansion

As a means to test this formalism, we have implemented the LPA' scheme. This

leads to very interesting discussions; the dimensional reduction still occurs, and it is in fact possible to define a zero-dimensional generating functional for this LPA' flow. It is a trivial modification of the LPA one, which consists only in changing the RG scale k for $\tilde{k} = \sqrt{Z_k}k$. As a consequence, the effective potential is unaffected by the field renormalization, and no corrections to the stochastic approach are found.

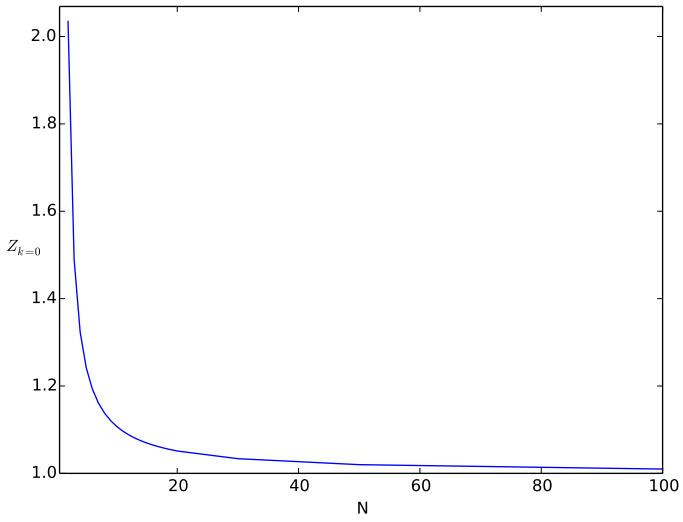


Figure 4.3: Renormalization of the field $Z_{k=0}$ from IR contributions as a function of N. Starting at Z_k=1 at the scale of the horizon, we find that the end value can be as much as doubled in $N = 2$ with our choice of initial conditions. As N grows larger, $Z_{k=0}$ decreases as the empirical law $\sim 1+1/N$.

4.4.3 Heavy UV regime

$$
\begin{aligned}
I_0+I_2+I_3 &= \frac{(2-\eta_k)k^2}{16i\bar{\nu}_l\bar{\nu}_t}\int_{p,p'} -\left(\frac{1}{\bar{\nu}_l}+\frac{1}{\bar{\nu}_t}\right)\left(\left(\frac{p}{p'}\right)^{\bar{\nu}_l+\bar{\nu}_t}+\left(\frac{p'}{p}\right)^{\bar{\nu}_l+\bar{\nu}_t}\right) log\frac{p'}{p}+\left(\left(\frac{p}{p'}\right)^{\bar{\nu}_t}-\left(\frac{p'}{p}\right)^{\bar{\nu}_t}\right)\left[\frac{1}{\bar{\nu}_l^2}\left(\left(\frac{k^2}{pp'}\right)^{\bar{\nu}_l}+\left(\frac{pp'}{k^2}\right)^{\bar{\nu}_l}-\left(\frac{p}{p'}\right)^{\bar{\nu}_l}-\left(\frac{p'}{p}\right)^{\bar{\nu}_l}\right)-\frac{1}{\bar{\nu}_t^2}\left(\left(\frac{p}{p'}\right)^{\bar{\nu}_t}-\left(\frac{p'}{p}\right)^{\bar{\nu}_t}\right)\right]\\
&= \frac{(2-\eta_k)k^2}{16i\bar{\nu}_l\bar{\nu}_t}\int_0^k\frac{dp}{p}p^{d-\gamma}\left[-ln\frac{k}{p}\left(\frac{p^{\bar{\nu}_l+\bar{\nu}_t}k^{\gamma-\bar{\nu}_l-\bar{\nu}_t}}{\gamma-\bar{\nu}_l-\bar{\nu}_t}+\frac{p^{-\bar{\nu}_l-\bar{\nu}_t}k^{\gamma+\bar{\nu}_l+\bar{\nu}_t}}{\gamma+\bar{\nu}_l+\bar{\nu}_t}\right)+k^\gamma\left(\frac{\left(\frac{p}{k}\right)^{\bar{\nu}_l+\bar{\nu}_t}}{(\gamma-\bar{\nu}_l-\bar{\nu}_t)^2}+\frac{\left(\frac{p}{k}\right)^{-\bar{\nu}_l-\bar{\nu}_t}}{(\gamma+\bar{\nu}_l+\bar{\nu}_t)^2}\right)-p^\gamma\left(\frac{1}{(\gamma-\bar{\nu}_l-\bar{\nu}_t)^2}+\frac{1}{(\gamma+\bar{\nu}_l+\bar{\nu}_t)^2}\right)\right]\left(\frac{1}{\bar{\nu}_l}+\frac{1}{\bar{\nu}_t}\right)\\
&+\left\{\frac{k^{\gamma+\bar{\nu}_l-\bar{\nu}_t}-p^{\gamma+\bar{\nu}_l-\bar{\nu}_t}}{\gamma+\bar{\nu}_l-\bar{\nu}_t}p^{\bar{\nu}_t-\bar{\nu}_l}-\frac{k^{\gamma+\bar{\nu}_l+\bar{\nu}_t}-p^{\gamma+\bar{\nu}_l+\bar{\nu}_t}}{\gamma+\bar{\nu}_l+\bar{\nu}_t}p^{-\bar{\nu}_t-\bar{\nu}_l}\right\}\left(\frac{1}{\bar{\nu}_l^2}\left(\frac{k}{p}\right)^{2\bar{\nu}_l}-\frac{1}{\bar{\nu}_l^2}-\frac{1}{\bar{\nu}_t^2}\right)+\left\{\frac{k^{\gamma-\bar{\nu}_l-\bar{\nu}_t}-p^{\gamma-\bar{\nu}_l-\bar{\nu}_t}}{\gamma-\bar{\nu}_l-\bar{\nu}_t}p^{\bar{\nu}_t+\bar{\nu}_l}-\frac{k^{\gamma-\bar{\nu}_l+\bar{\nu}_t}-p^{\gamma-\bar{\nu}_l+\bar{\nu}_t}}{\gamma-\bar{\nu}_l+\bar{\nu}_t}p^{-\bar{\nu}_t+\bar{\nu}_l}\right\}\left(\frac{1}{\bar{\nu}_l^2}\left(\frac{k}{p}\right)^{2\bar{\nu}_l}-\frac{1}{\bar{\nu}_l^2}-\frac{1}{\bar{\nu}_t^2}\right)\\
&\underset{H\to 0}{=} \frac{(2-\eta_k)k^{d+2}}{8di\bar{\nu}_l\bar{\nu}_t}\left[\left(\frac{1}{\bar{\nu}_l^2}+\frac{1}{\bar{\nu}_t^2}\right)\left(\frac{1}{\gamma-\bar{\nu}_l-\bar{\nu}_t}-\frac{1}{\gamma+\bar{\nu}_l+\bar{\nu}_t}\right)-\left(\frac{1}{\bar{\nu}_l}+\frac{1}{\bar{\nu}_t}\right)\left(\frac{1}{(\gamma-\bar{\nu}_l-\bar{\nu}_t)^2}+\frac{1}{(\gamma+\bar{\nu}_l+\bar{\nu}_t)^2}\right)\right]
\end{aligned}
$$

The first two lines must be symmetrize in $\bar{\nu}_t \leftrightarrow \bar{\nu}_l$. This is done in the last line by simply multiplying by two. By deriving with respect to γ^2, and evaluating at the minimum of the potential, we get the expression for the anomalous dimension :

$$
\eta_k = \frac{\rho U_k'^2\Omega_d}{(2\pi)^d}\frac{(2-\eta_k)k^{d+1}}{4dM_k(k+M_k)^3}\left[\left(\frac{1}{k}+\frac{1}{M_k}\right)\frac{3}{k+M_k}-\frac{1}{k^2}-\frac{1}{M_k^2}\right] \tag{4.114}
$$

where $M_k^2 = k^2 + m_k^2$.

4.5 first order derivative expansion and anomalous dimension in the symmetric phase

We now consider a first order derivative expansion, that is, Z_k depends on ϕ. The flow of $\Gamma_k^{(2)}$ then contains additional terms through $\Gamma^{(3)}$ and $\Gamma^{(4)}$:

$$\begin{aligned}
-\Gamma^{(3)}_{xyz} =& V^{(3)}\delta_{xy}\delta_{xy}\delta_{xz} + Z'_x\delta_{xz}\Box_x\delta_{xy} + Z'_y\delta_{yz}\Box_y\delta_{xy} + Z'_x\delta_{xy}\Box_x\delta_{xz} \\
&+ \frac{1}{2}\left(Z''_x\phi_x\delta_{xz}\Box_x\delta_{yx} + Z''_y\phi_y\delta_{yz}\Box_y\delta_{yx} + Z''_x\phi_x\delta_{xy}\Box_x\delta_{zx} \right) \\
&+ \frac{3}{2}Z''_x\delta_{yx}\delta_{xz}\Box_x\phi_x + \frac{3}{2}Z^{(3)}_x\delta_{yx}\delta_{xz}\phi_x\Box_x\phi_x
\end{aligned} \tag{4.115}$$

$$-\Gamma^{(4)}_{xyzt} = \frac{3}{2}\left(Z''_x\delta_{xy}\delta_{yz}\Box_z\delta_{zt} + Z''_y\delta_{yz}\delta_{zt}\Box_t\delta_{tx} + Z''_z\delta_{zt}\delta_{tx}\Box_x\delta_{xy} + Z''_t\delta_{tx}\delta_{xy}\Box_y\delta_{yz} \right) \tag{4.116}$$

In the symmetric phase, this results in a non-zero contribution to the running of Z_k : $\tilde{\partial}\int_q F(q,q)$.

Conclusion

The purpose of this thesis is to demonstrate the potential of NPRG techniques to study de Sitter physics. Following the steps of Refs. [65,66], we have shown that a formalism can be found that allows us to compute the effective potential on superhorizon scales. This not only corroborates the results of other methods, in particular the stochastic approach, but also provides an alternative mathematical approach (namely a flow equation) to compute the quantitites of interest. We have implemented a number of methods to solve this flow equation, from large N techniques to zero dimensional path integrals, that contribute to the arsenal of resummation tools in de Sitter space.

It is worth discussing again the dimensional reduction that occurs for light fields in the infrared flow. While this phenomenon is well understood in compact spaces, such as the sphere [64], or in finite volume [122], its origin is clearly different in de Sitter space. In particular, although the sphere is thought of as the Euclidean equivalent of de Sitter, we obtain the same flow function using very different regulators in the two cases. It seems that this asymptotic limit is somehow enforced in order to reproduce the stochastic solution (and thus also the spherical flow). This begs the question as to what would happen with a regulation scheme that respects all the de Sitter isometries.

The next step in this thesis was to go beyond the Local Potential Approximation. This follows the same line of thought as in statistical physics, where the NPRG has been largely implemented for many purposes. We have therefore discussed the derivative expansion in the general context of curved-space time, where matters are greatly more complicated. For instance, the meaning of large scale physics is unclear in the presence of an unspecified local curvature scale. The maximal symmetry of de Sitter space makes this matter simple enough to expand the effective action in terms of the Laplace-Beltrami operator. As a first step beyond the LPA, we then introduced a field-independent running of the kinetic term.

A challenge we faced was to extract a prescription for the flow of this field renormalization. In Euclidean theories, one can easily move to Fourier space and define this parameter as the quadratic coefficient of the inverse correlator. The impossibility to diagonalize time and spatial derivatives simultaneously in de Sitter space hinders this task. In particular, it does not seem possible to access the flow of Z_k through physical momentum dependencies. The solution we opted for was to focus on frequency dependency by building time dependent, spatially homogeneous states. Because of our regulation scheme, frequency and momentum dependencies are not equivalent. They provide different flows for Z_k In Minkowski space, however this effect is negligeable in

all situations where the anomalous dimension is small.

The first interesting question related to the renormalization of the field is its influence on the effective potential. There again, the equivalence with a zero-dimensional theory simplifies the problem drastically. In this case, we have shown that, while slowing the flow down, the running anomalous dimension leaves the effective potential (at the end of the flow) exactly unchanged. This is consistent with the results of Ref. [55], and hints that non-local contributions do not alter the result of the stochastic approach.

The role of the field renormalization, however restricted by this finding, is not necessarily non-existent. In the NPRG approach, although physical observables are defined at the end of the flow, it is generally understood that running quantities give an insight on the physics at intermediate scales. Because the anomalous dimension slows the flow, it could have nontrivial implications for inflationary models.

There are a number of prospects I have in mind following this thesis. The first one is to further improve the approximation scheme by allowing a field dependency of Z_k. It is the proper way of implementing the first order derivative expansion, and therefore provides more robust results with potentially new physics. Furthermore, this provides a handle on the field renormalization in the symmetric phase, which was not possible until now. The underlying question is wether the effective potential remains unaffected in this case or not, possibly bringing corrections to the stochastic approach.

The regulation of physical momenta, while providing an efficient formalism, raises a number of issues. In the mindset of providing a solid basis for NPRG techniques in de Sitter, it would be interesting to perform an analysis of the regulation scheme. This could be done in the manner of Ref. [116], by considering a numerical prefactor to the regulator function and analyzing the influence of this parameter on the results. The optimal regulator is then expected to minimize this sensitivity. Another handle on the shortcomings of the p-representation is to compute the modified Ward identities that follow from the broken isometries. This would provide a measurement of the error induced. Finally, it would be most interesting to bypass this question altogether by implementing a de Sitter invariant regulation scheme. Heat kernel methods, in particular, are well adapted to perform this. It would be interesting to adapt this tool to the problem at hand. As mentioned above, it is of prime interest to see wether the same results appear that corroborate the stochastic approach and other techniques.

In this thesis, it may seem to the unsuspecting reader that the NPRG is always implemented with the derivative expansion. Although the Wetterich equation is indeed complex enough that it requires some approximation scheme, there are many others capable of providing rich results. In particular, the derivative expansion does not resum nonlocal contributions to the correlator functions. An efficient technique to perform this is the Blaizot-Mendes-Wschebor method [117], which captures the full momentum dependency of correlators. It would be very interesting to adapt this method in the present out-of-equilibrium context[13]. This is all the more valuable that few nonperturbative methods exist to capture these physics.

[13]The BMW approximation has already been implemented for the out-of-equilibrium KPZ model [123].

I would like to conclude with the physical motivations that bring so much attention to quantum fields in de Sitter space. Inflationary physics and dark energy extend the focus outside of scalar fields, to vector particles [124], gauge interactions[14] [126] as well as graviton loops. Realistic models also require a finite duration e.g. with slow-roll parameters in quasi-de Sitter. The NPRG can be systematically implemented in these scenarii to provide further insight on the early and late universe.

[14] NPRG has recently been applied to scalar QED [125].

Appendices

What am I working on? Uhh... I'm working on something that will change the world, and human life as we know it.

– Jeff Goldblum as Seth Brundle, *The fly*

Contents

A Hankel functions cheat sheet 88
A.1 General relations 88
A.2 Infrared regime 88
A.3 Ultraviolet regime 89
B Explicit calculation of $B(\nu, k, x)$ 90
C Dimensionally reduced RG flow 92
D Dimensionally reduced integral for large N 93
E Truncation effects for $N = 1$ 95
F Correlator functions 97
G Ultraviolet flow of the inverse correlator 99
G.1 Tadpole contribution 99
G.2 Sunset contributions 100
H Infrared flow of the inverse correlator 102
H.1 Tadpole contribution 102
H.2 Sunset contributions 102
H.3 $0(N)$ case 104

A Hankel functions cheat sheet

The Hankel function, being the free mode function in de Sitter space, appears in a great number of the calculations along this thesis. We summarize here a number of useful relations that we have used to obtain the various limits of interest. See [127] for more details.

Let us start with the definition of the Hankel functions of first and second type from the Bessel functions:

$$H_\nu^{(1)}(p) = J_\nu(p) + iY_\nu(p), \qquad H_\nu^{(2)}(p) = J_\nu(p) - iY_\nu(p), \tag{A.1}$$

where

$$J_\nu(p) = \left(\frac{p}{2}\right)^\nu \sum_{k=0}^{\infty}(-1)^k \frac{(p/2)^{2k}}{k!\Gamma(\nu+k+1)}, \qquad Y_\nu(p) = \frac{J_\nu(p)\cos(\nu\pi) - J_{-\nu}(p)}{\sin(\nu\pi)}. \tag{A.2}$$

In what follows, as well as everywhere in the main text, we use only the Hankel function of first kind and note $H_\nu^{(1)}(p) = H_\nu(p)$.

A.1 General relations

When the order is an integer $n \in \mathbb{N}$,

$$H_n(p) = (-i)^{n+1}\frac{e^{ip}}{p}\sum_{k=0}^{n}\frac{i^k}{k!(2p)^k}\frac{(n+k)!}{(n-k)!} \tag{A.3}$$

The following identities hold for any order:

$$W\{H_\nu^{(1)}(p), H_\nu^{(2)}(p)\} = H_{\nu+1}^{(1)}(p)H_\nu^{(2)}(p) - H_\nu^{(1)}(p)H_{\nu+1}^{(2)}(p) \tag{A.4}$$

$$= H_\nu(p)H_\nu'^{*}(p) - H_\nu'(p)H_\nu^{*}(p) = -\frac{4i}{\pi p} \tag{A.5}$$

$$H_{\nu-1}(p) + H_{\nu+1}(p) = \frac{2\nu}{p}H_\nu(p) \tag{A.6}$$

$$H_{\nu-1}(p) - H_{\nu+1}(p) = 2H_\nu'(p) \tag{A.7}$$

$$H_\nu'(p) = H_{\nu-1}(p) - \frac{\nu}{p}H_\nu(p) = -H_{\nu+1}(p) + \frac{\nu}{p}H_\nu(p) \tag{A.8}$$

$$H_{-\nu}(p) = e^{i\pi\nu}H_\nu(p) \tag{A.9}$$

$$\tag{A.10}$$

A.2 Infrared regime

For $p \ll 1$ and $\mathrm{Re}[\nu] > 0$:

$$H_\nu(p) \sim \frac{1}{\Gamma(\nu+1)}\left(\frac{p}{2}\right)^\nu + \frac{1}{i\pi}\Gamma(\nu)\left(\frac{2}{p}\right)^\nu \tag{A.11}$$

$$H_{i\nu}(p) \sim \frac{1}{sinh(\pi\nu)}\left(\frac{e^{\pi\nu}}{\Gamma(1+i\nu)}\left(\frac{p}{2}\right)^{i\nu} - \frac{1}{\Gamma(1-i\nu)}\left(\frac{p}{2}\right)^{-i\nu}\right) \tag{A.12}$$

$$H_{i\nu-1}(p) \sim i\frac{e^{\pi\nu}}{\pi}\Gamma(1-i\nu)\left(\frac{p}{2}\right)^{i\nu-1} \tag{A.13}$$

A.3 Ultraviolet regime

When $p \gg 1$,

$$H_\nu(p) \sim \sqrt{\frac{2}{\pi p}} e^{ip - i\frac{\pi}{2}(\nu+\frac{1}{2})} \tag{A.14}$$

When $m, p \gg 1$,

$$H_{im}(p) = \sqrt{\frac{2}{\pi}} \frac{1}{(p^2+m^2)^{\frac{1}{4}}} \exp\left(i\sqrt{p^2+m^2} - im\ sinh^{-1}\left(\frac{m}{p}\right) + \frac{m\pi}{2} - i\frac{\pi}{4}\right) \tag{A.15}$$

$$H'_{im}(p) = \frac{i\sqrt{m^2+p^2}}{p} H_{im}(p) \tag{A.16}$$

B Explicit calculation of $B(\nu,k,x)$

The flow of the potential is given by

$$\dot{V}_k = \frac{1}{2}\int \frac{d^dp}{(2\pi)^d}\dot{R}_k(p)\frac{|\hat{u}_k(p)|^2}{Z_k p}, \tag{B.1}$$

where $\hat{u}_k$ is given by (F.3) and $\dot{R}_k(p) = Z_k\big[(2-\eta_k)k^2+\eta_k p^2\big]\theta(k^2-p^2)$. The LPA corresponds to $Z_k=1$ and $\eta_k=0$. Injecting this in the flow equation, we get

$$\dot{V}_k(\phi) = A_d k^{d+2}\big[(2-\eta_k)B(\nu_k,k,d)+\eta_k B(\nu_k,k,d+2)\big] \tag{B.2}$$

where $A_d = \dfrac{\pi\Omega_d}{8(2\pi)^d}$ and $B(\nu,k,x)$ is defined as

$$B(\nu,k,x) = \int_0^k dp\, p^{x-1}\left|c_k^+\left(\frac{p}{k}\right)^{\bar{\nu}} + c_k^-\left(\frac{k}{p}\right)^{\bar{\nu}}\right|^2. \tag{B.3}$$

We remind that $c_k^\pm = \frac{1}{2}\left[H_{\nu_k}(k)\pm\frac{k}{\bar{\nu}_k}H'_{\nu_k}(k)\right]$. The coefficients ν and $\bar{\nu}$ are either real or pure imaginary, and are related by $\bar{\nu}^2=\nu^2-k^2$. To simplify notations, we write

$$\nu_r = \mathrm{Re}[\nu], \qquad \bar{\nu}_r = \mathrm{Re}[\bar{\nu}], \tag{B.4}$$

$$\nu_i = i\mathrm{Im}[\nu], \qquad \bar{\nu}_i = i\mathrm{Im}[\bar{\nu}], \tag{B.5}$$

with the following properties:

$$\nu_i\nu_r = 0, \qquad \bar{\nu}_i\bar{\nu}_r = 0, \tag{B.6}$$

$$\nu_i+\nu_r = \nu, \qquad \bar{\nu}_i+\bar{\nu}_r = \bar{\nu}. \tag{B.7}$$

After direct integration,

$$\begin{aligned} B(\nu,k,x) &= \frac{e^{i\pi\nu_i}}{4x^2(x^2-4\bar{\nu}^2)}\Bigg[(x^2-4\bar{\nu}_i^2)(x-2\bar{\nu}_r)\left|H_\nu+\frac{k}{\bar{\nu}}H'_\nu\right|^2 + (x^2-4\bar{\nu}_i^2)(x+2\bar{\nu}_r)\left|H_\nu-\frac{k}{\bar{\nu}}H'_\nu\right|^2 \\ &\quad + 2(x^2-4\bar{\nu}_r^2)Re[(H_\nu+\frac{k}{\bar{\nu}}H'_\nu)(H_\nu-\frac{k}{\bar{\nu}}H'_\nu)^*(x-2\bar{\nu}_i)]\Bigg] \qquad \text{(B.8)} \\ &= \frac{e^{i\pi\nu_i}}{4x^2(x^2-4\bar{\nu}^2)}\Bigg[2x(x^2-4\bar{\nu}_i^2)(|H_\nu|^2+\left|\frac{k}{\bar{\nu}}H'_\nu\right|^2) - 8\bar{\nu}_r(x^2-4\bar{\nu}_i^2)Re[\frac{k}{\bar{\nu}}H^*_\nu H'_\nu] \\ &\quad + 2x(x^2-4\bar{\nu}_r^2)(|H_\nu|^2-\left|\frac{k}{\bar{\nu}}H'_\nu\right|^2) - 8i\bar{\nu}_i(x^2-4\bar{\nu}_r^2)Im[\frac{k}{\bar{\nu}}H^*_\nu H'_\nu]\Bigg] \qquad \text{(B.9)} \\ &= \frac{e^{i\pi\nu_i}}{x(x^2-4\bar{\nu}^2)}\Big[(x^2-2\nu^2+2k^2)|H_\nu|^2+2k^2|H'_\nu|^2-2xkRe[H^*_\nu H'_\nu]\Big]. \qquad \text{(B.10)} \end{aligned}$$

Alternatively, using (A.8) to express H'_ν in terms of $H_{\nu-1}$ or $H_{\nu+1}$,

$$\begin{aligned} B(\nu,k,x) =& \frac{e^{i\pi\nu_i}}{x(x^2-4\bar{\nu}^2)}\Big[(x^2-2\bar{\nu}^2+2|\nu|^2+2x\nu_r)|H_\nu|^2+2k^2|H_{\nu-1}|^2 \qquad \text{(B.11)} \\ &- 2xkRe[H_\nu H^*_{\nu-1}] - 4kRe[\nu H_\nu H^*_{\nu-1}]\Big] \qquad \text{(B.12)} \\ =& \frac{e^{i\pi\nu_i}}{x(x^2-4\bar{\nu}^2)}\Big[(x^2-2\bar{\nu}^2+2|\nu|^2-2x\nu_r)|H_\nu|^2+2k^2|H_{\nu+1}|^2 \\ &+ 2xkRe[H_\nu H^*_{\nu+1}] - 4kRe[\nu H_\nu H^*_{\nu+1}]\Big]. \qquad \text{(B.13)} \end{aligned}$$

Notice that the symmetry $\nu \to -\nu$ is respected for any value of this parameter (real or pure imaginary). This is clear at line (B.10) using $H_{-\nu}(p) = e^{i\pi\nu} H_\nu(p)$.

This computation is related to the notation of the main text (chapter **??**) by

$$B_d(\nu, k) = d(d^2 - 4\bar{\nu}^2) B(\nu, k, d). \tag{B.14}$$

It has the following asymptotic behaviors:

$\nu \in \mathbb{R}^*$	IR	UV
$B_d(\nu, k) \sim$	$(d^2 + 2d\nu)\frac{\Gamma^2(\nu)}{\pi^2}\left(\frac{2}{k}\right)^{2\nu}$	$\frac{8}{\pi}\sqrt{k^2 - \nu^2}, \quad k > \nu$
$B_d(i\nu, k) \sim$	$\frac{1}{sinh(\pi\nu)}\left[\frac{2(d^2 + 4\nu^2)}{\lvert\Gamma(1 + i\nu)\rvert^2} coth(\pi\nu) + 4\pi\nu Re\left[\frac{1}{\Gamma^2(1 + i\nu)}\left(\frac{k}{2}\right)^{2i\nu}\right]\right]$	$\frac{8}{\pi}\sqrt{k^2 + \nu^2}$
$B_d(0, k) \sim$	$\frac{4d^2}{\pi^2} log\left(\frac{k}{2}\right)^2 - \frac{8d}{\pi} log\left(\frac{k}{2}\right) + \mathcal{O}(k^0)$	$\frac{8k}{\pi}$

C Dimensionally reduced RG flow

In this section we show how the flow of the parameters describing the effective potential in the regime of dimensional reduction can be read off the equivalent zero-dimensional theory, Eq. (2.33). For the sake of the discussion we focus on the symmetric phase and we only consider the square mass and the quartic coupling, defined as

$$m_k^2 = U_k'(0) \quad \text{and} \quad \lambda_k = U_k''(0). \tag{C.1}$$

The discussion can easily be extended to any other coupling. At vanishing sources, the first nontrivial correlators have the following $O(N)$ structures

$$\langle \varphi_a \varphi_b \rangle = \delta_{ab} G_k \tag{C.2}$$

and

$$\langle \varphi_a \varphi_b \varphi_c \varphi_d \rangle = (\delta_{ab}\delta_{cd} + \delta_{ac}\delta_{bd} + \delta_{ad}\delta_{bc}) C_k^{(4)}. \tag{C.3}$$

The two- and four-point functions G_k and $C_k^{(4)}$ are related to the parameters of the effective potential $U_k(\rho)$ through the Legendre transform (2.34) as

$$G_k = \frac{1}{\Omega_{D+1}(k^2 + m_k^2)} \tag{C.4}$$

and

$$C_k^{(4)} = G_k^2 - \frac{\Omega_{D+1}\lambda_k}{N} G_k^4. \tag{C.5}$$

For a potential at the horizon scale of the form $U_{k_0}(\rho) \approx m_{k_0}^2 \rho + \lambda_{k_0}\rho^2/2$, the various correlators of the theory are obtained from the moments

$$\langle (\varphi_a \varphi_a)^q \rangle = \frac{\int_0^\infty d\varphi \varphi^{N+2q-1} e^{-\alpha\varphi^2 - \beta\varphi^4}}{\int_0^\infty d\varphi \varphi^{N-1} e^{-\alpha\varphi^2 - \beta\varphi^4}}, \tag{C.6}$$

where we introduced $\alpha = \Omega_{D+1}(k^2 + m_{k_0}^2)/2$ and $\beta = \Omega_{D+1}\lambda_{k_0}/(8N)$. For instance, one has $G_k = \langle \varphi_a \varphi_a \rangle / N$ and $C_k^{(4)} = \langle (\varphi_a \varphi_a)^2 \rangle / [N(N+2)]$. The moments (C.6) can easily be computed. For instance, in the limit $\beta/\alpha^2 \gg 1$, which corresponds to the critical case discussed in the main text, one has

$$\langle (\varphi_a \varphi_a)^q \rangle \approx \beta^{-\frac{q}{2}} \frac{\Gamma\left(\frac{N+2q}{4}\right)}{\Gamma\left(\frac{N}{4}\right)}. \tag{C.7}$$

Putting Eqs. (C.4)–(C.7) together, one obtains Eqs. (2.101)–(2.102). The other limit of interest is that of a would-be broken phase, corresponding to $\alpha < 0$ and $\beta/\alpha^2 \ll 1$. In that case, one gets

$$\langle (\varphi_a \varphi_a)^q \rangle \approx \left(\frac{|\alpha|}{2\beta} \right)^q, \tag{C.8}$$

from which Eq. (2.104) follows.

D Dimensionally reduced integral for large N

The generating functional of the zero-dimensional theory,

$$e^{-\Omega_{D+1}\mathcal{W}_k(J)}=\int d^N\varphi\, e^{-\Omega_{D+1}\left[V_{\text{eff}}(\varphi)+J\cdot\varphi+\frac{k^2}{2}\varphi^2\right]} \tag{D.1}$$

can be computed exactly for a ϕ^4 theory in the large N limit, reproducing the solution to the flow presented in section 2.4.2. For simpler notations, and proper $1/N$ scalings, let us compute

$$e^{NW(J)} = \int d^N\varphi \exp\left(-\frac{\alpha}{2}\varphi^2 - \frac{\beta}{2N}(\varphi^2)^2 + J\cdot\varphi\right), \tag{D.2}$$

where $\alpha = \Omega_{D+1}(m_{k_0}^2 + k^2)$ and $\beta = \Omega_{D+1}\lambda_{k_0}/4$. Using the identity

$$e^{-\frac{\beta}{2N}(\varphi^2)^2} = \sqrt{\frac{N}{2\pi}}\int d\chi \exp\left(-\frac{N}{2}\chi^2 + i\sqrt{\beta}\chi\varphi^2\right), \tag{D.3}$$

we write:

$$\begin{aligned} e^{NW(J)} &= \sqrt{\frac{N}{2\pi}}\int d\chi d^N\varphi \exp\left[-\left(\frac{\alpha}{2} - i\sqrt{\beta}\chi\right)\varphi^2 - \frac{N}{2}\chi^2 + J\cdot\varphi\right] \\ &= \sqrt{\frac{N}{2\pi}}\pi^{N/2}\int d\chi \exp\left(-N\left[\frac{1}{2}\chi^2 + \frac{1}{2}\ln\left(\frac{\alpha}{2} - i\sqrt{\beta}\chi\right) - \frac{j^2}{4(\frac{\alpha}{2} - i\sqrt{\beta}\chi)}\right]\right) \\ &\equiv \sqrt{\frac{N}{2\pi}}\pi^{N/2}\int d\chi \exp\left(-NF(\chi, j)\right) \end{aligned} \tag{D.4}$$

with $J_a = \sqrt{N}j_a$. We can now use the saddle point technique to compute the $N\to\infty$ limit. Defining $\bar\chi$ as

$$\left.\frac{\partial F}{\partial\chi}\right|_{\bar\chi} = 0 \iff i\bar\chi + \frac{\sqrt{\beta}}{2(\frac{\alpha}{2} - i\sqrt{\beta}\bar\chi)} + \frac{\sqrt{\beta}j^2}{4(\frac{\alpha}{2} - i\sqrt{\beta}\bar\chi)^2} = 0, \tag{D.5}$$

the saddle point approximation gives

$$W(j) = -F(\bar\chi(j), j) + C(N), \tag{D.6}$$

where $C(N)$ is a constant depending on N only. We discard it as it is irrelevant to the computation of the effective potential. The average field is defined as

$$\phi_a \equiv \frac{\partial W}{\partial j_a} = \frac{j_a}{2(\frac{\alpha}{2} - i\sqrt{\beta}\bar\chi)} \iff j_a = 2\mathcal{K}(\phi)\phi_a, \tag{D.7}$$

where we have introduced $\mathcal{K} = \frac{\alpha}{2} - i\sqrt{\beta}\bar\chi$. To compute the effective potential, we take the Legendre transform

$$\begin{aligned} V(\phi) &= -W(j) + j\phi \\ &= -\frac{(\frac{\alpha}{2} - \mathcal{K})^2}{2\beta} + \frac{1}{2}\ln\mathcal{K} + \mathcal{K}\phi^2. \end{aligned} \tag{D.8}$$

To find $\mathcal{K}$ as a function of ϕ, we write (D.5) as

$$\mathcal{K} = \frac{\alpha}{2} + \frac{\beta}{2\mathcal{K}} + \beta\phi^2, \tag{D.9}$$

which gives:

$$\mathcal{K}(\phi) = \frac{\alpha}{4} + \frac{\beta}{2}\phi^2 + \sqrt{\left(\frac{\alpha}{4} + \frac{\beta}{2}\phi^2\right)^2 + \frac{\beta}{2}} \tag{D.10}$$

Mixing this properly into Eq. (D.8),

$$V(\phi) - V(0) = \frac{\mathcal{K}^2(\phi) - \mathcal{K}^2(0)}{2\beta} + \frac{1}{2}\ln\frac{\mathcal{K}(\phi)}{\mathcal{K}(0)}. \tag{D.11}$$

This reproduces Eq. (2.67) and (2.68) with the substitutions

$$\alpha \to \Omega_{D+1}(m_{k_0}^2 + k^2), \tag{D.12}$$

$$\beta \to \Omega_{D+1}\frac{\lambda_{k_0}}{4}, \tag{D.13}$$

$$V(\phi) \to \Omega_{D+1}\big[U_k(\rho) + k^2\rho\big], \tag{D.14}$$

$$\mathcal{K}(\phi) \to \frac{\Omega_{D+1}}{2}M_k^2(\rho). \tag{D.15}$$

There is one subtlety here to identify both computations: we have integrated the flow from k_0 to k and identified the potential at k_0 as the bare potential. Strictly speaking, this is only true if $k_0 \gg k$. In this limit, both results are indeed identical.

E Truncation effects for $N = 1$

Although the dimensional reduction is responsible for symmetry restoration in the infrared for all N, this behavior is not captured by a field expansion around the potential minimum when there are no Goldstone modes. Indeed, using such an expansion in the case $N = 1$, we find a spurious, nontrivial phase structure with a line of fixed points that we now describe. Using the lowest order polynomial

$$U_k(\rho) = \frac{\lambda_k}{2}(\rho - \bar{\rho}_k)^2, \tag{E.1}$$

with the notation (2.52), we reduce the functional flow to that of two parameter defined as

$$U_k'(\bar{\rho}_k) = 0 \quad \text{and} \quad U_k''(\bar{\rho}_k) = \lambda_k. \tag{E.2}$$

The corresponding flows are

$$\dot{\bar{\rho}}_k = -\frac{\dot{U}_k'(\bar{\rho}_k)}{U_k''(\bar{\rho}_k)} \quad \text{and} \quad \dot{\lambda}_k = \dot{U}_k''(\bar{\rho}_k), \tag{E.3}$$

where we have already neglected third order derivatives. In the light IR regime $m_k, k \ll 1$, the flow function reduces to

$$\dot{U}_k = \frac{1}{\Omega_{D+1}} \frac{k^2}{k^2 + U_k' + 2\rho U_k''} \tag{E.4}$$

and we get

$$\dot{\bar{\rho}}_k = \frac{3}{\Omega_{D+1}} \frac{k^2}{(k^2 + 2\lambda_k \bar{\rho}_k)^2}, \qquad \dot{\lambda}_k = \frac{18\lambda_k^2}{\Omega_{D+1}} \frac{k^2}{(k^2 + 2\lambda_k \bar{\rho}_k)^3}. \tag{E.5}$$

When looking for critical properties, it is important to work with properly rescaled quantities which have autonomous flows. This is necessary to obtain fixed point solutions which, when they exist, describe critical regimes. In flat space, this scaling is directly related to the dimensionality of each quantity, e.g. $\bar{\rho}_k k^{2-D}$ and $\lambda_k k^{D-4}$, and translates the absence of any fixed scale in the critical flow. Here the dimension is effectively zero, and performing this change of variables reveals no fixed points. However, the fact that we appear to be in zero dimensions is the signature of a non-flowing scale, the Hubble scale H. As a consequence, we are not as restricted as in flat space to build dimensionless quantities and our search for fixed points must exhaust all possibilities before we are able to conclude. As it turns out, exhausting all possibilities, we find the exotic dimensioning

$$\lambda_k = l_k k^{\frac{2}{3}}, \qquad \bar{\rho}_k = r_k k^{\frac{2}{9}}, \tag{E.6}$$

for which we get the following flow equations:

$$\dot{r}_k = -\frac{2}{9} r_k + \frac{3}{4\Omega_{D+1} l^2 r^2} \qquad \dot{l}_k = -\frac{2}{3} l_k + \frac{9}{4\Omega_{D+1} l r^3} \tag{E.7}$$

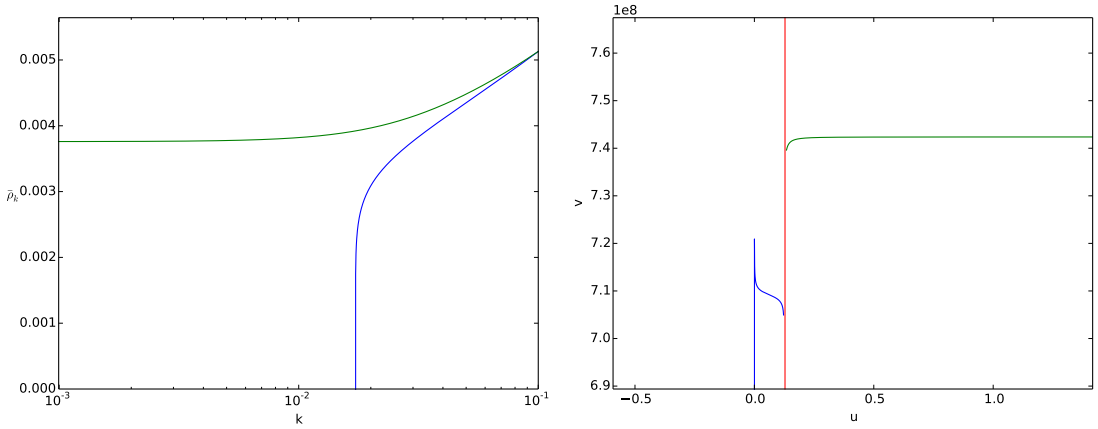


Figure E.1: Flow of the potential minimum (left) for two sets of initial conditions close to criticality. A small variation in the initial coupling affects the symmetry restoration. On the right, we plot u_k versus v_k. The green curve corresponds to a flow in the broken phase characterized by $v_k = \text{const}$. On the other side of the critical line $u_k = u^*$ (in red), we find a flow which restores the symmetry (in blue). A rapid exit of the regime where $k^2 \ll m_k^2$ means that v_k is no longer a constant, and in fact diverges at the scale of restoration.

when we are sufficiently deep in the infrared for the regulator k^2 to be small with respect to the mass $2\lambda_k\bar{\rho}_k = 2l_k r_k k^{8/9}$. Fixed points are found by canceling both flows. Both equations give the same condition:

$$l_*^2 r_*^3 = \frac{27}{8\Omega_{D+1}} \equiv u_*. \tag{E.8}$$

Defining $u_k \equiv l_k^2 r_k^3$ and $v_k = l_k / r_k^3$, we get

$$\dot{u}_k = -2(u_k - u_*) \quad \text{and} \quad \dot{v}_k = 0. \tag{E.9}$$

The line $u = u^*$ is composed of repulsive fixed points. These are indeed critical points, since the mass goes to zero at the end of the flow and it separates a broken and a symmetric phase (see figure E.1). For $u_k > u^*$, $\bar{\rho}_k$ flows to a positive constant. For $u_k < u^*$, it reaches zero at a finite scale[15].

We therefore find a possible symmetry breaking in the effective potential. This is inconsistent with the argument of convexification explained in the main text, and is an artifact of the field expansion.

[15]In this case, the regulator can no longer be neglected with respect to the mass and must be reintroduced in the flow equations.

F Correlator functions

For a single field, the two-point function is decomposed as

$$\hat{G}(p,p') = \hat{F}(p,p') - \frac{i}{2}\text{sign}_{\hat{C}}(p-p')\hat{\rho}(p,p'). \tag{F.1}$$

The statistical and spectral correlators are respectively

$$\hat{F}_k = \frac{1}{Z_k}\,\text{Re}[\hat{u}_k(p)\hat{u}_k^*(p')] \quad \text{and} \quad \hat{\rho}_k = -\frac{2}{Z_k}\,\text{Im}[\hat{u}_k(p)\hat{u}_k^*(p')]. \tag{F.2}$$

With the Litim regulator, the mode function writes

$$\begin{aligned} \hat{u}_k(p) &= \sqrt{\frac{\pi p}{4}}e^{i\varphi_k}\left[c_k^+\left(\frac{p}{k}\right)^{\bar{\nu}_k} + c_k^-\left(\frac{k}{p}\right)^{\bar{\nu}_k}\right] \quad \text{for } p \le k, \\ \hat{u}_k(p) &= \sqrt{\frac{\pi p}{4}}e^{i\varphi_k}H_{\nu_k}(p) \qquad\qquad\qquad\qquad \text{for } p \ge k, \end{aligned} \tag{F.3}$$

where

$$\varphi_k = \frac{\pi}{2}\nu_k + \frac{\pi}{4}, \qquad \nu_k = \sqrt{\frac{d^2}{4} - \frac{V_k''}{Z_k}}, \qquad \bar{\nu}_k^2 = \nu_k^2 - k^2, \tag{F.4}$$

$H_\nu(p)$ is the Hankel function of the first kind, and the coefficients

$$c_k^\pm = \frac{1}{2}\left[H_{\nu_k}(k) \pm \frac{k}{\bar{\nu}_k}H'_{\nu_k}(k)\right] \tag{F.5}$$

have the following exact properties:

$$Im[c_k^+ c_k^{-*}] = \begin{cases} \dfrac{1}{\pi\bar{\nu}_k} & \text{if } \bar{\nu}_k \in \mathbb{R} \\ -\dfrac{i\pi k^2}{16\bar{\nu}_k}Re[H_{\nu_k}^* H'_{\nu_k}] & \text{if not} \end{cases} \tag{F.6}$$

$$|c_k^+|^2 - |c_k^-|^2 = \begin{cases} \dfrac{ik}{2\bar{\nu}_k} & \text{if } \bar{\nu}_k \in i\mathbb{R} \\ \dfrac{\pi k^2}{4\bar{\nu}_k}Re[H'_{\nu_k} H_{\nu_k}^*] & \text{if not} \end{cases} \tag{F.7}$$

Correlators at $p, p' < k$

$$\forall\ \bar{\nu}_k, \quad \hat{\rho}_k(p,p') = -\frac{\sqrt{pp'}}{\bar{\nu}_k}\sinh\left(\bar{\nu}_k(t-t')\right) \qquad t = \ln\frac{p}{k},\ t' = \ln\frac{p'}{k} \tag{F.8}$$

If $\bar{\nu}_k \in \mathbb{R}$,

$$\hat{F}_k(p,p') = \frac{\pi}{4}\sqrt{pp'}\left(|c_k^+|^2 e^{\bar{\nu}_k(t+t')} + |c_k^-|^2 e^{-\bar{\nu}_k(t+t')} + 2Re[c_k^+ c_k^{-*}]\cosh\left(\bar{\nu}_k(t-t')\right)\right) \tag{F.9}$$

If $\bar{\nu}_k \in i\mathbb{R}$,

$$\hat{F}_k(p,p') = \frac{\pi}{4}\sqrt{pp'}e^{-\pi m_k}\Big(\{|c_k^+|^2+|c_k^-|^2\}\cosh\left(\bar{\nu}_k(t-t')\right) + 2Re[c_k^+c_k^{-*}]\cosh\left(\bar{\nu}_k(t+t')\right) + 2iIm[c_k^+c_k^{-*}]\sinh\left(\bar{\nu}_k(t+t')\right)\Big) \quad \text{(F.10)}$$

where we note

$$m_k^2 = V_k'', \qquad M_k^2 = m_k^2 + k^2. \quad \text{(F.11)}$$

Limit $V_k'', k \gg 1$:

$$\hat{F}_k(p,p') = \frac{\sqrt{pp'}}{2M_k}\left[\left(\frac{p}{p'}\right)^{\bar{\nu}_k} + \left(\frac{p'}{p}\right)^{\bar{\nu}_k}\right] \qquad \bar{\nu}_k \simeq iM_k \quad \text{(F.12)}$$

Limite $V_k'', k \ll 1$:

$$\hat{F}_k(p,p') = \frac{2^d\Gamma^2(d/2)}{4\pi}(pp')^{\frac{1}{2}-\bar{\nu}_k} \quad \text{(F.13)}$$

G Ultraviolet flow of the inverse correlator

In this appendix we detail the computation of the integrals (4.53-4.58) in the limit where $m_k, k \gg 1$ for a single scalar field.

- The spectral and statistical correlators are given by (F.8) and (F.12) respectively, which are combinations of (imaginary) power laws.
- As in the main text, we use the notation $M_k^2 = m_k^2 + k^2$. In this limit, $\bar{\nu}_k = iM_k$.
- We remind that I_1 and I_4 do not contribute in the flat space limit (see main text discussion).

We start with the (easiest) tadpole contribution. It also serves as a pedagogical example for insights on the computation of the other terms.

G.1 Tadpole contribution

We highlight in red the leading order contribution whenever there is a sum:

$$J \equiv \int_0^k dp\, p^{d-2} \int_p^k \frac{dr}{r^2} \hat{\rho}_k(p,r) \left[(2-\eta_k)k^2 + \eta_k r^2\right] \hat{F}_k(r,p) \tag{G.1}$$

$$= -\frac{1}{4iM_k^2} \left[(2-\eta_k)k^2 \int_0^k \frac{dp}{p} p^d \int_p^k \frac{dr}{r} \left[\left(\frac{p}{r}\right)^{\bar{\nu}_k} - \left(\frac{r}{p}\right)^{\bar{\nu}_k} \right] \left[\left(\frac{p}{r}\right)^{\bar{\nu}_k} + \left(\frac{r}{p}\right)^{\bar{\nu}_k} \right] \right.$$
$$\left. \eta_k \int_0^k dp\, p^{d-2} \int_p^k \frac{dr}{r} r^2 \left[\left(\frac{p}{r}\right)^{\bar{\nu}_k} - \left(\frac{r}{p}\right)^{\bar{\nu}_k} \right] \left[\left(\frac{p}{r}\right)^{\bar{\nu}_k} + \left(\frac{r}{p}\right)^{\bar{\nu}_k} \right] \right] \tag{G.2}$$

$$= -\frac{1}{4iM_k^2} \left[(2-\eta_k)k^2 \int_0^k \frac{dp}{p} p^d \left\{ \frac{1}{-2\bar{\nu}_k} \left[\left(\frac{p}{k}\right)^{2\bar{\nu}_k} - 1 \right] - \frac{1}{2\bar{\nu}_k} \left[\left(\frac{k}{p}\right)^{2\bar{\nu}_k} - 1 \right] \right\} \right.$$
$$\left. + \eta_k \int_0^k \frac{dp}{p} p^d \left\{ \frac{1}{2-2\bar{\nu}_k} \left[k^2 \left(\frac{p}{k}\right)^{2\bar{\nu}_k} - p^2 \right] - \frac{1}{2+2\bar{\nu}_k} \left[k^2 \left(\frac{k}{p}\right)^{2\bar{\nu}_k} - p^2 \right] \right\} \right] \tag{G.3}$$

$$= -\frac{k^{d+2}}{4iM_k^2} \left[\frac{(2-\eta_k)}{2\bar{\nu}_k} \left(\frac{1}{d+2\bar{\nu}_k} + \frac{1}{d-2\bar{\nu}_k} - \frac{2}{d} \right) \right.$$
$$\left. + \eta_k \left(\frac{1}{2\bar{\nu}_k - 2} \left\{ \frac{1}{d-2\bar{\nu}_k} + \frac{1}{d+2} \right\} + \frac{1}{2\bar{\nu}_k + 2} \left\{ \frac{1}{d-2\bar{\nu}_k} + \frac{1}{d+2} \right\} \right) \right] \tag{G.4}$$

To take the limit $H \to 0$, we must replace explicit occurrences of H. In this case, it means $\bar{\nu}_k \to \bar{\nu}_k/H$. We see that the terms in red are then dominant with respect to the other terms. The resulting limit is

$$J = \frac{1}{4M_k^3} \left(\frac{2-\eta_k}{d} + \frac{\eta_k}{d+2} \right) \tag{G.5}$$

Let us stress in this simple case what becomes of the two terms that stem from $\dot{R}_k$ (in blue in (G.1)). The term proportional to η_k initially adds a r^2 factor in the integrand compared to the term proportionnal to $2-\eta_k$. This results in the modification of a number of denominators, e.g. $\pm 2\bar{\nu}_k \to 2 \pm 2\bar{\nu}_k$. Because we take the limit $H \to 0$, these modifications are negligible everywhere except when $d \to d+2$. This results in the above factorization. The same discussion happens for the other integrals I_j. We will therefore compute the $2-\eta_k$ contributions and conclude by factorizing.

G.2 Sunset contributions

In the limit $H \to 0$, each individual contribution I_0, I_2, I_3 has a dominant term $\propto H^3/M_k^3$, which is not the expected $\propto H^5/M_k^5$. These spurious terms cancel out with each other, as can be expected, and we will therefore compute the sum $I_0 + I_2 + I_3$ directly to be as efficient in this calculation as possible.

As discussed above, we will compute the contribution $\propto 2 - \eta_k$ only. The reader can convince himself, by repeating the same steps, that the term $\propto \eta_k$ gives the same result with the denominator $d \to d + 2$. Noting I the term of interest,

$$I_0 + I_2 + I_3 = \left[(2 - \eta_k) + \frac{d}{d+2}\eta_k\right] I \tag{G.6}$$

In a concise notation,

$$I = k^2 \int_{p,q} \left[-\int_p^k \frac{dr}{r^2} \hat{\rho}_k \hat{F}_k \hat{\rho}_k + \int_q^k \frac{dr}{r^2} \hat{F}_k \hat{\rho}_k \hat{\rho}_k - \int_p^q \frac{dr}{r^2} \hat{\rho}_k \hat{\rho}_k \hat{F}_k \right] \tag{G.7}$$

where

$$\int_{p,q} = \int_0^k \frac{dp}{p^2} p^d \int_p^k \frac{dq}{q^2} \tag{G.8}$$

and the arguments of the correlator functions are always $(p, r), (r, q), (p, q)$ in this order. The H^3/M_k^3 terms we discussed arise from $\int dr/r$ terms. We gather these together by breaking the first term as $\int_p^k = \int_p^q + \int_q^k$:

$$I = k^2 \int_{p,q} \left[+ \int_q^k \frac{dr}{r^2} \big(\hat{F}_k \hat{\rho}_k - \hat{\rho}_k \hat{F}_k\big) \hat{\rho}_k - \int_p^q \frac{dr}{r^2} \big(\hat{\rho}_k \hat{\rho}_k \hat{F}_k + \hat{\rho}_k \hat{F}_k \hat{\rho}_k\big) \right] \tag{G.9}$$

$$\begin{aligned} &= \frac{k^2}{4M_k^3} \int_{p,q} pq \left\{ \int_q^k \frac{dr}{r} \left[\left(\frac{pq}{r^2}\right)^{\bar{\nu}_k} - \left(\frac{r^2}{pq}\right)^{\bar{\nu}_k} \right] \left[\left(\frac{p}{q}\right)^{\bar{\nu}_k} - \left(\frac{q}{p}\right)^{\bar{\nu}_k} \right] \right. \\ &\qquad \left. + \int_p^q \frac{dr}{r} \left[\left(\frac{p}{r}\right)^{\bar{\nu}_k} - \left(\frac{r}{p}\right)^{\bar{\nu}_k} \right] \left[\left(\frac{pr}{q^2}\right)^{\bar{\nu}_k} - \left(\frac{q^2}{pr}\right)^{\bar{\nu}_k} \right] \right\} \end{aligned} \tag{G.10}$$

We have performed a number of cancellations here. Integrating over r,

$$\begin{aligned} I = \frac{k^2}{4M_k^3} \int_{p,q} pq \left\{ \frac{1}{2\bar{\nu}_k} \left[\left(\frac{p}{q}\right)^{\bar{\nu}_k} - \left(\frac{q}{p}\right)^{\bar{\nu}_k} \right] \left[2\left(\frac{p}{q}\right)^{\bar{\nu}_k} + 2\left(\frac{q}{p}\right)^{\bar{\nu}_k} - \left(\frac{pq}{k^2}\right)^{\bar{\nu}_k} - \left(\frac{k^2}{pq}\right)^{\bar{\nu}_k} \right] \right. \\ \left. + \log\frac{q}{p} \left[\left(\frac{p}{q}\right)^{2\bar{\nu}_k} + \left(\frac{q}{p}\right)^{2\bar{\nu}_k} \right] \right\} \end{aligned} \tag{G.11}$$

We will now perform the integrals over p and q. It proves simpler to inverse the order of integration by using the relation $\int_0^k dp \int_p^k dq = \int_0^k dq \int_0^q dp$. The logarithm is integrated using

$$\int_0^q \frac{dp}{p} \ln\frac{k}{p} \left(\frac{p}{k}\right)^{\epsilon} = \frac{1}{\epsilon^2}. \tag{G.12}$$

After integration over p, we therefore obtain

$$I = \frac{k^2}{4M_k^3}\int_0^k \frac{dq}{q} q^d \Bigg\{ \frac{1}{2\bar{\nu}_k}\left[\frac{2}{d-\omega+2\bar{\nu}_k} - \frac{2}{d-\omega-2\bar{\nu}_k}\right] + \frac{1}{(d-\omega+2\bar{\nu}_k)^2} + \frac{1}{(d-\omega+2\bar{\nu}_k)^2}\Bigg\} \quad \text{(G.13)}$$

We have discarded negligible terms in the first line, owing to the fact that

$$\int_0^k \frac{dq}{q} q^d \left(\frac{p}{k}\right)^{2\bar{\nu}_k} \ll \int_0^k \frac{dq}{q} q^d, \quad \text{that is} \quad \frac{1}{d+2\bar{\nu}_k} \ll \frac{1}{d}. \quad \text{(G.14)}$$

The last integration is straightforward, and only dominant contributions remain. Substituting $\bar{\nu}_k = iM_k$ in this limit, and gathering all terms, we find that

$$I = -\frac{k^{d+2}}{4dM_k^3}\frac{2\omega^2+24M_k^2}{(\omega^2+4M_k^2)^2}. \quad \text{(G.15)}$$

We do not compute the terms I_0 and I_4 in this limit. We refer to the main text where it is demonstrated that these terms vanish at leading order in this limit.

H Infrared flow of the inverse correlator

In this appendix we detail the computation of the integrals (4.53-4.58) in the limit where $m_k, k \ll 1$ for a single scalar field. The spectral and statistical correlators are given by (F.8) and (F.13) respectively, which are combinations of real power laws. To compute the leading order contribution of these integrals, the smart way is to understand that it is given by integration of power laws such as

$$\int_0^k \frac{dp}{p}\left(\frac{p}{k}\right)^\epsilon = \frac{1}{\epsilon} \qquad \text{or} \qquad \int_0^k \frac{dp}{p}\left(\frac{p}{k}\right)^\epsilon \ln\frac{k}{p} = \frac{1}{\epsilon^2}, \tag{H.1}$$

where ϵ is a small parameter, either $d-2\bar{\nu}$, ω or a combination of the two. In other words, we will always select terms which give either a small positive power law or a logarithm. With this in mind, we start with the simplest integral, the tadpole contribution.

H.1 Tadpole contribution

We highlight in red the leading order contribution whenever there is a sum:

$$\begin{aligned}
J &\equiv \int_0^k dp\, p^{d-2} \int_p^k \frac{dr}{r^2}\hat{\rho}_k(p,r)\left[(2-\eta_k)k^2 + \eta_k r^2\right]\hat{F}_k(r,p) && \text{(H.2)}\\
&= -\frac{2^d\Gamma^2(d/2)}{8\pi\bar{\nu}_k Z_k^2}\int_0^k \frac{dp}{p}p^d \int_p^k \frac{dr}{r}\left[\left(\frac{p}{r}\right)^{\bar{\nu}_k} - \left(\frac{r}{p}\right)^{\bar{\nu}_k}\right]\left[(2-\eta_k)k^2 + \eta_k r^2\right](ps)^{-\bar{\nu}_k} && \text{(H.3)}\\
&= \frac{2^d\Gamma^2(d/2)}{8\pi\bar{\nu}_k Z_k^2}(2-\eta_k)k^2\int_0^k \frac{dp}{p}p^{d-2\bar{\nu}_k}\ln\frac{k}{p} && \text{(H.4)}\\
&= \frac{2^d\Gamma^2(d/2)}{8\pi\bar{\nu}_k Z_k^2}\frac{(2-\eta_k)k^{d-2\bar{\nu}_k+2}}{(d-2\bar{\nu}_k)^2} && \text{(H.5)}
\end{aligned}$$

which is indeed the result (4.64), keeping in mind that $\bar{\nu}_k = d/2$ at leading order.

H.2 Sunset contributions

Just as for the tadpole contribution, we keep only terms for which the integration over r produces a logarithm. We remind the expression of the integration measure

$$A_k(p,q,r) = p^d\left(\frac{q}{p}\right)^\omega \frac{(2-\eta_k)k^2 + \eta_k r^2}{(pqr)^2}, \tag{H.6}$$

so that

$$I_0 \equiv -\int_0^k dp \int_p^k dq \int_p^k dr\, A_k(p,q,r)\hat{\rho}_k(p,r)\hat{F}_k(r,q)\hat{\rho}_k(p,q) \tag{H.7}$$

$$\to \frac{2^d\Gamma^2(d/2)}{16\pi\bar{\nu}_k^2 Z_k^3}(2-\eta_k)k^2 \int_0^k \frac{dp}{p}p^d \int_p^k \frac{dq}{q}\left(\frac{q}{p}\right)^\omega \left[\left(\frac{p}{q}\right)^{\bar{\nu}_k} - \left(\frac{q}{p}\right)^{\bar{\nu}_k}\right] \frac{1}{(pq)^{\bar{\nu}_k}} \ln\frac{k}{p} \tag{H.8}$$

$$I_2 \equiv \int_0^k dp \int_p^k dq \int_q^k dr\, A_k(p,q,r)\hat{F}_k(p,r)\hat{\rho}_k(r,q)\hat{\rho}_k(p,q) \tag{H.9}$$

$$\to \frac{2^d\Gamma^2(d/2)}{16\pi\bar{\nu}_k^2 Z_k^3}(2-\eta_k)k^2 \int_0^k \frac{dp}{p}p^d \int_p^k \frac{dq}{q}\left(\frac{q}{p}\right)^\omega \left[\left(\frac{p}{q}\right)^{\bar{\nu}_k} - \left(\frac{q}{p}\right)^{\bar{\nu}_k}\right] \frac{1}{(pq)^{\bar{\nu}_k}} \ln\frac{k}{q} \tag{H.10}$$

$$I_3 \equiv -\int_0^k dp \int_p^k dq \int_p^q dr\, A_k(p,q,r)\hat{\rho}_k(p,r)\hat{\rho}_k(r,q)\hat{F}_k(p,q) \tag{H.11}$$

$$\to -\frac{2^d\Gamma^2(d/2)}{16\pi\bar{\nu}_k^2 Z_k^3}(2-\eta_k)k^2 \int_0^k \frac{dq}{q} \int_0^q \frac{dp}{p}p^d\left(\frac{q}{p}\right)^\omega \left[\left(\frac{p}{q}\right)^{\bar{\nu}_k} + \left(\frac{q}{p}\right)^{\bar{\nu}_k}\right] \frac{1}{(pq)^{\bar{\nu}_k}} \ln\frac{q}{p} \tag{H.12}$$

Applying the same principle of keeping the dominant contribution, we see that we must select the "growing mode" which is the positive power law of (q/p). It is the only one which systematically produces integrals of the type (H.1). Discarding the other (decaying) mode, we see that $I_2 + I_3 = I_0$, simply by adding logarithms. As a result, the leading order is simply

$$I_0 + I_2 + I_3 = -\frac{2^d\Gamma^2(d/2)}{8\pi\bar{\nu}_k^2 Z_k^3}(2-\eta_k)k^2 \int_0^k \frac{dp}{p}p^d \int_p^k \frac{dq}{q}\left(\frac{q}{p}\right)^\omega \left(\frac{q}{p}\right)^{\bar{\nu}_k} \frac{1}{(pq)^{\bar{\nu}_k}} \ln\frac{k}{p} \tag{H.13}$$

$$= \frac{2^d\Gamma^2(d/2)}{8\pi\bar{\nu}_k^2 Z_k^3}(2-\eta_k)k^2 \int_0^k \frac{dp}{p}p^{d-\omega-2\bar{\nu}_k} \ln\frac{k}{p}\frac{p^\omega - k^\omega}{\omega} \tag{H.14}$$

$$= \frac{2^d\Gamma^2(d/2)}{8\pi\bar{\nu}_k^2 Z_k^3}\frac{(2-\eta_k)k^{2+d-2\bar{\nu}_k}}{\omega}\left(\frac{1}{(d-2\bar{\nu}_k)^2} - \frac{1}{(d-2\bar{\nu}_k-\omega)^2}\right). \tag{H.15}$$

This reproduces the result in the main text.

$\mathbf{I_1 + I_4}$

We now compute the non dominant contributions, which are the integrals involving a momentum above k. It is more convenient to compute the sum $I_1 + I_4$ rather than the individual terms:

$$I_1{+}I_4 \equiv -\int_0^k dp \int_k^\infty dq \int_p^k dr\, A_k(p,q,r)\hat{\rho}_k(p,r)\left[\hat{F}_k(r,q)\hat{\rho}_k(p,q) + \hat{\rho}_k(r,q)\hat{F}_k(p,q)\right] \tag{H.16}$$

$$= 2\int_0^k dp \int_k^\infty dq \int_p^k dr\, A_k(p,q,r)\hat{\rho}_k(p,r)\mathrm{Im}[u_k(p)u_k(r)u_k^*(q)^2], \tag{H.17}$$

$$= 2\mathrm{Im}\left[f(\omega)\int_k^\infty \frac{dq}{q^{2-\omega}}u_k^*(q)^2\right] \tag{H.18}$$

where we have used the decomposition in terms of the mode function (F.2) as well as the complex identity $\mathrm{Re}(z_1)\mathrm{Im}(z_2) + \mathrm{Im}(z_1)\mathrm{Re}(z_2) = \mathrm{Im}(z_1 z_2)$. The integrals over p and

r are power laws and can be computed exactly:

$$f(\omega) \equiv \int_0^k dp \int_p^k dr\, A_k(p,1,r)\hat{\rho}_k(p,r)u_k(p)u_k(r). \tag{H.19}$$

The integral over r is

$$\begin{aligned}
&\frac{1}{k^2}\int_p^k \frac{dr}{r}\left[\left(\frac{p}{r}\right)^{\bar{\nu}_k} - \left(\frac{r}{p}\right)^{\bar{\nu}_k}\right]\left[c_k^+\left(\frac{r}{k}\right)^{\bar{\nu}_k} + c_k^-\left(\frac{k}{r}\right)^{\bar{\nu}_k}\right]\left[(2-\eta_k)k^2 + \eta_k r^2\right] = \\
&(2-\eta_k)\left\{\frac{c_k^+ - c_k^-}{2\bar{\nu}_k}\left(x^{\bar{\nu}_k} - x^{-\bar{\nu}_k}\right) - \ln x\left(c_k^+ x^{\bar{\nu}_k} - c_k^- x^{-\bar{\nu}_k}\right)\right\} \\
&+\eta_k\left\{\frac{c_k^+}{2+2\bar{\nu}_k}\left(x^{\bar{\nu}_k+2} - x^{-\bar{\nu}_k}\right) + \frac{c_k^-}{2-2\bar{\nu}_k}\left(x^{\bar{\nu}_k} - x^{2-\bar{\nu}_k}\right) + \frac{1-x^2}{2}\left(c_k^+ x^{\bar{\nu}_k} - c_k^- x^{-\bar{\nu}_k}\right)\right\}
\end{aligned} \tag{H.20}$$

where $x = p/k$. Integrating over x is straightforward as well. Interestingly, the result can be factorized as

$$f(\omega) = -\frac{\pi\bar{\nu}_k e^{2i\varphi_k}k^{d+2-\omega}}{2(d-\omega)}(2-\eta_k)\left(\frac{c_k^+}{d+2\bar{\nu}_k-\omega} + \frac{c_k^-}{d-2\bar{\nu}_k-\omega}\right)^2, \tag{H.21}$$

where we remind that $\varphi_k = \frac{\pi}{2}\nu_k + \frac{\pi}{4}$. As a result,

$$I_1+I_4 = -\frac{\pi^2 e^{-2\pi\mathrm{Im}\nu_k}k^{d+2-\omega}}{8(d-\omega)}(2-\eta_k)\mathrm{Im}\left[\bar{\nu}_k\int_k^\infty \frac{dq}{q}q^\omega H_\nu^*(q)^2\left(\frac{c_k^+}{d+2\bar{\nu}_k-\omega} + \frac{c_k^-}{d-2\bar{\nu}_k-\omega}\right)^2\right]. \tag{H.22}$$

In the light infrared,

$$H_\nu(k) \sim \frac{1}{i\pi}\Gamma(\nu)\left(\frac{2}{k}\right)^\nu + \frac{1}{\nu\Gamma(\nu)}\left(\frac{k}{2}\right)^\nu \tag{H.23}$$

$$c_k^\pm \sim \frac{1}{i\pi}\Gamma(\nu)\left(\frac{2}{k}\right)^\nu\left(1 \mp \frac{\nu_k}{\bar{\nu}_k}\right) + \frac{1}{\nu\Gamma(\nu)}\left(\frac{k}{2}\right)^\nu\left(1 \pm \frac{\nu_k}{\bar{\nu}_k}\right). \tag{H.24}$$

In particular, $c_k^- \gg c_k^+$. Eq. (H.22) is the imaginary part of the product of four terms with pure imaginary dominant contribution. To compute non-zero contributions, we must consider the real part of one of the four terms. Exhausting all possibilities, we find that there are no contributions of same order as the other integrals, so that it is an m_k^2/H^2 type correction.

H.3 $0(N)$ case

We now perform the equivalent computations in the case of an $0(N)$ symmetry. the tadpole contribution J is trivially generalized (it is the same computation):

$$J^{T,L} = \frac{2^d\Gamma^2(d/2)}{8\pi\bar{\nu}_k^{T,L}Z_k^2}\frac{(2-\eta_k)k^{d-2\bar{\nu}_k^{T,L}+2}}{(d-2\bar{\nu}_k^{T,L})^2}. \tag{H.25}$$

The sunset contributions now mix transverse and longitudinal modes in a nontrivial (and symmetrize way):

$$I_0 \equiv -\int_0^k dp \int_p^k dq \int_p^k dr\, A_k(p,q,r)\hat{\rho}_k^T(p,r)\hat{F}_k^T(r,q)\hat{\rho}_k^L(p,q) \quad + \quad T \leftrightarrow L, \tag{H.26}$$

$$I_2 \equiv \int_0^k dp \int_p^k dq \int_q^k dr\, A_k(p,q,r)\hat{F}_k^T(p,r)\hat{\rho}_k^T(r,q)\hat{\rho}_k^L(p,q) \quad + \quad T \leftrightarrow L, \tag{H.27}$$

$$I_3 \equiv -\int_0^k dp \int_p^k dq \int_p^q dr\, A_k(p,q,r)\hat{\rho}_k^L(p,r)\hat{\rho}_k^L(r,q)\hat{F}_k^T(p,q) \quad + \quad T \leftrightarrow L. \tag{H.28}$$

Following the same steps, Eq. (H.13) now becomes

$$I_0 + I_2 + I_3 = -\frac{2^d\Gamma^2(d/2)}{8\pi\bar{\nu}_k^L\bar{\nu}_k^T Z_k^3}(2-\eta_k)k^2 \int_0^k \frac{dp}{p}p^d \int_p^k \frac{dq}{q}\left(\frac{q}{p}\right)^{\omega+\bar{\nu}_k^L} \frac{1}{(pq)^{\bar{\nu}_k^T}} \ln\frac{k}{p} + T \leftrightarrow L \tag{H.29}$$

$$\begin{aligned} &= \frac{2^d\Gamma^2(d/2)}{8\pi\bar{\nu}_k^L\bar{\nu}_k^T Z_k^3}\frac{(2-\eta_k)k^{2+d-2\bar{\nu}_k}}{\bar{\nu}_k^L - \bar{\nu}_k^T + \omega}\left(\frac{1}{(d-\bar{\nu}_k^L-\bar{\nu}_k^T)^2} - \frac{1}{(d-2\bar{\nu}_k^T-\omega)^2}\right) \\ &+ \frac{2^d\Gamma^2(d/2)}{8\pi\bar{\nu}_k^L\bar{\nu}_k^T Z_k^3}\frac{(2-\eta_k)k^{2+d-2\bar{\nu}_k}}{\bar{\nu}_k^T - \bar{\nu}_k^L + \omega}\left(\frac{1}{(d-\bar{\nu}_k^L-\bar{\nu}_k^T)^2} - \frac{1}{(d-2\bar{\nu}_k^L-\omega)^2}\right). \end{aligned} \tag{H.30}$$

This reproduces the result in the main text. The contributions I_1 and I_4 are, as previously, negligible in this limit.

List of Figures

1.1 Cosmology and the inflation era . . . 3
1.2 Self-interacting potential of the inflaton field . . . 4
1.3 de Sitter hyperboloid . . . 6
1.4 Closed time path contour in the in-in formalism . . . 7
1.5 Closed momentum contour in the p-representation . . . 9
1.6 one-point function . . . 11
1.7 infrared regulator . . . 15
1.8 Diagrammatic representation of the Wetterich equation . . . 17
1.9 theory space of action functionals . . . 19

2.1 Regulated one-point function . . . 24
2.2 curvature effects in the potential flow in de Sitter space . . . 25
2.3 Different regimes of the β-function . . . 27
2.4 β function of the potential . . . 28
2.5 slope of the β function of the potential . . . 29
2.6 Symmetry restoration in the large N limit . . . 37
2.7 β function of the potential minimum in the large N limit . . . 40
2.8 Flow of the potential minimum in the large N limit . . . 41
2.9 mass generation in the IR close to UV criticality . . . 42
2.10 mass generation in the IR far from UV criticality . . . 43
2.11 causal patches and symmetry restoration . . . 45
2.12 Potential flow of a single field in the IR . . . 46

3.1 Diagrammatic representation of $\dot{\Gamma}_k^{(2)}$ . . . 53

4.1 delayed LPA' flow . . . 77
4.2 anomalous dimension for various N . . . 78
4.3 Renormalization of the field as a function of N . . . 79

E.1 truncation effects in $N = 1$ . . . 96

Bibliography

[1] Paul R. Anderson and R. Holman. Effective Potential for the O(n) Symmetric Model in Static Homogeneous Space-Times. *Phys. Rev.*, D34:2277, 1986.

[2] E. Elizalde, K. Kirsten, and S. D. Odintsov. Effective Lagrangian and the back reaction problem in a selfinteracting O(N) scalar theory in curved space-time. *Phys. Rev.*, D50:5137–5147, 1994.

[3] N. C. Tsamis and R. P. Woodard. One loop graviton selfenergy in a locally de Sitter background. *Phys. Rev.*, D54:2621–2639, 1996.

[4] V. K. Onemli and R. P. Woodard. Superacceleration from massless, minimally coupled phi**4. *Class. Quant. Grav.*, 19:4607, 2002.

[5] T. Brunier, V. K. Onemli, and R. P. Woodard. Two loop scalar self-mass during inflation. *Class. Quant. Grav.*, 22:59–84, 2005.

[6] D. Boyanovsky, Hector J. de Vega, and Norma G. Sanchez. Quantum corrections to the inflaton potential and the power spectra from superhorizon modes and trace anomalies. *Phys. Rev.*, D72:103006, 2005.

[7] Martin S. Sloth. On the one loop corrections to inflation and the CMB anisotropies. *Nucl. Phys.*, B748:149–169, 2006.

[8] David Seery. One-loop corrections to a scalar field during inflation. *JCAP*, 0711:025, 2007.

[9] Yuko Urakawa and Kei-ichi Maeda. One-loop Corrections to Scalar and Tensor Perturbations during Inflation in Stochastic Gravity. *Phys. Rev.*, D78:064004, 2008.

[10] Donald Marolf and Ian A. Morrison. The IR stability of de Sitter QFT: results at all orders. *Phys. Rev.*, D84:044040, 2011.

[11] Stefan Hollands. Correlators, Feynman diagrams, and quantum no-hair in deSitter spacetime. *Commun. Math. Phys.*, 319:1–68, 2013.

[12] Atsushi Higuchi, Donald Marolf, and Ian A. Morrison. On the Equivalence between Euclidean and In-In Formalisms in de Sitter QFT. *Phys. Rev.*, D83:084029, 2011.

[13] Takahiro Tanaka and Yuko Urakawa. Loops in inflationary correlation functions. *Class. Quant. Grav.*, 30:233001, 2013.

[14] V. K. Onemli. Quantum corrected mode function and power spectrum for a scalar field during inflation. *Phys. Rev.*, D89:083537, 2014.

[15] Matti Herranen, Tommi Markkanen, and Anders Tranberg. Quantum corrections to scalar field dynamics in a slow-roll space-time. *JHEP*, 05:026, 2014.

[16] Matti Herranen, Asgeir Osland, and Anders Tranberg. Quantum corrections to inflaton dynamics: The semiclassical approach and the semiclassical limit. *Phys. Rev.*, D92(8):083530, 2015.

[17] S. W. Hawking. Particle Creation by Black Holes. *Commun. Math. Phys.*, 43:199–220, 1975. [,167(1975)].

[18] W. G. Unruh. Notes on black hole evaporation. *Phys. Rev.*, D14:870, 1976.

[19] R. Brout, S. Massar, R. Parentani, and Ph. Spindel. A Primer for black hole quantum physics. *Phys. Rept.*, 260:329–454, 1995.

[20] Graham M. Shore. Radiatively Induced Spontaneous Symmetry Breaking and Phase Transitions in Curved Space-Time. *Annals Phys.*, 128:376, 1980.

[21] I. L. Buchbinder, S. D. Odintsov, and I. L. Shapiro. *Effective action in quantum gravity*. 1992.

[22] E. Elizalde and S. D. Odintsov. Renormalization group improved effective potential for gauge theories in curved space-time. *Phys. Lett.*, B303:240–248, 1993. [Russ. Phys. J.37,25(1994)].

[23] Viatcheslav F. Mukhanov, H. A. Feldman, and Robert H. Brandenberger. Theory of cosmological perturbations. Part 1. Classical perturbations. Part 2. Quantum theory of perturbations. Part 3. Extensions. *Phys. Rept.*, 215:203–333, 1992.

[24] Jacques Bros, Henri Epstein, and Ugo Moschella. Lifetime of a massive particle in a de Sitter universe. *JCAP*, 0802:003, 2008.

[25] Dileep P. Jatkar, Louis Leblond, and Arvind Rajaraman. On the Decay of Massive Fields in de Sitter. *Phys. Rev.*, D85:024047, 2012.

[26] Tomislav Prokopec, Ola Tornkvist, and Richard P. Woodard. Photon mass from inflation. *Phys. Rev. Lett.*, 89:101301, 2002.

[27] Tomislav Prokopec and Ewald Puchwein. Photon mass generation during inflation: de Sitter invariant case. *JCAP*, 0404:007, 2004.

[28] H. V. Peiris et al. First year Wilkinson Microwave Anisotropy Probe (WMAP) observations: Implications for inflation. *Astrophys. J. Suppl.*, 148:213–231, 2003.

[29] S. Perlmutter et al. Measurements of Omega and Lambda from 42 high redshift supernovae. *Astrophys. J.*, 517:565–586, 1999.

[30] Renaud Parentani. The Inflationary paradigm: Predictions for CMB. *Comptes Rendus Physique*, 4:935–943, 2003.

[31] D. Langlois. Lectures on inflation and cosmological perturbations. *Lect. Notes Phys.*, 800:1–57, 2010.

[32] N. C. Tsamis and R. P. Woodard. Stochastic quantum gravitational inflation. *Nucl. Phys.*, B724:295–328, 2005.

[33] Steven Weinberg. Quantum contributions to cosmological correlations. *Phys. Rev.*, D72:043514, 2005.

[34] Julien Serreau. Nonperturbative infrared enhancement of nonGaussian correlators in de Sitter space. *Phys. Lett.*, B728:380–385, 2014.

[35] A. M. Polyakov. Infrared instability of the de Sitter space. 2012.

[36] Paul R. Anderson and Emil Mottola. Instability of global de Sitter space to particle creation. *Phys. Rev.*, D89:104038, 2014.

[37] Paul R. Anderson, Carmen Molina-Paris, and Emil Mottola. Cosmological Horizon Modes and Linear Response in de Sitter Spacetime. *Phys. Rev.*, D80:084005, 2009.

[38] Steven Weinberg. Quantum contributions to cosmological correlations. II. Can these corrections become large? *Phys. Rev.*, D74:023508, 2006.

[39] Juergen Berges and Julien Serreau. Progress in nonequilibrium quantum field theory. In *5th Internationa Conference on Strong and Electroweak Matter (SEWM 2002) Heidelberg, Germany, October 2-5, 2002*, 2003.

[40] Juergen Berges and Julien Serreau. Progress in nonequilibrium quantum field theory II. In *6th International Conference on Strong and Electroweak Matter (SEWM 2004) Helsinki, Finland, June 16-19, 2004*, 2004.

[41] J. Berges and Sz. Borsanyi. Progress in nonequilibrium quantum field theory. III. *Nucl. Phys.*, A785:58–67, 2007.

[42] Alexei A. Starobinsky. Stochastic de Sitter (inflationary) stage in the early universe. *Lect. Notes Phys.*, 246:107–126, 1986.

[43] Alexei A. Starobinsky and Junichi Yokoyama. Equilibrium state of a self interacting scalar field in the De Sitter background. *Phys. Rev.*, D50:6357–6368, 1994.

[44] V. K. Onemli. Vacuum Fluctuations of a Scalar Field during Inflation: Quantum versus Stochastic Analysis. *Phys. Rev.*, D91:103537, 2015.

[45] Bjorn Garbrecht, Florian Gautier, Gerasimos Rigopoulos, and Yi Zhu. Feynman Diagrams for Stochastic Inflation and Quantum Field Theory in de Sitter Space. *Phys. Rev.*, D91:063520, 2015.

[46] Björn Garbrecht, Gerasimos Rigopoulos, and Yi Zhu. Infrared correlations in de Sitter space: Field theoretic versus stochastic approach. *Phys. Rev.*, D89:063506, 2014.

[47] Meindert van der Meulen and Jan Smit. Classical approximation to quantum cosmological correlations. *JCAP*, 0711:023, 2007.

[48] C. P. Burgess, L. Leblond, R. Holman, and S. Shandera. Super-Hubble de Sitter Fluctuations and the Dynamical RG. *JCAP*, 1003:033, 2010.

[49] Arvind Rajaraman. On the proper treatment of massless fields in Euclidean de Sitter space. *Phys. Rev.*, D82:123522, 2010.

[50] M. Beneke and P. Moch. On "dynamical mass" generation in Euclidean de Sitter space. *Phys. Rev.*, D87:064018, 2013.

[51] E. T. Akhmedov. IR divergences and kinetic equation in de Sitter space. Poincare patch: Principal series. *JHEP*, 01:066, 2012.

[52] Bjorn Garbrecht and Gerasimos Rigopoulos. Self Regulation of Infrared Corrections for Massless Scalar Fields during Inflation. *Phys. Rev.*, D84:063516, 2011.

[53] Daniel Boyanovsky. Condensates and quasiparticles in inflationary cosmology: mass generation and decay widths. *Phys. Rev.*, D85:123525, 2012.

[54] R. Parentani and J. Serreau. Physical momentum representation of scalar field correlators in de Sitter space. *Phys. Rev.*, D87:045020, 2013.

[55] Florian Gautier and Julien Serreau. Infrared dynamics in de Sitter space from Schwinger-Dyson equations. *Phys. Lett.*, B727:541–547, 2013.

[56] Ahmed Youssef and Dirk Kreimer. Resummation of infrared logarithms in de Sitter space via Dyson-Schwinger equations: the ladder-rainbow approximation. *Phys. Rev.*, D89:124021, 2014.

[57] D. Boyanovsky. Effective field theory during inflation: Reduced density matrix and its quantum master equation. *Phys. Rev.*, D92(2):023527, 2015.

[58] Jürgen Berges, Nikolaos Tetradis, and Christof Wetterich. Nonperturbative renormalization flow in quantum field theory and statistical physics. *Phys. Rept.*, 363:223–386, 2002.

[59] Bertrand Delamotte. An Introduction to the nonperturbative renormalization group. *Lect. Notes Phys.*, 852:49–132, 2012.

[60] Holger Gies. Introduction to the functional RG and applications to gauge theories. *Lect. Notes Phys.*, 852:287–348, 2012.

[61] M. Reuter. Nonperturbative evolution equation for quantum gravity. *Phys. Rev.*, D57:971–985, 1998.

[62] Holger Gies and Stefan Lippoldt. Renormalization flow towards gravitational catalysis in the 3d Gross-Neveu model. *Phys. Rev.*, D87:104026, 2013.

[63] Ilya L. Shapiro, Poliane Morais Teixeira, and Andreas Wipf. On the functional renormalization group for the scalar field on curved background with non-minimal interaction. *Eur. Phys. J.*, C75:262, 2015.

[64] Dario Benedetti. Critical behavior in spherical and hyperbolic spaces. *J. Stat. Mech.*, 1501:P01002, 2015.

[65] Ali Kaya. Exact renormalization group flow in an expanding Universe and screening of the cosmological constant. *Phys.Rev.*, D87(12):123501, 2013.

[66] Julien Serreau. Renormalization group flow and symmetry restoration in de Sitter space. *Phys.Lett.*, B730:271–274, 2014.

[67] Bharat Ratra. Restoration of Spontaneously Broken Continuous Symmetries in de Sitter Space-Time. *Phys. Rev.*, D31:1931–1955, 1985.

[68] F. D. Mazzitelli and J. P. Paz. Gaussian and $1/N$ Approximations in Semiclassical Cosmology. *Phys. Rev.*, D39:2234, 1989.

[69] T. M. Janssen, S. P. Miao, T. Prokopec, and R. P. Woodard. The Hubble Effective Potential. *JCAP*, 0905:003, 2009.

[70] Julien Serreau. Effective potential for quantum scalar fields on a de Sitter geometry. *Phys. Rev. Lett.*, 107:191103, 2011.

[71] Albert Einstein. Cosmological Considerations in the General Theory of Relativity. *Sitzungsber. Preuss. Akad. Wiss. Berlin (Math. Phys.)*, 1917:142–152, 1917.

[72] Jerry B. Griffiths and Jiří Podolský. *Exact Space-Times in Einstein's General Relativity.* Cambridge University Press, 2009.

[73] Arno A. Penzias and Robert Woodrow Wilson. A Measurement of excess antenna temperature at 4080-Mc/s. *Astrophys. J.*, 142:419–421, 1965.

[74] Shaun Cole et al. The 2dF Galaxy Redshift Survey: Power-spectrum analysis of the final dataset and cosmological implications. *Mon. Not. Roy. Astron. Soc.*, 362:505–534, 2005.

[75] et.al. Hinshaw, G. F. Nine-year Wilkinson Microwave Anisotropy Probe (WMAP) Observations: Cosmological Results. *The Astrophysical Journal, Supplement*, 2012.

[76] Keith A. Olive, Gary Steigman, and Terry P. Walker. Primordial nucleosynthesis: Theory and observations. *Phys. Rept.*, 333:389–407, 2000.

[77] Daniel Baumann. Inflation. In *Physics of the large and the small, TASI 09, proceedings of the Theoretical Advanced Study Institute in Elementary Particle Physics, Boulder, Colorado, USA, 1-26 June 2009*, pages 523–686, 2011.

[78] Andreas Albrecht and Paul J. Steinhardt. Cosmology for Grand Unified Theories with Radiatively Induced Symmetry Breaking. *Phys. Rev. Lett.*, 48:1220–1223, 1982.

[79] Andrei D. Linde. A New Inflationary Universe Scenario: A Possible Solution of the Horizon, Flatness, Homogeneity, Isotropy and Primordial Monopole Problems. *Phys. Lett.*, B108:389–393, 1982.

[80] N. Bartolo, E. Komatsu, Sabino Matarrese, and A. Riotto. Non-Gaussianity from inflation: Theory and observations. *Phys. Rept.*, 402:103–266, 2004.

[81] Juan Maldacena. Non-gaussian features of primordial fluctuations in single field inflationary models. *Journal of High Energy Physics*, 2003(05):013, 2003.

[82] Julian S. Schwinger. Brownian motion of a quantum oscillator. *J. Math. Phys.*, 2:407–432, 1961.

[83] Jürgen Berges. Introduction to nonequilibrium quantum field theory. *AIP Conf. Proc.*, 739:3–62, 2005. [,3(2004)].

[84] Xavier Busch and Renaud Parentani. Dispersive fields in de Sitter space and event horizon thermodynamics. *Phys. Rev.*, D86:104033, 2012.

[85] Julian Adamek, Xavier Busch, and Renaud Parentani. Dissipative fields in de Sitter and black hole spacetimes: quantum entanglement due to pair production and dissipation. *Phys. Rev.*, D87:124039, 2013.

[86] Paul R. Anderson, Wayne Eaker, Salman Habib, Carmen Molina-Paris, and Emil Mottola. Attractor states and infrared scaling in de Sitter space. *Phys. Rev.*, D62:124019, 2000.

[87] E. Mottola. Particle Creation in de Sitter Space. *Phys. Rev.*, D31:754, 1985.

[88] Christopher J. Fewster and Rainer Verch. The Necessity of the Hadamard Condition. *Class. Quant. Grav.*, 30:235027, 2013.

[89] T. S. Bunch and P. C. W. Davies. Quantum Field Theory in de Sitter Space: Renormalization by Point Splitting. *Proc. Roy. Soc. Lond.*, A360:117–134, 1978.

[90] J. P. Blaizot, Edmond Iancu, and A. Rebhan. Approximately selfconsistent resummations for the thermodynamics of the quark gluon plasma. 1. Entropy and density. *Phys. Rev.*, D63:065003, 2001.

[91] Gerasimos Rigopoulos. Fluctuation-dissipation and equilibrium for scalar fields in de Sitter. 2013.

[92] F. J. Dyson. The S matrix in quantum electrodynamics. *Phys. Rev.*, 75:1736–1755, 1949.

[93] Julian S. Schwinger. On the Green's functions of quantized fields. 1. and 2. *Proc. Nat. Acad. Sci.*, 37:452–455, 1951.

[94] Florian Gautier and Julien Serreau. Scalar field correlator in de Sitter space at next-to-leading order in a 1/N expansion. *Phys. Rev.*, D92(10):105035, 2015.

[95] Jean Zinn-Justin. Quantum field theory and critical phenomena. *Int. Ser. Monogr. Phys.*, 113:1–1054, 2002.

[96] Thomas Gasenzer and Jan M. Pawlowski. Towards far-from-equilibrium quantum field dynamics: A functional renormalisation-group approach. *Phys. Lett.*, B670:135–140, 2008.

[97] Leonie Canet, Hugues Chate, and Bertrand Delamotte. General framework of the non-perturbative renormalization group for non-equilibrium steady states. *J. Phys.*, A44:495001, 2011.

[98] J. Berges and David Mesterhazy. Introduction to the nonequilibrium functional renormalization group. *Nucl. Phys. Proc. Suppl.*, 228:37–60, 2012.

[99] Daniel F. Litim. Optimized renormalization group flows. *Phys. Rev.*, D64:105007, 2001.

[100] Christof Wetterich. Exact evolution equation for the effective potential. *Phys. Lett.*, B301:90–94, 1993.

[101] Kenneth G. Wilson. Renormalization group and critical phenomena. 1. Renormalization group and the Kadanoff scaling picture. *Phys. Rev.*, B4:3174–3183, 1971.

[102] Joseph Polchinski. Renormalization and Effective Lagrangians. *Nucl. Phys.*, B231:269–295, 1984.

[103] E. V. Gorbar. Dynamical symmetry breaking in spaces with constant negative curvature. *Phys. Rev.*, D61:024013, 2000.

[104] Gianrocco Lazzari and Tomislav Prokopec. Symmetry breaking in de Sitter: a stochastic effective theory approach. 2013.

[105] B. L. Hu and D. J. O'Connor. Symmetry Behavior in Curved Space-time: Finite Size Effect and Dimensional Reduction. *Phys. Rev.*, D36:1701, 1987.

[106] Marco D'Attanasio and Tim R. Morris. Large N and the renormalization group. *Phys. Lett.*, B409:363–370, 1997.

[107] N. Tetradis and D. F. Litim. Analytical solutions of exact renormalization group equations. *Nucl. Phys.*, B464:492–511, 1996.

[108] J. P. Blaizot, Ramon Mendez Galain, and Nicolas Wschebor. A New method to solve the non perturbative renormalization group equations. *Phys. Lett.*, B632:571–578, 2006.

[109] Leonard Fister and Jan Martin Pawlowski. Functional renormalization group in a finite volume. *Phys. Rev.*, D92(7):076009, 2015.

[110] Tomislav Prokopec. Symmetry breaking and the Goldstone theorem in de Sitter space. *JCAP*, 1212:023, 2012.

[111] Takashi Arai. Nonperturbative Infrared Effects for Light Scalar Fields in de Sitter Space. *Class. Quant. Grav.*, 29:215014, 2012.

[112] Diana L. Lopez Nacir, Francisco D. Mazzitelli, and Leonardo G. Trombetta. Hartree approximation in curved spacetimes revisited: The effective potential in de Sitter spacetime. *Phys. Rev.*, D89:024006, 2014.

[113] Daniel Boyanovsky. Spontaneous symmetry breaking in inflationary cosmology: on the fate of Goldstone Bosons. *Phys. Rev.*, D86:023509, 2012.

[114] Urko Reinosa and Zsolt Szep. Broken phase scalar effective potential and Phi-derivable approximations. *Phys. Rev.*, D83:125026, 2011.

[115] M. Beneke and P. Moch. On "dynamical mass" generation in euclidean de sitter space. *Phys. Rev. D*, 87:064018, Mar 2013.

[116] Leonie Canet, Bertrand Delamotte, Dominique Mouhanna, and Julien Vidal. Optimization of the derivative expansion in the nonperturbative renormalization group. *Phys. Rev.*, D67:065004, 2003.

[117] F. Benitez, J. P. Blaizot, H. Chate, B. Delamotte, R. Mendez-Galain, and N. Wschebor. Non-perturbative renormalization group preserving full-momentum dependence: implementation and quantitative evaluation. *Phys. Rev.*, E85:026707, 2012.

[118] N. D. Mermin and H. Wagner. Absence of ferromagnetism or antiferromagnetism in one- or two-dimensional isotropic heisenberg models. *Phys. Rev. Lett.*, 17:1133–1136, Nov 1966.

[119] J M Kosterlitz and D J Thouless. Ordering, metastability and phase transitions in two-dimensional systems. *Journal of Physics C: Solid State Physics*, 6(7):1181, 1973.

[120] Martin Hasenbusch. Monte carlo studies of the three-dimensional ising model in equilibrium. *International Journal of Modern Physics C*, 12(07):911–1009, 2001.

[121] Jean-Paul Blaizot. Renormalization group flow equations with full momentum dependence. *Phil. Trans. Roy. Soc. Lond.*, A369:2735–2758, 2011.

[122] Leonard Fister and Jan M. Pawlowski. Functional renormalization group in a finite volume. *Phys. Rev. D*, 92:076009, Oct 2015.

[123] Thomas Kloss, Léonie Canet, Bertrand Delamotte, and Nicolás Wschebor. Kardar-Parisi-Zhang equation with spatially correlated noise: A unified picture from non-perturbative renormalization group. *Phys. Rev.*, E89(2):022108, 2014.

[124] Shun-Pei Miao and R. P. Woodard. Leading log solution for inflationary Yukawa. *Phys. Rev.*, D74:044019, 2006.

[125] Fransisco Fabian Gonzales. Scalar quantum electrodynamics in de Sitter space from the non-perturbative renormalization group. *Master's thesis*, advisor: Tomislav Prokopec, 2016.

[126] T. Prokopec, N. C. Tsamis, and R. P. Woodard. Stochastic Inflationary Scalar Electrodynamics. *Annals Phys.*, 323:1324–1360, 2008.

[127] NIST Digital Library of Mathematical Functions. http://dlmf.nist.gov/, Release 1.0.11 of 2016-06-08.

Abstract

The study of cosmology draws us to the topic of quantum fields in curved space-time. In particular, light scalar fields offer a simple mechanism for inflation and primordial fluctuations. When computing loop corrections to these models however, infrared and secular divergences appear which call for resummation techniques. To this end, we implement the nonperturbative renormalization group for quantum scalar fields on a fixed de Sitter background. First, the Local Potential Approximation (LPA) is applied. We show that there is always symmetry restoration due to infrared effects, and that mass is generated in agreement with the stochastic approach. Next, we study the flat space limit of our formalism by taking the curvature $H \to 0$, and we check that it reproduces a number of known results. Finally, we discuss the derivative expansion, which goes beyond the LPA. Its implementation seems too complex in general curved space-times, but de Sitter symmetries allow for a simpler representation. We define a prescription for all orders of the expansion, and discuss the flow of the first order term in the simple case where we neglect the field dependency (LPA').

Key words: quantum field theory, nonperturbative renormalization group, de Sitter space

Résumé

La cosmologie moderne amène à étudier la théorie quantique des champs en espace-temps courbe. Les champs scalaires légers, notamment, génèrent un mécanisme simple pour l'inflation et les fluctuations primordiales. Cependant, les calculs de boucles de ces modèles contiennent des divergences infrarouges et séculaires qui requièrent des techniques de resommation. Dans ce but, on implémente le groupe de renormalisation non perturbatif pour des champs scalaires en espace-temps de De Sitter. Dans un premier temps, on applique l'Approximation de Potentiel Local (APL). On démontre que les effets infrarouges sont responsables d'une restauration de la symétrie, et qu'une masse est générée en accord avec l'approche stochastique. On étudie ensuite la limite d'espace-temps plat de notre formalisme en prenant la courbure $H \to 0$, ce qui reproduit un certain nombre de résultats connus. Enfin, on s'intéresse à l'expansion dérivative, qui va au-delà de l'APL. Son implémentation semble trop complexe dans le cas général d'un espace-temps courbe, mais les symétries de De Sitter permettent de trouver une représentation simple. On définit une prescription pour tous les ordres de l'expansion, puis on implémente le flot du terme de premier ordre dans le cas simple où la dépendance en champ est négligée.

Mots clés : théorie quantique des champs, groupe de renormalisation non perturbatif, espace-temps de De sitter.